London Dispersion and Solvent Effects on Azobenzene Switches

Inauguraldissertation zur Erlangung des Doktorgrades der naturwissenschaftlichen Fachbereiche im Fachgebiet Chemie der Justus-Liebig-Universität Gießen

vorgelegt von
Marcel A. Strauß

aus Singlis

Betreuer
Prof. Dr. Hermann A. Wegner

Gießen 2021

London Dispersion and Solvent Effects on Azobenzene Switches

Inauguraldissertation zur Erlangung des Doktorgrades der naturwissenschaftlichen Fachbereiche im Fachgebiet Chemie der Justus-Liebig-Universität Gießen

vorgelegt von

Marcel A. Strauß

aus Singlis

Betreuer

Prof. Dr. Hermann A. Wegner

Gießen 2021

We are trying to prove ourselves wrong as quickly as possible, because only in that way we can find progress.

– Richard P. Feynman

Versicherung nach §17 der Promotionsordnung

Ich erkläre: Ich habe die vorgelegte Dissertation selbstständig und ohne unerlaubte fremde Hilfe und nur mit den Hilfen angefertigt, die ich in der Dissertation angegeben habe. Alle Textstellen, die wörtlich oder sinngemäß aus veröffentlichten Schriften entnommen sind, und alle Angaben, die auf mündlichen Auskünften beruhen, sind als solche kenntlich gemacht. Ich stimme einer evtl. Überprüfung meiner Dissertation durch eine Antiplagiat-Software zu. Bei den von mir durchgeführten und in der Dissertation erwähnten Untersuchungen habe ich die Grundsätze guter wissenschaftlicher Praxis, wie sie in der „Satzung der Justus-Liebig-Universität Gießen zur Sicherung guter wissenschaftlicher Praxis“ niedergelegt sind, eingehalten.

Marcel André Strauß	Ort, Datum

Dekan:	Prof. Dr. Thomas Wilke
Erstgutachter:	Prof. Dr. Hermann A. Wegner
Zweitgutachter:	Prof. Dr. Peter R. Schreiner, PhD

Contents

1 Abstract

Molecular photoswitches based on azobenzenes represent a widespread tool to manipulate properties of systems in the solid or liquid state as well as in solution by using light. In order to optimize the design of these azoswitches, comprehensive knowledge of all internal and external factors altering their properties is necessary. This includes photochromic but also thermodynamic and kinetic influences on their switching behavior.

As part of this thesis, fundamental studies concerning the effect of London dispersion interactions on the stability of the *cis*-isomer of azobenzenes were conducted. In this context, multiple alkyl substituted azobenzenes were prepared and used as probes to determine the stabilizing contributions on the *cis*-state in dependence of the substituent length and position. It was possible to identify dispersion interactions originating from alkyl-aryl interactions as the main contributor to the stabilization of the *cis*-isomer. Surprisingly, even flexible alkyl chains like *n*-butyl can lead to an about five times higher half-life of the *cis*-isomer compared to the methyl-substituted derivative.

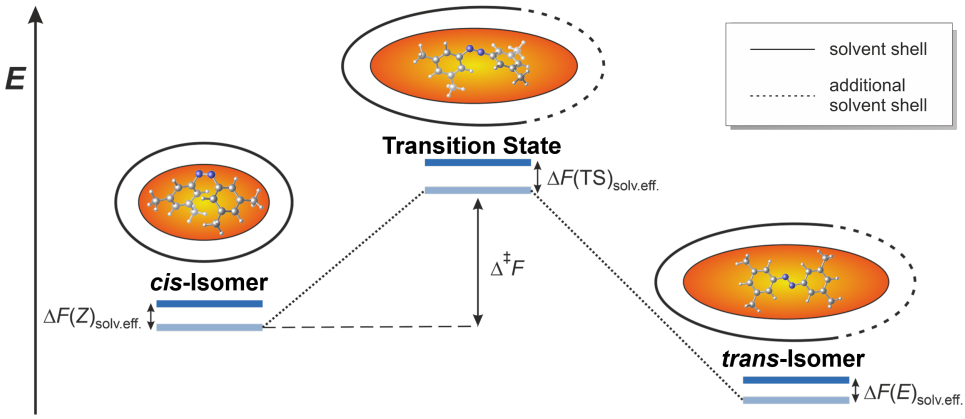

Figure 1: Relative energies of the *cis-trans*-isomerization of an azobenzene derivative. Changes in the solvent accessible surface due to the isomerization results in increased solute solvent interactions in the transition state and for the *trans*-isomer. The figure was adapted from figure 1 in reference 45. ©2021 with permission of John Wiley & Sons, Inc.

Additionally, changes induced by different solvent environments were investigated. Replacing *n*-octane as the solvent with *iso*-octane, increased the activation barrier for the thermal *cis-trans*-isomerization by about 0.1 kcal mol^{-1}, resulting in 20% higher half-lives. Cyclooctane had a destabilizing effect of the same magnitude except for a bulky *tert*-butyl substituted derivative, which was similarly stabilized as in *iso*-octane. It was further demonstrated that intramolecular dispersion interactions are not canceled in solution, since the overall trend of half-lives in dependence of the substituent chain length is constant in all investigated solvents.

Moreover, several molecular systems for the investigation of London dispersion interactions were reviewed. Advantages and disadvantages of the different concepts were addressed, revealing the necessity to gain a deeper insight into London dispersion interactions between different molecular structures and especially concerning the solvent environment.

Further studies were conducted in order to analyze the influence of an electronically decoupled ammonium tag attached to the azobenzene scaffold in different solvents. Such an ammonium functionality represents a common motif for biological active compounds, enhancing their solubility in aqueous environments even allowing binding with biological receptors. Photochromic as well as kinetic properties of the *cis-trans* isomerization were determined and compared to unsubstituted azobenzene. In this way, background data for the use of ammonium tagged azobenzenes for versatile applications in different systems could be provided.

2 Zusammenfassung

Molekulare Photoschalter auf der Basis von Azobenzolen stellen ein weit verbreitetes Werkzeug dar, um Eigenschaften von Systemen im festen oder flüssigen Zustand sowie in Lösung mit Hilfe von Licht zu beeinflussen. Um das Design dieser Azoschalter zu optimieren, ist eine umfassende Kenntnis aller internen und externen Faktoren notwendig, die ihre Eigenschaften verändern können. Dazu gehören photochrome, aber auch thermodynamische und kinetische Einflüsse auf ihr Schaltverhalten.

Im Rahmen dieser Arbeit wurden grundlegende Untersuchungen zum Einfluss von London Dispersionswechselwirkungen auf die Stabilität des *cis*-Isomers von Azobenzolen durchgeführt. Dazu wurden mehrere Alkyl-substituierte Azobenzole hergestellt und als Sensor verwendet, um die stabilisierende Wirkung auf das *cis*-Isomer in Abhängigkeit von der Substituentenlänge und -position zu bestimmen. Es war möglich, Dispersionswechselwirkungen, die von Alkyl-Aryl-Wechselwirkungen herrühren, als den Hauptfaktor zur Stabilisierung des *cis*-Isomers zu identifizieren. Überraschenderweise konnte festgestellt werden, dass sogar flexible Alkylketten wie *n*-Butyl zu einer etwa fünfmal höheren Halbwertszeit des *cis*-Isomers im Vergleich zum Methyl-substituierten Derivat führen.

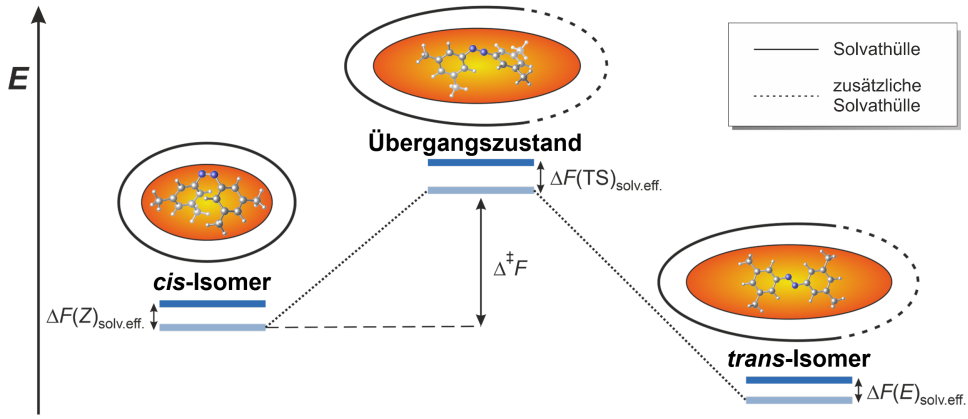

Figure 2: Relative Energien der *cis-trans*-Isomerisierung eines Azobenzolderivats. Änderungen in der lösungsmittelzugänglichen Oberfläche aufgrund der Isomerisierung führen zu erhöhten Wechselwirkungen zwischen gelöster Substanz und dem Lösungsmittel im Übergangszustand und für das *trans*-Isomer. Die Abbildung wurde von Abbildung 1 in Referenz 45 adaptiert. ©2021 mit Genehmigung von John Wiley & Sons, Inc.

Außerdem wurden die durch unterschiedliche Lösungsmittelumgebungen induzierten Effekte untersucht. Das Ersetzen von *n*-Octan als Lösungsmittel durch *iso*-Octan erhöhte die Aktivierungsbarriere für die thermische *cis-trans*-Isomerisierung um etwa 0,1 kcal mol^{-1}, was zu 20% höheren Halbwertszeiten führte. Cyclooctan hatte einen destabilisierenden Effekt in der gleichen Größenordnung, mit Ausnahme für ein *tert*-Butyl-substituiertes Derivat, das ähnlich stabilisiert wurde wie in *iso*-Octan. Es wurde weiterhin gezeigt, dass intramolekulare Dispersionswechselwirkungen in Lösung nicht aufgehoben werden, da der Gesamttrend der Halbwertszeiten in Abhängigkeit von der Kettenlänge der Substituenten in allen untersuchten Lösungsmitteln konstant ist.

Darüber hinaus wurden verschiedene molekulare Systeme für die Untersuchung von London Dispersionswechselwirkungen evaluiert. Es wurden Vor- und Nachteile der verschiedenen Konzepte adressiert und die Notwendigkeit aufgezeigt, einen tieferen Einblick in die London Dispersionswechselwirkungen zwischen verschiedenen molekularen Strukturen und insbesondere in Bezug auf die Lösungsmittelumgebung zu gewinnen.

Weitere Studien wurden durchgeführt, um den Einfluss eines elektronisch entkoppelten Ammonium-Tags, das an ein Azobenzolgerüst gebunden ist, in verschiedenen Lösungsmitteln zu analysieren. Eine solche Ammoniumgruppe stellt ein gängiges Motiv für biologisch aktive Verbindungen dar, welches deren Löslichkeit in wässriger Umgebung erhöht und sogar die Bindung an biologische Rezeptoren ermöglicht. Sowohl die photochromen als auch die kinetischen Eigenschaften der *cis-trans*-Isomerisierung wurden bestimmt und mit unsubstituiertem Azobenzol verglichen. Auf diese Weise konnten Hintergrunddaten für den Einsatz von Ammonium-markierten Azobenzolen für vielseitige Anwendungen in verschiedenen Systemen geliefert werden.

3 Introduction

Molecular photoswitches based on azobenzenes represent a widespread group of compounds with versatile applications. Their high potential in controlling biological mechanisms,[1–3] selectivity and activity of catalysts[4,5] and functions in material science,[6,7] make it necessary to fully understand every factor influencing their photochemical properties. One factor, which has been neglected in the past are the stabilizing effects of London dispersion on the *cis*-form of azobenzenes. Especially, in the prominent case of all-*meta tert*-butyl azobenzene, attractive dispersion interactions as cause for the low isomerization rate of its *cis*-isomer were not considered.[8] With the changed perception of large alkyl groups not only as steric factors but also as dispersion energy donors,[9] a new evaluation of its influence on azobenzene based photoswitches becomes necessary. The following chapters provide a comprehensive introduction and may guide the reader through the interlinked effects caused by London dispersion interactions and the solvent environment on the stability of azobenzenes.

3.1 London Dispersion – an Ubiquitous Force

In 1930, Fritz London found a way to estimate the strength of molecular interactions described by the attractive part of the van der Waals equation.[10] Such small attractive forces derive from instantaneous dipole-induced dipole interactions and represent the origin of major attractive forces between non-polar or weak polar molecules. Due to the connection with the optical dispersion theory, he named it *dispersion effect*. This relation can further be demonstrated by the *Clausius-Mossotti* equation 1.[11] Here, P_m stands for the molar polarization, ε_r for the relative permittivity, M_m is the molar mass, ρ the density, N_A the Avogadro constant and ε_0 the vacuum permittivity. The polarizability α then describes the tendency of a substance to establish an electric dipole, when exposed to an electric field.[12] The source for the electric field can also be a light wave, connecting dispersion theory with the induced polarization of atoms or molecules. Replacing the relative permittivity ε_r in equation 1 with the square of the refractive index n leads to the *Lorentz-Lorenz* equation, further emphasizing the relation of optical dispersion to the polarizability α.[11]

$$P_m = \frac{\varepsilon_r - 1}{\varepsilon_r + 2}\frac{M_m}{\rho} = \frac{N_A}{3\varepsilon_0}\alpha \tag{1}$$

The equation below represents an approximation for the calculation of the dispersion energy between fragments consisting of the atoms A & B.[13] The C_6^{AB} dispersion coefficient describes the specific polarizability of the atoms involved. The fast decrease of the dispersion forces with growing interatomic distance between the atoms can be derived from the r_{AB}^6 dependence of the term.

$$E_{disp} = -\sum_{AB}^{atom\ pairs} \frac{C_6^{AB}}{r_{AB}^6} \tag{2}$$

3.1.1 Influences of London Dispersion on Inter- and Intramolecular Association

The strength of one dispersion interaction is usually quite weak, but increases already considerably with increasing size of the electron shell of the interacting atoms. This can be well illustrated by the dissociation energies of noble gas dimers.[14] While for the He_2 dimer only 22 cal mol^{-1} of energy uptake lead to dissociation, this value rises already to 84 and 285 cal mol^{-1} for the Ne_2 and Ar_2 dimers, respectively. The interaction energies from dispersion forces start to get significant for hydrocarbons, especially alkanes. For a series of all-*trans* *n*-alkanes, they rise steadily from -0.4 for the methane dimer **1** up to -2.7 kcal mol^{-1} for the butane dimer **4** (Figure 3).[15] However, one has to keep in mind, that the results from these coupled-cluster computations cover only a part of the possible arrangements of the alkane chains to each other. Considering the whole conformer ensemble, lower total interaction energies have to be expected.

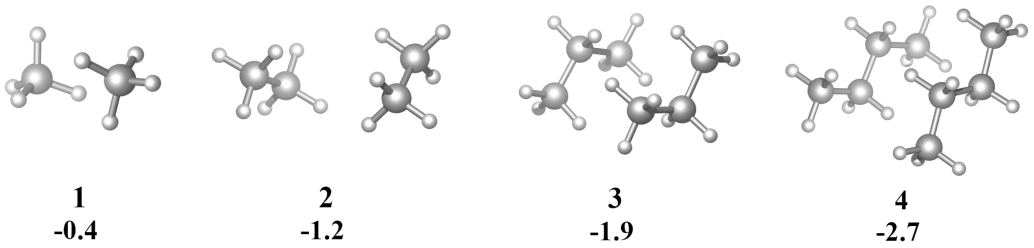

Figure 3: Dimers of small alkanes ranging from methane **1** to *n*-butane **4**. Interaction energies are given in kcal mol^{-1} at the CCSD(T)/cc-pVTZ level of theory.[15] The figure was created using the information from reference 15.

Even for benzene, dispersion interactions play a major role for molecular association. Computations clearly showed, that not the intuitive "Sandwich" dimer **5**, but a parallel displaced structure **6** and a T-shaped structure **7** provide the best arrangement (Scheme 1).[16] It can further be seen, that the optimal distance between the molecules is reduced with increasing electrostatic interactions. Nevertheless, in all cases London dispersion dominates the interaction energies.

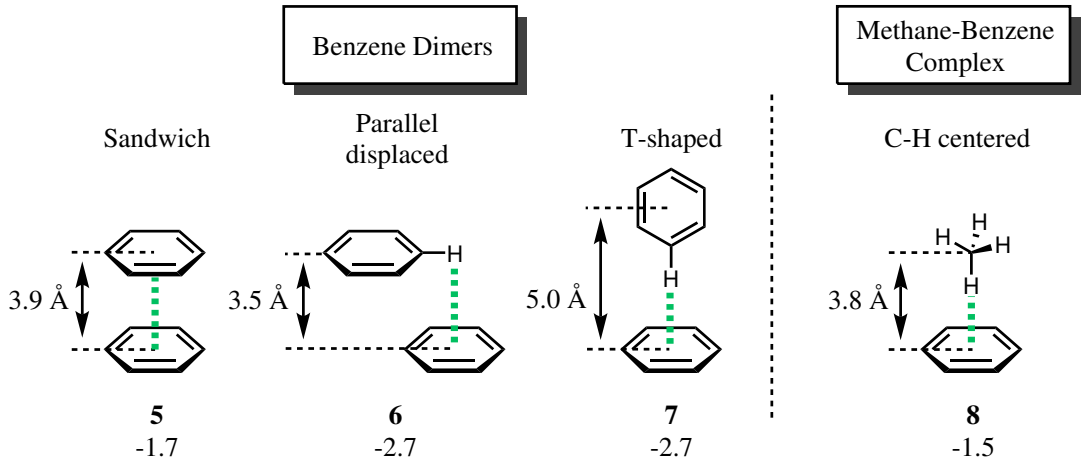

Scheme 1: Examples of extreme bonding situations stabilized by London dispersion. The scheme was created according to Figure 1 in reference 18. Energies are given in kcal mol^{-1} and calculated at the CCSD(T)/CBS(Δha(TQ)Z) level of theory.[16]

This is also true for the C–H···π interaction in the methane-benzene complex **8**.[17] Although electrostatic interactions determine the orientation of the C–H bond in this alkyl-aryl interaction, the major contribution to the attraction comes from the long-range London dispersion interaction. For complexes between benzene and unsaturated hydrocarbons, an increase of the electrostatic interaction energies was determined. However, in all cases London dispersion forces are the dominant factor in the total interaction energy. Further computational studies on graphane layers revealed, that the association energy between these layers is in the same order of magnitude as between graphene layers.[18] The dispersion interactions caused by the polarizable C–H and C–C σ-bonds in graphane as well as those originating mainly from π-π interactions in graphene lead to association energies of about 1.2 kcal mol^{-1} per carbon atom. This illustrates that the attractive influence of large sp^3-hybridized hydrocarbons is not to be neglected.

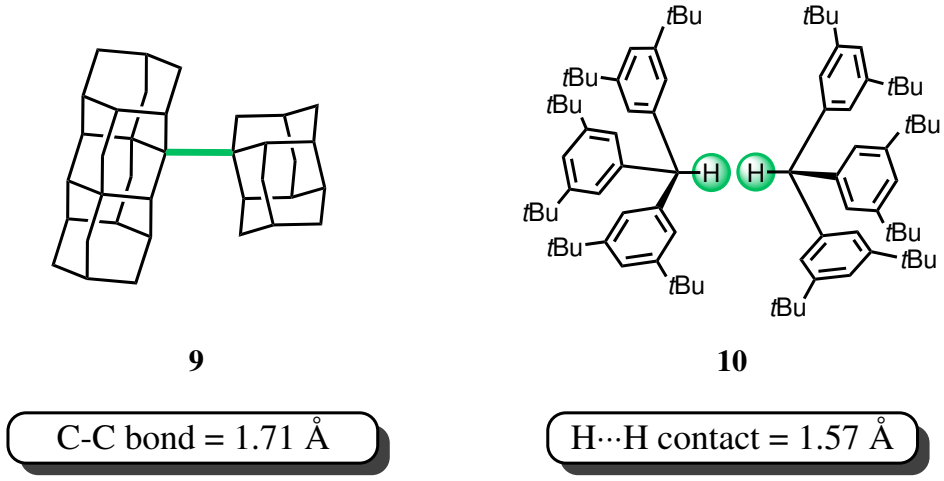

9 **10**

Scheme 2: Examples of extreme bonding situations stabilized by London dispersion. Left: A C-C bond of 1.71 Å in a tetramantane-diamantane dimer **9**.[19] Right: A very short intermolecular H···H contact of 1.57 Å in a triarylmethane dimer **10**.[20]

The arrangement of diamondoids on metal surfaces shows how London dispersion forces can steer the self-assembly of molecular layers.[21] The highly ordered regions of [121]tetramantane on Au(111) or Cu(111) surfaces exhibit a structure, which maximizes the number of close contacts between the hydrocarbons. The interaction energy for the most stable tetramantane dimer could be calculated with 8.8 kcal mol^{-1}, with 7.2 kcal mol^{-1} attributable to London dispersion interactions. This value already exceeds the strength of a hydrogen bond in a water dimer with only 4.4 kcal mol^{-1}.[22] Recent research projects draw the attention to the possibilities of using London dispersion forces to create unusual bonding situations. Despite their enormous size, repulsive forces are overcome in the formation of a tetramantane-diamantane dimer.[19] In this way, London dispersion interactions stabilize an extremely long C-C bond of 1.71 Å. The same concept can be applied in the opposite direction. A triarylmethane dimer substituted with *tert*-butyl groups crystallizes in such a way, that the central C-H bond points directly head-to-head to another triarylmethane structure.[20] This leads to the formation of a very short intermolecular H···H contact of only 1.57 Å. Further DFT computations revealed that crystal packing effects contribute to the compression of the H···H contact. However, the major

contributions stabilizing this exceptional arrangement originate from intermolecular London dispersion interactions between the *tert*-butyl substituents at the edges of the dimer.

The increasing attention regarding possibilities to control molecular properties by London dispersion led to an intensification of efforts to discover unexpected influences of these non-covalent forces in many fields of chemistry.[9] Metal complexes can often be stabilized by additional dispersion interactions emerging from their ligands.[23–25] This can even lead to the formation of adducts with simple alkanes.[26] Also in organocatalysis, the often invoked argument of steric hindrance for selectivity is sometimes not accurate. That dispersion interactions determine the stereochemical outcome of organocatalyzed reactions could be demonstrated for a Mukaiyama-Michael reaction,[27] an asymmetric Diels-Alder reaction[28] and the Corey-Bakshi-Shibata reduction[29] for example. Furthermore, attractive non-covalent interactions also stabilize intermediates for carbene triggered transformations.[30]

3.1.2 Solvent Influence on London Dispersion

Although today a powerful toolbox of computational methods exists to accurately describe London dispersion interactions also for large compounds, the determination of the influence of solvents is not trivial.[31–34] As a consequence, several molecular systems were designed to investigate London dispersion interactions in solution.[35] Some systems work as balances others are based on the interruption of the London forces upon dissociation of polarizable moieties. A few studies raised the question, whether dispersion interactions are still of relevance in solution.[36,37] Their results suggested, that intramolecular dispersion interactions are compensated by competitive solute-solvent interactions or superimposed by much stronger solvophobic effects in polar solvents. This is in so far not surprising, since especially linear alkanes tend to adopt a more compact conformation to reduce their surface exposed to a polar solvent.[38] For a system based on a proton-bound dimer a compensation of the dispersion interactions in solution compared to gas-phase measurements between 60-80% was observed.[39,40] Experimental results for alkyl substituted azobenzenes, however, corroborated the assumption, that dispersion interactions of relevant magnitude are definitely present in apolar alkanes as solvent.[41] Further investigations of London forces between linear alkyl chains demonstrated, that even differences caused by one additional methylene unit in the alkane substituents can be detected.[42] This is not a trivial task, regarding the fact, that interactions between *n*-alkane chains show strong anisotropy additionally to their high conformational flexibility.[43] With azobenzene based molecular probes, differences in stabilizing effects upon elongation of the attached *n*-alkyl substituents could be determined with high accuracy.[44] The stronger increase in *cis*-isomer stabilization from methyl to *n*-butyl substituents derive from strong alkyl-aryl interactions for the shorter chains. Solvophobic effects become relevant for *n*-hexyl or longer chains. The sensitivity of this system goes so far, that even changes of the stability between a series of *n*-alkanes as solvents can be detected.[45] Surprisingly, differences in solvation, when replacing *n*-octane as solvent with its constitutional isomer *iso*-octane, leads to a 20% increase in stabilization for the *cis*-azobenzenes with four ethyl or longer substituents. To avoid distortions in the determination of of the solvent influence on intramolecular dispersion interactions caused by local dipoles from the test systems, a purely hydrocarbon based molecular probe can be

of advantage.[46] Such a 1,4-substituted cycloocta-1,3,5,7-tetraene (1,4-COT) **11** can undergo a bond shift to the 1,6-substituted cycloocta-1,3,5,7-tetraene (1,6-COT) **13**. While in the 1,4-COT isomer **11** and the planar transition state **12** no dispersion forces between the polarizable *tert*-butyl substituents can be established, the 1,6-COT isomer **13** exhibits just the correct geometry for dispersion interactions between the substituents and is always energetically favored. Different solvents shift the isomer ratio only slightly. Especially in polar and chlorinated solvents the folded 1,6-COT **13** is preferred to an even higher degree. The investigation could clearly confirm, that though entropic influences from solvent reorganization partially attenuate London dispersion interactions, they still contribute most to enthalpy and therefore the free energy preference for 1,6-COT **13**.

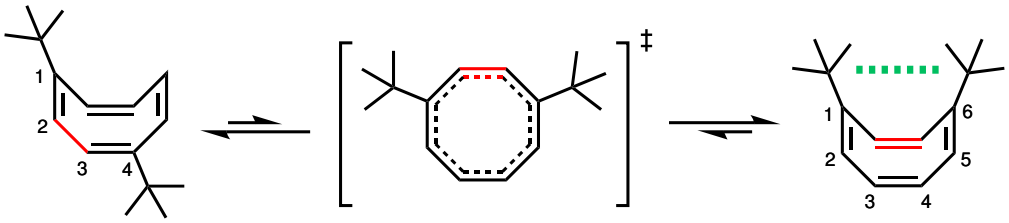

11 1,4-COT no dispersion contact

12 transition state

13 1,6-COT dispersion contact

Scheme 3: Interconversion of a cycloocta-1,3,5,7-tetraene based molecular balance from the 1,4- **11** to the 1,6-substituted bond shift isomer **13** *via* a planar transition state **12**. London dispersion interactions can only be established in the isomer **13**.[46]

These studies demonstrated that the by Fritz London described fundamental dispersion forces can be attenuated by solvent effects but they are not completely canceled out. All this provides an impetus to evaluate the reflexive association of large molecular moieties with steric repulsion more cautiously. Sometimes you just have to look at a picture from a greater distance to recognize the attraction in a larger structure.

3.2 Azobenzene as Photoswitch

Azobenzene was already discovered during the lifetime of Justus von Liebig. Starting from nitrobenzene, Mitscherlich reported its first synthesis in 1834.[47,48] Although Noble presented a convenient and reliable procedure for the preparation of larger amounts only 22 years later, there was still no practical application for this substance until then.[49] Despite its orange-red colour and its good crystallizability, unsubstituted azobenzene was not suitable for fulfilling the demand for synthetic dyes and pigments of the chemical industry of that time.[50] It took until 1861 when Ch. Mène discovered a synthesis of 4-aminoazobenzene, the first azobenzene derivative suitable for dyeing of cotton and silk, which is known as *Aniline Yellow* **14**.[51] With the discovery of the diazotisation reaction in 1858, Peter Griess laid the foundation for the facile synthesis of a large variety of azo compounds.[52,53] During the following years more and more azo dyes were discovered and found their way into industrial production as replacement for expensive natural dyes like carmine, quercitron or campeche logwood.[54] The successful application of azo compounds as organic pigments was then finally initiated 1899 by the development of *Lithol Red R* **15** by Paul Julius, also establishing BASF as a global manufacturer for dyes and pigments.[55,56]

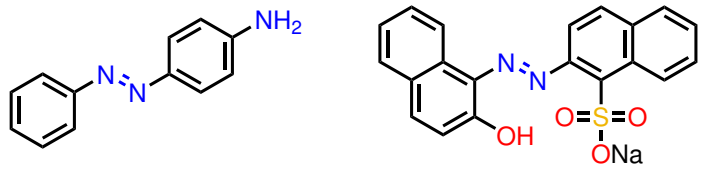

14 *Aniline Yellow* **15** *Lithol Red R*

(a)

(b)

Figure 4: a) The first derivatives of azobenzene used as dyes and pigments.[51,56] b) Orange-red crystals of azobenzene **16**.

A further research area and a new field of application became accessible when Hartley discovered that light irradiation leads to the interconversion of azobenzene between two isomeric structures in 1937.[57] The isomerization from the *trans*- to the thermally less stable *cis*-isomer can only be achieved by light due to the high energetic difference between the two isomers of 11.3 kcal mol^{-1}.[58] The back-isomerization can be initiated by irradiation at a different wavelength or by heating the compound. Compared to other photo-switchable molecules like spiropyran, dithienylethene or dihydroazulene, azobenzene undergoes a large structural change of the geometry upon isomerization. The distance between the carbon atoms in *para*-position for *trans*-azobenzene is 9.1 Å,[59] whereas this value is reduced to 6.2 Å[60] in *cis*-azobenzene (Scheme 4). This movement can be used to perform mechanical work. Incorporated in a polyazopeptide, which was covalently coupled to an AFM tip and a supporting glass slide, it was shown that switching is possible even against an external force up to 500 pN.[61] Azobenzene shows two significant absorption bands in the UV-Vis spectrum. Of these, the π-π*-band at around 320 nm bears the highest and the n-π*-band at around 440 nm the lowest extinction coefficient.[62] While switching the *trans*-azobenzene to the *cis*-isomer, the absorption band at 320 nm is decreasing and the one at 440 nm is increasing with increasing *cis*-isomer content.

This allows convenient monitoring of changes in the relative isomer composition by UV-Vis spectroscopy. The exact photostationary composition depends on the irradiation wavelength enabling the adjustment of the *cis*-isomer content as desired.[63]

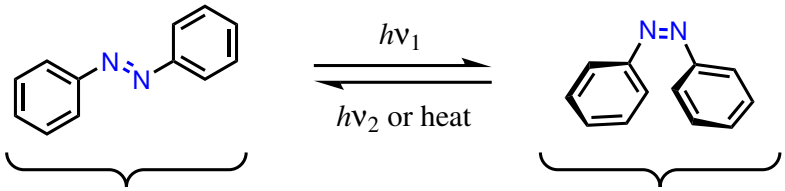

9.1 Å
16
trans-Azobenzene

6.2 Å
17
cis-Azobenzene

Scheme 4: Geometrical changes of the azobenzene structure upon isomerization.

With regard to possible applications, the isomerization process was extensively studied (Scheme 5). Two main pathways, proceeding *via* a rotational or an inversion mechanism, were already discussed at an early stage.[64] For the thermal *cis*- to *trans*-isomerization, some experimental results supported the inversion mechanism.[65–67] Others pointed to a rotational pathway.[68] Computational studies supported to a high degree the inversion mechanism for thermal *cis*- to *trans*-isomerization.[69] The rotational pathway postulates a breakage of the N=N π-bond, which enables rotation around the N–N bond. In this way mainly the dihedral Ph–N=N–Ph angle is altered, leaving the N=N–Ph angles almost unchanged. The inversion mechanism is thought to proceed by an in-plane bending of either one or in the case of concerted inversion both of the N=N–Ph angles meanwhile changing the hybridization of the nitrogen atoms. Small rotation around the N–Ph bonds leads then to the final structures.[70] Furthermore, a combination of both pathways termed as inversion-assisted rotation taking place under harsh conditions was also introduced recently.[71]

It was further observed that the quantum yield for the photoisomerization shows an unusual dependence on the wavelength and for the π-π^* excitation to S_2 was always lower than for the n-π^* photoexcitation to S_1. This is in so far interesting, as it represents a violation of Kasha's rule due to the absence of detectable side reactions. The fluorescence quantum yields for *trans*- and *cis*-azobenzene were determined to be in the range of 10^{-5} and 10^{-6} respectively.[72] One interpretation is that n-π^* excitation triggers isomerization *via* inversion, whereas isomerization proceeds *via* rotation upon π-π^* excitation.[73,74] Other studies propose the reversed order. Here, photoexcitation to S_1 leads to isomerization *via* rotation, whereas excitation to a higher state can give access to an inversion driven isomerization pathway.[70,75,76] The idea of different isomerization pathways accessible through different irradiation wavelengths is supported by photoexcitation experiments with azo compounds with bridged phenyl rings blocking one isomerization pathway.[77,78] As a result, the observed quantum yields for the π-π^* and the n-π^* photoexcitation were identical in these cases, indicating that the same isomerization pathway takes place independent of the irradiation wavelength. Though, even higher excited states might contribute to the observed photoreactivity.[73,79] The role of triplet states is rarely considered for thermal *cis*- to *trans*-isomerization but might provide an additional decay channel.[76] However, comparison of quantum yields for several photoisomerization experiments led to the

assumption that the direct photochemical isomerization takes place in the singlet domain.[80] Nonetheless, the mechanism for photoisomerization is still under debate. Newer computational results further indicate, that – especially for push-pull azobenzenes – replacing an apolar with a polar solvent changes the pathway for thermal isomerization from an inversion to a rotation driven mechanism.[8] This shows how external influences make it difficult to establish a universal isomerization concept.

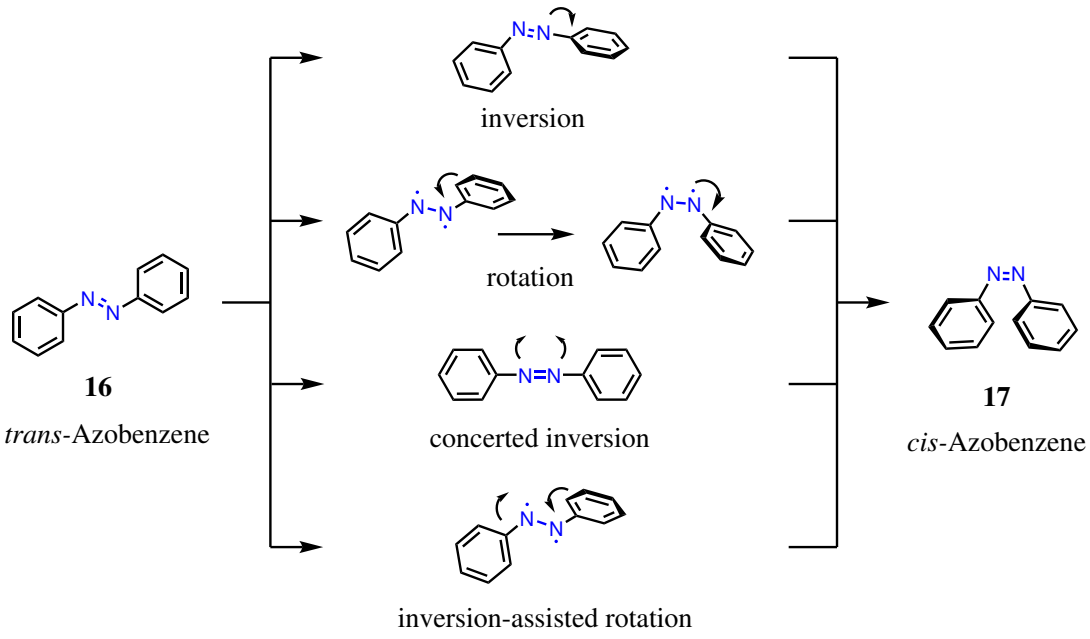

Scheme 5: Proposed mechanisms for the isomerization of azobenzene.[64,69–71]

3.2.1 Catalysts and Sensitizers for Isomerization

Multiple ways have been investigated in order to steer thermal or photoisomerization of azobenzenes by using different catalysts. Early studies showed that the thermal conversion from *cis*- to *trans*-azobenzene can be promoted by a large variety of catalysts.[81] Most of them form bimolecular complexes with the azobenzenes. Among these are numerous Brønsted or Lewis acids like hydrochloric or oxalic acid, zinc chloride, thiourea and thiophenol. Furthermore, tri-coordinate phosphorous compounds,[82] transition-metal complexes[83] or iodine[84,85] can accelerate the *cis-trans* conversion. The early studies of Schulte-Frohlinde indicated that substances with a higher redox potential such as elemental sodium or zinc dust on the one hand and tetra halogenated quinones and lead dioxide on the other hand were also suitable catalysts.[81] Electron-transfer reactions, leading to the reversible formation of azobenzene radicals and therefore lowering the isomerization barrier, were later investigated in more detail. The nature of the radical not seemed to be important since *cis*-azobenzene radical cations as well as anions exhibited a drastically reduced half-life. In case of the *cis*-azobenzene radical anion in a first study its life-time was estimated with 0.1 ms at room temperature in dimethylformamide.[86] An investigation of a variety of electrochemically generated radical anions of *cis*-azobenzenes demonstrated that the rate for the *cis-trans* isomerization of the anion radical species is up to 10^{13} times faster than for the corresponding neutral azobenzenes. Also iridium complexes

as photoelectron transfer agents could be used to create the radical anions. The experimental results clearly indicate that the process is catalytic in electrons. After isomerization of the *cis*-azobenzene anion radical to the *trans*-anion radical, the electron is transferred to a neutral *cis*-azobenzene molecule resulting in chain propagation.[87] The same principal can be applied for azobenzene radical cations. Computations predict 14-17 times faster *cis-trans* isomerization rates for the radical cations. They can be prepared by chemical oxidation with triaryl amine radical cations or Ceric ammonium nitrate. Additionally, in case of electron rich azobenzenes, photoinduced electron transfer with methylene blue provides another possibility. Here, quantum yields >1 support the proposed catalytic oxidation mechanism driving the radical chain reaction. For other azobenzene derivatives methylene blue operated as sensitizer as indicated by the lower quantum yields.[88]

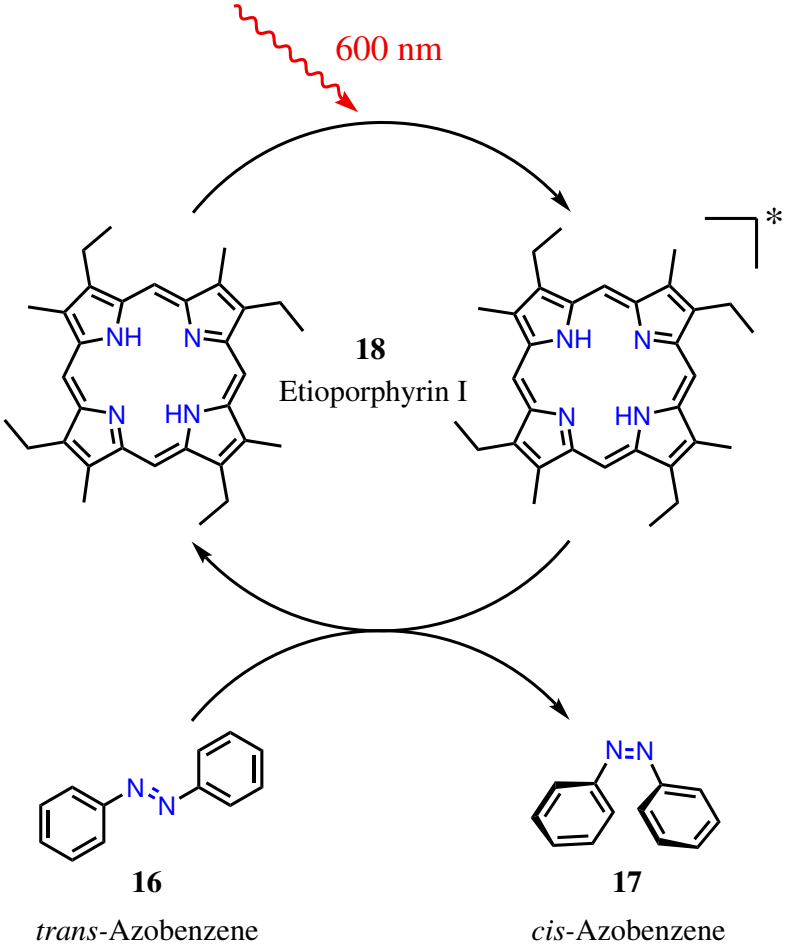

Scheme 6: Operating principle of a photosensitizer for the isomerization of azobenzene.[89]

The use of sensitizers provides an additional handle to steer the photoisomerization of azobenzenes. While triplet energy donors based on carbonyl or aromatic compounds can sensitize the *cis*- to *trans*-isomerization efficiently, conversion from *trans*- to *cis*-azobenzene was only poorly initiated by these sensitizers.[90] Dyes with low-lying triplet states like rose Bengal, eosin Y, fluoroscein or methylene blue were better suited to sensitize the photoisomerization.[91] It is even possible to use sensitizers like etioporphyrin I for the *trans*- to *cis*-photoisomerization (Scheme 6). In this way, the sample can be irradiated at wavelengths >600 nm enabling switching of the azo compounds.[89] However, often a higher quantum yield for the direct compared to

the sensitized *trans*- to *cis*-photoisomerization was observed.[80]

3.2.2 Internal Influences on Isomerization

The list of internal influences on isomerization include electronic and steric effects caused by different substituents attached to the azobenzene or replacement of a phenyl ring with a heteroaryl ring. Therefore, not only the type of substituent is important, but also the position and its interplay with other substituents attached. Alkyl substituents already alter the electronic properties of the azobenzene scaffold compared to the parent molecule. However, an increase of the isomerization rate was observed independent of the substituents attached in the 4,4'-positions relative to the central azo bond (Scheme 7).[92]

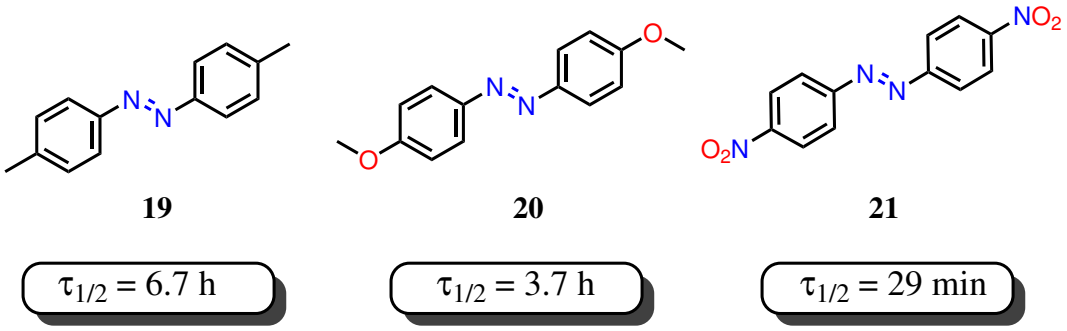

Scheme 7: Half-lives of the corresponding *cis*-isomers of several 4,4'-disubstituted azobenzenes at 35 °C in cyclohexane.[92]

One methyl substituent is sufficient to reduce the half-life of the azobenzene derivative **22** in benzene by around 10 h compared to the unsubstituted azobenzene with a half-life of 32.3 h (Scheme 8).[93] The position of the substituent relative to the central azo bond is crucial to alter the electronic properties and the stability of the *cis*-isomer. This is further demonstrated by the 10% difference in half-lives of **22** and **23**. Interestingly, increasing the size of the alkyl substituent in **23** also leads to increasing half-lives, which can even exceed the half-life of unsubstituted azobenzene.[93] This can be rationalized by stronger alkyl-aryl interactions, stabilizing the *cis*-isomer, as could be supported by a later study.[44] The fastest isomerization can be observed for push-pull azobenzenes as **24**. The substituents in these compounds stabilize the dipolar transition state, which leads to the accelerated thermal isomerization.[94]

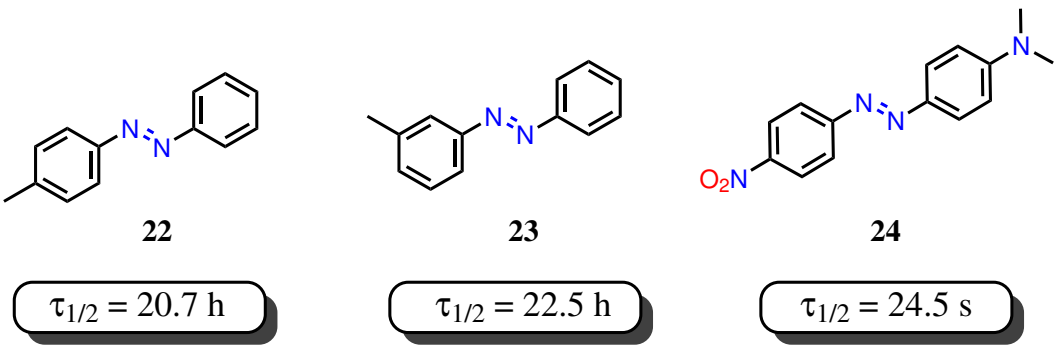

Scheme 8: Half-lives of the corresponding *cis*-isomers of several substituted azobenzenes at 35 °C in benzene[93] and toluene[94] for **24**.

Substituents in *ortho*-position relative to the azo functionality, exhibit a stronger steric influence apart from electronic effects (Scheme 9). This is demonstrated by the non-planar structure of the *trans*-isomer of these compounds. However, the steric influence has to be very high to prevent isomerization upon photoexcitation. Even with four *iso*-propyl substituents in **25** or one methyl and one *tert*-butyl-substituent on each side as in **26**, the corresponding *cis*-isomers could be isolated. Only with *tert*-butyl substituents in all four *ortho*-positions, this was no longer possible and switching of **27** was also not observed by spectroscopic techniques.[95]

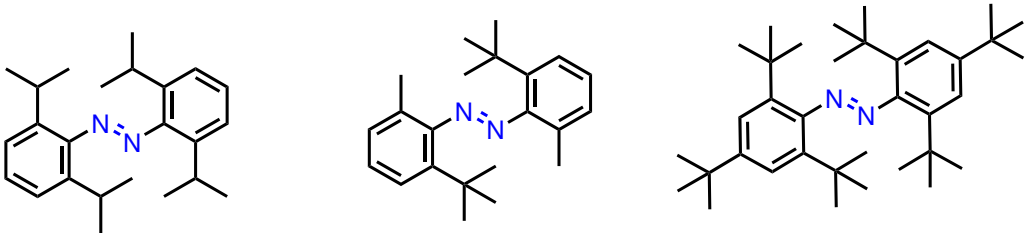

25 **26** **27**

switchable switchable not switchable

Scheme 9: Several azobenzenes with large alkyl substituents in *ortho*-position, of which some can still undergo isomerization.[95]

Halogen atoms as *ortho*-substituents exhibit, apart from a steric influence, a much higher effect on the electronic configuration of the azobenzene compounds. Fluorine atoms in *ortho*-position are capable of reducing the electron density in the N=N bond, which results in a lower energy of the n-orbital. This allows to shift the absorption of the n-π*-band of the *cis*-isomer to lower wavelengths, resulting in a better separation from the n-π*-band of the *trans*-isomer. In this way, an efficient switching between both isomers in the visible region with green or blue light is possible, accompanied by selective addressing of photostationary states with more than 80% of the respective isomer. The installation of additional electron-withdrawing substituents in *para*-position leads to an even higher separation of the n-π*-bands, resulting in improved photochromic properties. Furthermore, thermodynamic parameters are improved by fluorination as demonstrated by a half-life of ca. 700 days at 25 °C for the *cis*-isomer of *ortho*-tetrafluoroazobenzene.[96] By installing four chlorine atoms as *ortho*-substituents, a similar effect can be observed. Due to larger chlorine atoms compared to fluorine, a higher distortion of the *trans*-isomer geometry follows. This is reflected in the N=N–C=C dihedral angle, which for the *trans*-isomer of the tetrafluoroazobenzene **28** is 18.2° [96] and for tetrachloroazobenzene **29** is 48.9° (Scheme 10).[63] This further destabilizes the *trans*-isomer, reducing the energy difference to the *cis*-isomer. For *trans*-decafluoroazobenzene the N=N–C=C dihedral angle is reduced even further to 4.2° as revealed by a crystallographic investigation.[97] This is most likely caused by further reduced electron density along the N=N-bond, leading to less repulsion between the fluorine substituents in *ortho*-position and the lone-pair orbitals of the nitrogen atoms. How important the interplay between steric and electronic influences of substituents in tuning the half-lives of the *cis*-isomer is, can be further demonstrated with compound **30**. Though computations show that the N=N–C=C dihedral angle of 32.7° for its *trans*-isomer is

just between the values for **28** and **29**,[96] with 14 days the half-life of its *cis*-form is the shortest of these three compounds.[98] However, isomerization with visible light is also possible with this configuration. Here, the methoxy substituents lead to a 36 nm red shift of the n-π*-band of the *trans*-isomer. The resulting separation from the n-π*-band of the *cis*-isomer allows photoisomerization with light of around 530 or 450 nm, respectively and between 80 to 85% of the corresponding isomer in the photostationary state.

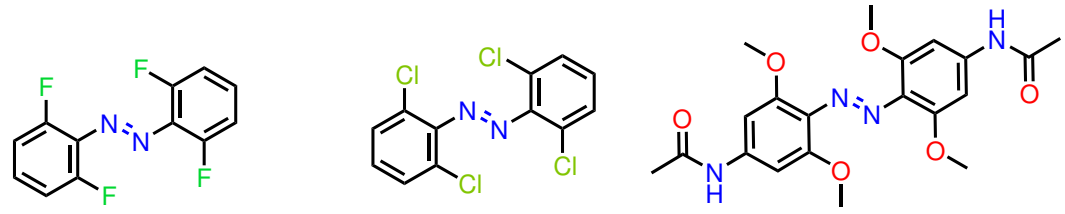

28 **29** **30**

$\tau_{1/2}$ = 700 d $\tau_{1/2}$ = 38 d $\tau_{1/2}$ = 14 d

Scheme 10: Several azobenzenes with electron-withdrawing or electron-donating substituents in *ortho*-position. Half-lives of the corresponding *cis*-isomer are given for 25 °C in DMSO as solvent.[63,96,98]

Alkyl-substituents can not only cause repulsive interactions as *ortho*-substituents for example, but also contribute to attractive interactions, when placed in *meta*-position relative to the central azo bond. Contrary to intuition, larger groups lead to a higher stabilization of the *cis*-isomer of these azobenzene derivatives. This is especially pronounced by the more than 27 times longer half-life of the adamantyl substituted compound **32** compared to all-*meta* methyl azobenzene with a half-life of only 2.2 h in DMSO at 53 °C (Scheme 11).[41] Although cyclohexyl substituents are significantly more flexible than adamantyl groups, they still increase the half-life of the *cis*-state by a factor of 10. Further computational studies showed that the increase of the half-lives caused by these alkyl substituents is mainly based on a thermodynamic stabilization of the *cis*-isomer.[41] The reason for this stabilization are attractive London dispersion interactions emerging in a range of 3-5 Å. If these substituents are placed in the *meta*-positions relative to the azo bond, they are exactly facing each other in this distance. This stabilizing effect is observed even for more flexible *n*-alkyl chains as substituents.[44] Here, an increase of the half-lives in *n*-decane as solvent with increasing chain length up to *n*-butyl as substituents is observed, before the isomerization accelerates again for longer chains. Although the effect here is less pronounced than for the more rigid alkyl substituents, they reach up to a five times longer half-life at the maximum. Further investigation of derivatives with different substitution patterns and a NOESY NMR investigation revealed, that not only alkyl-alkyl interactions are responsible for the stabilization by London dispersion. Especially alkyl-aryl interactions seem to contribute to a major extent to these experimental findings. These interactions can be visualized by NCI analysis. Figure 5 shows the computed structure of the lowest energy conformer of the *cis*-isomer of all-*meta* *n*-butyl azobenzene. The green surfaces in the middle nicely depict how the interlocked alkyl chains interact with each other, but also more in-

tensively with the opposing aryl ring. These results show the significance of the underestimated effect of London dispersion forces on the stabilization of the *cis*-isomer of azobenzenes.

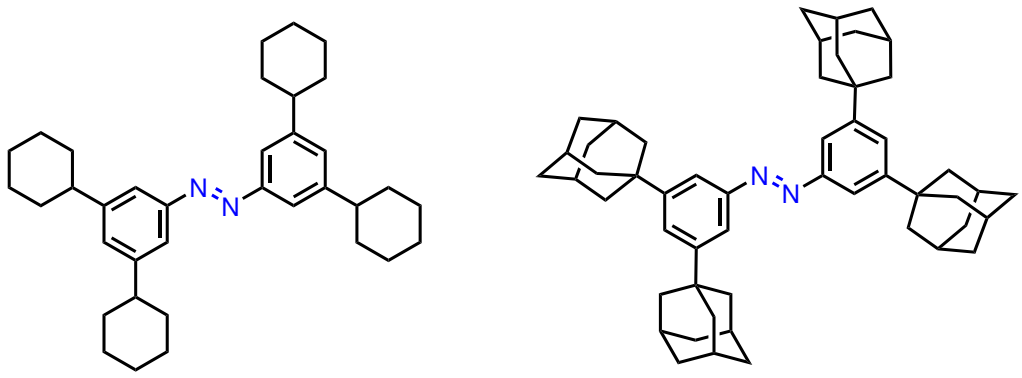

31 **32**

$\tau_{1/2}$ = 23.3 h $\tau_{1/2}$ = 60.5 h

Scheme 11: Azobenzene derivatives with large polarizable alkyl substituents in *meta*-position. Half-lives of the corresponding *cis*-isomer are given for 53 °C in DMSO as solvent.[41]

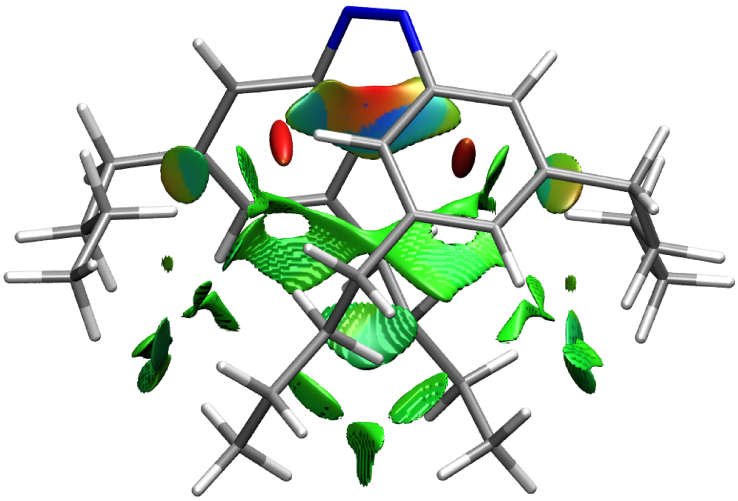

Figure 5: NCI analysis of the optimized structure for the lowest energy conformer of *cis*-isomer of all-*meta n*-butyl azobenzene [PBE0-D3BJ/def2-TZVP]. Green surfaces represent locations of weak attractive interactions.[45] ©2021 with permission of John Wiley & Sons, Inc.

In the case of multiphotochromic systems, the connectivity pattern and type of junction plays an important role. An investigation of bisazobenzenes provides valuable insights into the position dependency of the degree of π-conjugation and the resulting properties (Scheme 12).[99] Theoretical calculations demonstrated that excitonic interactions between the azo units in *ortho*-bisazobenzene **33** are possible, which explains the thermal half-life of the corresponding *cis*-isomer of 1.6 ms. The *meta-cis*-bisazobenzene **34** has a half-life similar to the monomeric azobenzene of more than 2 days. Both azobenzene units show nearly independent switching.

The highest degree of π-conjugation exhibits the *para*-bisazobenzene **35**. This results in high planarity and the lowest quantum yield for *trans*-*cis*-isomerization of all three compounds. The half-life of its *cis*-isomer was determined with 10 h.

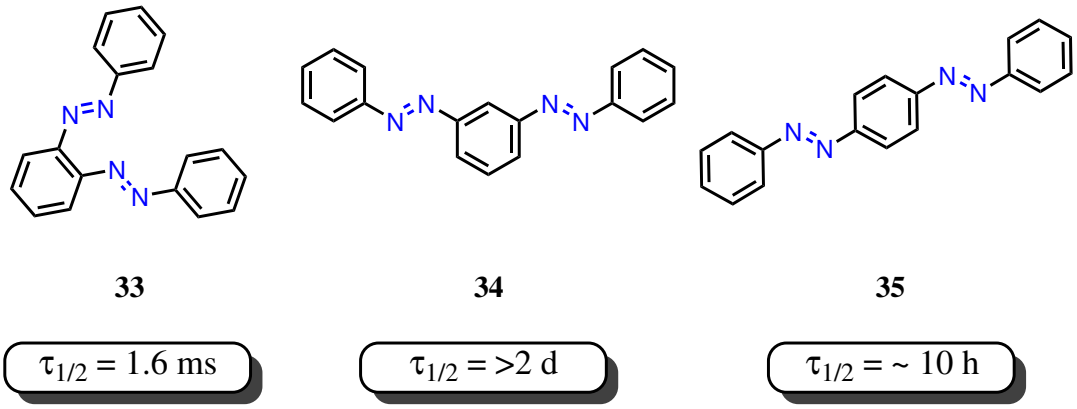

Scheme 12: Half-lives of the corresponding *cis*-isomers of several bisazobenzenes at 22 °C in ethanol.[99]

Cyclization of three azobenzenes to an *ortho*-connected cyclotrisazobenzene leads to a compound for which photochemical isomerization is not possible at all.[100] After photoexcitation, this compound undergoes ultrafast non-radiative relaxation. The high strain efficiently prevents isomerization of the azo units favoring the fast non-radiative relaxation back to the initial all-*trans* form. Structural strain not only prevents isomerization of azobenzenes, but in some cases also inverts the usual stability in azobenzenes. In the cases presented in Scheme 13, the *cis*-isomer is thermodynamically more stable than the *trans*- or mixed isomers. The azobenzenophane **36** can be photochemically switched to the *trans*-*trans* isomer and afterwards undergoes thermal *trans*-*cis* isomerization in two steps.[101]

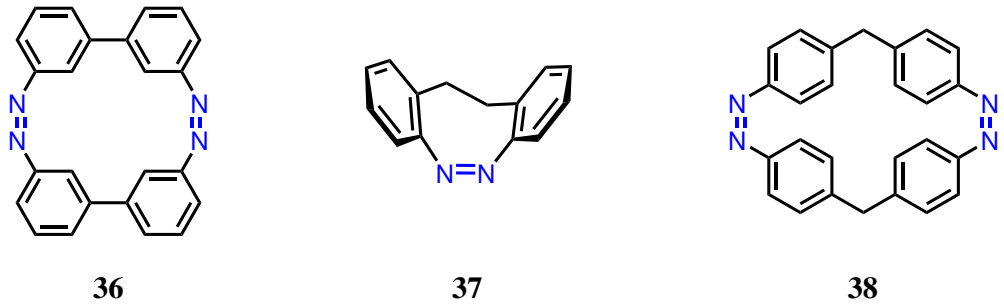

Scheme 13: Three azobenzene derivatives for which the *cis*-isomer is thermodynamically more stable than the *trans*-isomer.[101–103]

The bridged azobenzene derivative **37** investigated by Herges, Renth and Temps showed efficient photoswitching between 100% *cis*- or 90% *trans*-isomer.[102] This is enabled by the good separation of the n-π^* bands of the isomers. Additionally, a distinct photochromic effect in *n*-hexane was observed, changing the colour of the solution from yellow for the *cis*-isomer to a bright red for the *trans*-enriched isomer. The methylene bridges in bisazobenzenophane **38** prevent electronic coupling between both azo groups.[103] However, neither heating nor prolonged irradiation led to a recognizable accumulation of the (*trans*, *cis*)- or (*trans*, *trans*)-isomer. Also

here, the all-*cis*-isomer was identified by computations as the most stable structure. Further investigations of **38** in combination with ultrafast transient absorption experiments showed that it can be switched nevertheless. Internal molecular strain, resulting from the *cis*- to *trans*-isomerization, though leads to a high thermal relaxation rate. The half-life of the (*trans*, *cis*)-isomer was therefore determined with 7.7 ms by flash photolysis experiments.[104]

3.2.3 Heteroaryl-based Azo Photoswitches

The replacement of phenyl rings in azo compounds with heteroaryls offers many new possibilities to tune the properties of azo photoswitches. With changed ring sizes and incorporation of heteroatoms in the aryl rings, even new configurations can be adopted. In principle, all heteroaryls can be used for the design of azo switches. Early computations already showed, that azo compounds including furan, benzofuran or thiophene units instead of one phenyl ring exhibit a significant red-shift of the π-π*-band up to 33 nm compared to unsubstituted azobenzene.[105] From the variety of *N*-heterocycles, azo compounds with pyrrole,[106] pyrazole,[106,107] imidazole,[108] triazoles,[109–111] tetrazole,[112] pyridine,[113] pyrimidine[114,115] or tetrazine[116] have been prepared. Overall, heteroaryl azo compounds with π-π* absorption bands in the range of 278-560 nm were presented.[117] Upon photoisomerization 1,1'-Azobis-1,2,3-triazole even shows a new absorption maximum emerging at around 600 nm, giving the *cis*-isomer a blue colour.[111] The half-lives of the *cis*-isomer of heteroaryl azo switches are in a range of ~1000 days for **39**[106] to 2 µs at 25 °C in DMSO for **40** and for some derivatives even in the nanosecond range (Scheme 14a).[115] Also for the azoheteroarenes, the placement of the point of connection between the azo-bond and the heteroaryl ring has a strong effect on the thermal isomerization rate of the *cis*-isomer. This shortens the half-life from 1000 days for a 1-methyl-pyrazole azo derivative connected at the 4-position to 74 days when connected at the 3-position.[118] Similar observations were made for azoheteroarenes incorporating imidazoles. Five-membered heteroarenes as building blocks for azo photoswitches can give access to new T-shaped *cis*-isomers (**41**) as depicted below in Scheme 14b.[106] These conformers are stabilized by C–H···π interactions. When increasing the steric demand by methylation directly adjacent to the azo bond (**42**) or by using larger six-membered heteroarenes, a twisted conformation is adopted in the *cis*-state. Other computational studies showed, how the attachement of alkyl bridges to phenyl-azoheteroarenes could be used to modify and even reverse their *trans-cis* thermal stability by introducing macrocyclic strain.[119]

N-heterocycles in azo photoswitches offer another advantage apart from the tunable optical and thermodynamic properties as they are promising candidates for photo-dissociable ligands especially when containing imidazole[108] or pyridine[113] moieties. In the photostationary state up to 98% of the *cis*-isomer for the imidazole derivative[108] and 63% for the pyridine derivative[113] can be reached. A pyrimidine ring in an azo compound can increase its biocompatibility and the solubility of these photoswitches in aqueous media.[114] A very fast thermal isomerization in the nanosecond range of the *cis*-isomer could be used to trigger fast photo-induced responses in biological systems. However, considering safe handling, there seems to be a limit to the number of nitrogen atoms incorporated in an azo compound. If heteroaryls with a high number of nitrogen atoms as in the case of amino-4-nitro-1,2,3-triazoles are used to construct

an azo photoswitch, one might end up with a very explosive compound.[120] Interestingly, the *cis*- and *trans*-isomers feature differing sensitivities and detonation behavior.

Sulfur can also be introduced into heteroarenes coupled to azo photoswitches. With thiazole arenes, these azo switches can be easily modified by methylation to obtain cationic species, which reduces the relaxation time for the thermal *cis*- to *trans*-isomerization by up to 3×10^6.[121] Also thiophene moieties as part of azoheteroarenes led to intriguing properties of these photoswitches. Such an azothiophene can exhibit high photoisomerization quantum yields and fatigue resistance.[122] The π-π^* absorption of these compounds is highly red-shifted and they show excellent photoconversion levels with 95 to 99% *cis*-isomer at the photostationary state.[123] Their half-lives for the thermal *cis*- to *trans*-isomerization at 25 °C in acetonitrile are between 9.2 and 0.1 h and therefore in the medium range. However, in the *cis*-state, these molecules also adopt a T-shaped geometry. This structure is stabilized by rare lone-pair–π interactions, which are directly affected by the electronic influence of the substituents. The good charge delocalization alongside fused thiophene units already led to advantegous applications in electronic devices.[124] The attachment of multiple thiophenes to an azophotoswitch can in the same way be used to further red-shift the absorption maximum of these compounds in the visible region.[125]

(a)

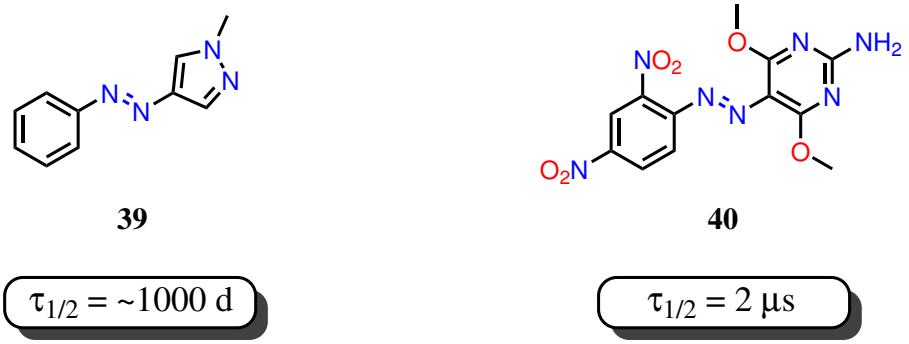

39 **40**

$\tau_{1/2}$ = ~1000 d $\tau_{1/2}$ = 2 µs

(b)

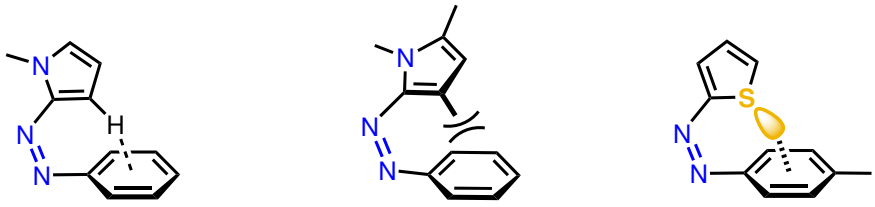

41 **42** **43**

T-shaped *cis*-isomer twisted *cis*-isomer T-shaped *cis*-isomer

Scheme 14: a) Examples of heteroaryl azo switches with a pyrazole[106] or pyrimidine ring.[115] Half-lives of the corresponding *cis*-isomer are given for 25 °C in DMSO as solvent. b) Azo photoswitches with five-membered heteroaryls can adopt new T-shaped geometries in the *cis*-state.[106,122] These conformers are either stabilized by C–H···π or lone-pair–π interactions. Increasing steric strain results in a twisted conformation.

3.2.4 Environmental Influences on Isomerization

The environment plays an important role for the switching of azo compounds. Investigations in the gas phase can therefore be advantageous for analyzing a system in the absence of environmental influences first. In this way, Andersson and coworkers found a significant blue-shift of the π-π* band of *trans*-azobenzene to 301 nm in the gas phase.[126] The activation energy for thermal *cis*-*trans*-isomerization was determined with 28.2 kcal mol^{-1}. A mild alternative for transferring a compound from the solution to the gas phase is the electrospray ionization. By measuring the photoinduced fragmentation of an azobenzene derivative as a function of time its absorption in the gas phase was studied.[127] The investigated ammonium-tagged azobenzene molecule exhibits also a blue shift of the n-π* band to 435 nm in the gas phase compared to 442 nm in methanol. Additionally, the increasing n-π* absorbance of the *cis*-isomer could be depicted by this technique. Cammenga and coworkers conducted several studies to determine the activation energy of the thermal isomerization for *cis*-azobenzene in the melt for which they found a value between 24.5 to 24.7 kcal mol^{-1}.[66,128] In the solid state, investigations are far more complex, since additional to the pure crystalline conformers, *cis*-azobenzene forms two eutectic mixtures with *trans*-azobenzene.[129] At temperatures above the stable eutectic temperature of 41.4°C the activation energy of 25.6 kcal mol^{-1} was lower than for measurements below the eutectic temperature. Here, with continuous formation of *trans*-azobenzene, the isomerization mechanism suddenly changes increasing the activation barrier from 26.3 to 27.7 kcal mol^{-1}. The isomerization in the crystalline state can also be triggered by irradiation with visible light.[130] A single crystal of a perhalogenated *cis*-azobenzene could be transformed into a polycrystalline aggregate of its *trans*-isomer in a photomechanical transformation thus undergoing distinct and thermally irreversible changes of the crystal shape.

External stimuli for the *cis*-*trans*-isomerization apart from heat can derive from electric fields, pressure, surrounding matrices, solvents or surface interactions. In a computational study the influence of oriented external electric fields was further examined, showing that the quantum yield of photoisomerization is likely to be significantly decreased or enhanced through applied electric fields of specific orientations and strengths.[131] In addition, a manipulation of the *cis*-*trans*-isomerization barrier by $\pm$10 kcal mol^{-1} should be possible. Minor pressure variations seem to have no effect on the thermal *cis*-*trans* isomerization. So changes in the isomerization rate in the gas phase by applying different pressures in the range of 13 to 130 kPa were not detected.[126] In the range of 100 kPa to 210,000 kPa different observations for different azo photoswitches in methanol were made.[132] For a bridged azobenzene derivative a slower isomerization rate was detected, whereas for unsubstituted azobenzene as well as for a morpholinocarbonyl substituted one, an acceleration of the isomerization with increasing pressure was determined. This indicates differences in the isomerization mechanism.

The driving force for the isomerization of azobenzene derivatives mostly exceeds retaining effects from solid environments. Even embedded in solid matrices like poly(methyl methacrylate) the isomerization can still take place.[67] In some cases, however, influences from the surrounding environment cannot be independently investigated. Especially when azobenzenes are covalently implemented in solid structures, they often also carry additional substituents. This makes it necessary to determine the photophysical properties for each system individu-

ally. Nevertheless, incorporated in solid environments, azobenzenes can have a large structural effect on the surrounding matrices, rendering these compounds interesting for an application in photoresponsive materials. As part of polymer films, the azo moieties allow precise bending of the polymeric structure with high local resolution upon irradiation with light.[133] The azo switches can be connected to the polymer main chain and the side chains. When properly designed, the absorption of the azo units can be altered in a way, that the azo moieties in the main and in the side chains can be switched independently.[134] Apart from polymers, they were also inserted into metal-organic frameworks (MOFs). They can be introduced by adsorption or by covalently attaching it to the linkers. Adsorbed azobenzene molecules could then change the structure of the host MOF reversibly upon irradiation with light or heating.[135] In this way the nitrogen adsorption properties of the MOF system could be altered. The size of the pore volume in MOFs is essential for their photochromic properties. On the one hand, smaller pores hinder the *cis-trans*-isomerization but allow alteration of carbon dioxide adsorption capacity.[136] Larger pores on the other hand show no photomodulation of carbon dioxide uptake but have better solid-state photochromic properties.

An azobenzene derivative absorbed on an Au(111) surface shows a by a factor of four reduced activation barrier for thermal *cis-trans*-isomerization compared to measurements in cyclohexane.[137] Increasing the distance between the azobenzene moiety and the surface by attaching large bulky substituents can decrease the coupling of the azobenzene and the surface and therefore increase the molecular photomechanical activity.[138] Surface effects can also be caused by nanoparticles.[139] Gold nanoparticles can in this way accelerate the thermal *cis-trans* isomerization of several azobenzene derivatives by a factor of 10 to 10^6. This effect is reduced by competitive adsorption of certain solvent molecules on the nanoparticles' surface.

3.2.5 Solvent Effects on Isomerization

Many studies conducted in the liquid state provide the opportunity to get a comprehensive impression of the different effects of solvents on the azobenzene system. One of this is solvatochromism, which shifts the absorption bands of the photochromic systems in different solvents and can for some compounds easily exceed 75 nm.[140] If substituents on the azobenzene can act as hydrogen bond acceptors, even acidochromism can occur in sufficient acidic environments. It is even possible that solvatochromism affects the π-π^* and the n-π^* bands independently, leading to shifts of varying degree.[141] Another important topic comprises changes in the isomerization behavior of azobenzenes caused by different solvents. The type of substituents attached to the azobenzene scaffold, however, determines whether a change from a non-polar to a polar solvent leads to an acceleration or a deceleration of the thermally induced *cis-trans*-isomerization. Azobenzenes with electron-donating and electron-withdrawing substituents tend to undergo thermal isomerization *via* a rotational mechanism.[142] In case of such a push-pull-system as in 4-(diethylamino)-4'-nitro-azobenzene, solvents with a higher polarity or more acidic protons can better stabilize the dipolar transition state. This results in an acceleration of the isomerization rate and the half-life of the *cis*-isomer is drastically reduced. This effect can increase the isomerization rate by a factor of 3800 when replacing benzene with DMSO for example.[92] If the thermal isomerization proceeds *via* an inversion mechanism,

a different tendency can be seen as calorimetrically determined enthalpies of solvent transfer for unsubstituted azobenzene showed.[65] Changing the solvent from cyclohexane to cyclohexanone, a stabilization of the *cis*-isomer was observed. Additionally, the transition state was destabilized as determined from kinetic measurements. Both effects contribute to a significant increase of the thermal half-life of the *cis*-isomer. The same effect was observed for *meta* alkyl-substituted azobenzenes, indicating that these compounds isomerize *via* the same mechanism.[41,44] The general solvent effect on the *cis-trans*-isomerization of azobenzene can be regarded as a sum of several parameters.[143] One term describes the direct solute-solvent interactions. These can be caused by van der Waals forces or hydrogen bonding for example. The second parameter includes the energy required to form cavities inside the liquid for the solute molecule. This parameter is mainly dependent on the surface tension of the solvent. A third parameter covers the reduction of intramolecular interactions caused by competitive interactions of the molecular groups of the solute with the solvent molecules. This term can often be neglected for small to medium-sized molecules. In some cases, the surface tension is the main contributor to the solvent effect. This can lead to changes in the *cis-trans*-isomerization rate of up to 20%, when replacing *n*-octane with *iso*-octane as solvent for example.[45]

All this shows that even after more than 180 years, research on azo compounds still reveals unknown features of this fascinating molecule. Therefore it is very likely that we will still find many versatile applications for azo switches in the future, which we just cannot imagine yet.

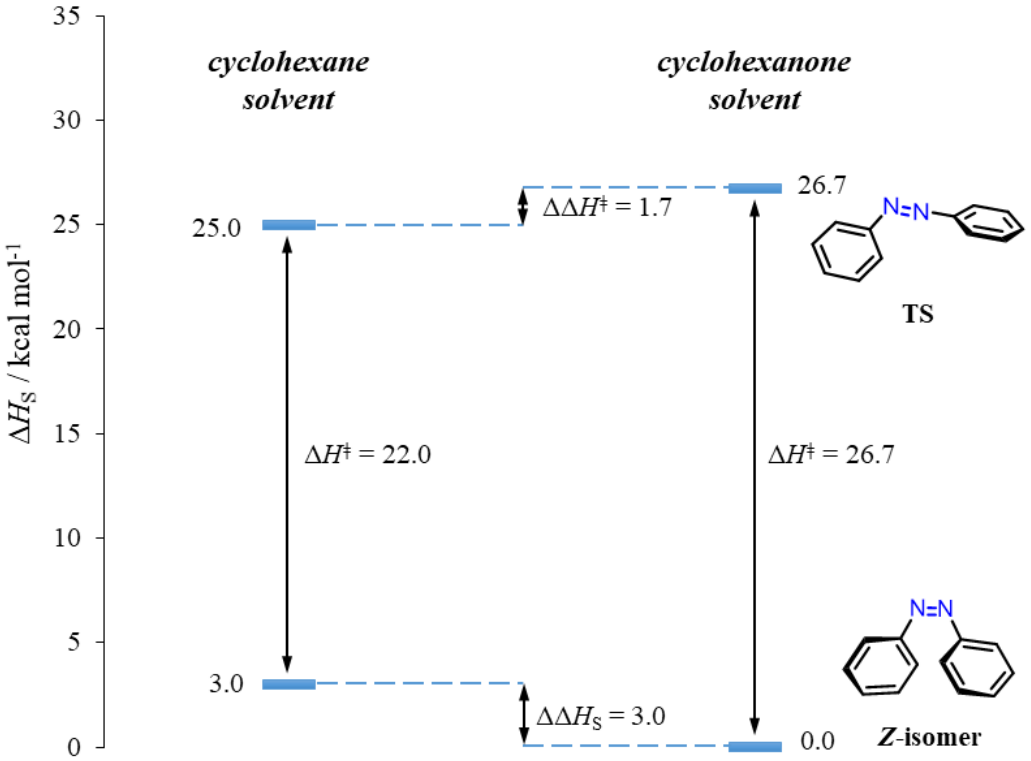

Scheme 15: Effects of solvent transfer from cyclohexane to cyclohexanone on the thermal isomerization of *cis*-azobenzene.[65]

3.3 References

[1] Polosukhina, A.; Litt, J.; Tochitsky, I.; Nemargut, J.; Sychev, Y.; de Kouchkovsky, I.; Huang, T.; Borges, K.; Trauner, D.; van Gelder, R. N.; Kramer, R. H. *Neuron* **2012**, *75*, 271–282.

[2] Borowiak, M.; Nahaboo, W.; Reynders, M.; Nekolla, K.; Jalinot, P.; Hasserodt, J.; Rehberg, M.; Delattre, M.; Zahler, S.; Vollmar, A.; Trauner, D.; Thorn-Seshold, O. *Cell* **2015**, *162*, 403–411.

[3] Schierling, B.; Noël, A.-J.; Wende, W.; Le Hien, T.; Volkov, E.; Kubareva, E.; Oretskaya, T.; Kokkinidis, M.; Römpp, A.; Spengler, B.; Pingoud, A. *Proc. Natl. Acad. Sci. U S A* **2010**, *107*, 1361–1366.

[4] Niedek, D.; Erb, F. R.; Topp, C.; Seitz, A.; Wende, R. C.; Eckhardt, A. K.; Kind, J.; Herold, D.; Thiele, C. M.; Schreiner, P. R. *J. Org. Chem.* **2020**, *85*, 1835–1846.

[5] Blanco, V.; Leigh, D. A.; Marcos, V. *Chem. Soc. Rev.* **2015**, *44*, 5341–5370.

[6] Ferri, V.; Elbing, M.; Pace, G.; Dickey, M. D.; Zharnikov, M.; Samorì, P.; Mayor, M.; Rampi, M. A. *Angew. Chem. Int. Ed.* **2008**, *47*, 3407–3409.

[7] Danowski, W.; van Leeuwen, T.; Browne, W. R.; Feringa, B. L. *Nanoscale Adv.* **2021**, *3*, 24–40.

[8] Dokić, J.; Gothe, M.; Wirth, J.; Peters, M. V.; Schwarz, J.; Hecht, S.; Saalfrank, P. *J. Phys. Chem. A* **2009**, *113*, 6763–6773.

[9] Wagner, J. P.; Schreiner, P. R. *Angew. Chem. Int. Ed.* **2015**, *54*, 12274–12296.

[10] London, F. *Z. Physik* **1930**, *63*, 245–279.

[11] Mayerhöfer, T. G.; Popp, J. *ChemPhysChem* **2020**, *21*, 1218–1223.

[12] Truhlar, D. G. *J. Chem. Educ.* **2019**, *96*, 1671–1675.

[13] Stefan Grimme, In *The chemical bond*; Frenking, G., Shaik, S. S., Eds.; Wiley-VCH Verlag: Weinheim, 2014; pp 477–499.

[14] Ogilvie, J. F.; Wang, F. Y. *J. Mol. Struct.* **1992**, *273*, 277–290.

[15] Tsuzuki, S.; Honda, K.; Uchimaru, T.; Mikami, M. *J. Chem. Phys.* **2006**, *124*, 114304.

[16] Sherrill, C. D.; Takatani, T.; Hohenstein, E. G. *J. Phys. Chem. A* **2009**, *113*, 10146–10159.

[17] Tsuzuki, S.; Honda, K.; Uchimaru, T.; Mikami, M.; Tanabe, K. *J. Am. Chem. Soc.* **2000**, *122*, 3746–3753.

[18] Fokin, A. A.; Gerbig, D.; Schreiner, P. R. *J. Am. Chem. Soc.* **2011**, *133*, 20036–20039.

[19] Fokin, A. A.; Chernish, L. V.; Gunchenko, P. A.; Tikhonchuk, E. Y.; Hausmann, H.; Serafin, M.; Dahl, J. E. P.; Carlson, R. M. K.; Schreiner, P. R. *J. Am. Chem. Soc.* **2012**, *134*, 13641–13650.

[20] Rösel, S.; Quanz, H.; Logemann, C.; Becker, J.; Mossou, E.; Cañadillas-Delgado, L.; Caldeweyher, E.; Grimme, S.; Schreiner, P. R. *J. Am. Chem. Soc.* **2017**, *139*, 7428–7431.

[21] Ebeling, D.; Šekutor, M.; Stiefermann, M.; Tschakert, J.; Dahl, J. E. P.; Carlson, R. M. K.; Schirmeisen, A.; Schreiner, P. R. *ACS nano* **2017**, *11*, 9459–9466.

[22] Fileti, E. E.; Chaudhuri, P.; Canuto, S. *Chem. Phys. Lett.* **2004**, *400*, 494–499.

[23] Ahlquist, M. S. G.; Norrby, P.-O. *Angew. Chem. Int. Ed.* **2011**, *50*, 11794–11797.

[24] Liptrot, D. J.; Guo, J.-D.; Nagase, S.; Power, P. P. *Angew. Chem. Int. Ed.* **2016**, *55*,

14766–14769.

[25] Lyngvi, E.; Sanhueza, I. A.; Schoenebeck, F. *Organometallics* **2015**, *34*, 805–812.

[26] Jung, J.; Löffler, S. T.; Langmann, J.; Heinemann, F. W.; Bill, E.; Bistoni, G.; Scherer, W.; Atanasov, M.; Meyer, K.; Neese, F. *J. Am. Chem. Soc.* **2020**, *142*, 1864–1870.

[27] Kemppainen, E. K.; Sahoo, G.; Piisola, A.; Hamza, A.; Kótai, B.; Pápai, I.; Pihko, P. M. *Chem. Eur. .J.* **2014**, *20*, 5983–5993.

[28] Yepes, D.; Neese, F.; List, B.; Bistoni, G. *J. Am. Chem. Soc.* **2020**, *142*, 3613–3625.

[29] Eschmann, C.; Song, L.; Schreiner, P. R. *Angew. Chem. Int. Ed.* **2021**, *60*, 4823–4832.

[30] Yatham, V. R.; Harnying, W.; Kootz, D.; Neudörfl, J.-M.; Schlörer, N. E.; Berkessel, A. *J. Am. Chem. Soc.* **2016**, *138*, 2670–2677.

[31] Riplinger, C.; Pinski, P.; Becker, U.; Valeev, E. F.; Neese, F. *J. Chem. Phys.* **2016**, *144*, 24109.

[32] Grimme, S.; Hansen, A.; Brandenburg, J. G.; Bannwarth, C. *Chem. Rev.* **2016**, *116*, 5105–5154.

[33] Caldeweyher, E.; Bannwarth, C.; Grimme, S. *J. Chem. Phys.* **2017**, *147*, 34112.

[34] Caldeweyher, E.; Ehlert, S.; Hansen, A.; Neugebauer, H.; Spicher, S.; Bannwarth, C.; Grimme, S. *J. Chem. Phys.* **2019**, *150*, 154122.

[35] Strauss, M. A.; Wegner, H. A. *Eur. J. Org. Chem.* **2019**, *2019*, 295–302.

[36] Yang, L.; Adam, C.; Nichol, G. S.; Cockroft, S. L. *Nat. Chem.* **2013**, *5*, 1006–1010.

[37] Hwang, J.; Dial, B. E.; Li, P.; Kozik, M. E.; Smith, M. D.; Shimizu, K. D. *Chem. Sci.* **2015**, *6*, 4358–4364.

[38] Ray, C.; Brown, J. R.; Kirkpatrick, A.; Akhremitchev, B. B. *J. Am. Chem. Soc.* **2008**, *130*, 10008–10018.

[39] Pollice, R.; Bot, M.; Kobylianskii, I. J.; Shenderovich, I.; Chen, P. *J. Am. Chem. Soc.* **2017**, *139*, 13126–13140.

[40] Pollice, R.; Fleckenstein, F.; Shenderovich, I.; Chen, P. *Angew. Chem. Int. Ed.* **2019**, *58*, 14281–14288.

[41] Schweighauser, L.; Strauss, M. A.; Bellotto, S.; Wegner, H. A. *Angew. Chem. Int. Ed.* **2015**, *54*, 13436–13439.

[42] van Craen, D.; Rath, W. H.; Huth, M.; Kemp, L.; Räuber, C.; Wollschläger, J. M.; Schalley, C. A.; Valkonen, A.; Rissanen, K.; Albrecht, M. *J. Am. Chem. Soc.* **2017**, *139*, 16959–16966.

[43] Tsuzuki, S.; Honda, K.; Uchimaru, T.; Mikami, M. *J. Phys. Chem. A* **2004**, *108*, 10311–10316.

[44] Strauss, M. A.; Wegner, H. A. *Angew. Chem. Int. Ed.* **2019**, *58*, 18552–18556.

[45] Strauss, M. A.; Wegner, H. A. *Angew. Chem. Int. Ed.* **2021**, *60*, 779–786.

[46] Schümann, J. M.; Wagner, J. P.; Eckhardt, A. K.; Quanz, H.; Schreiner, P. R. *J. Am. Chem. Soc.* **2021**, *143*, 41–45.

[47] Mitscherlich, E. *Ann. Pharm.* **1834**, *12*, 305–311.

[48] Mitscherlich, E. *Ann. Pharm.* **1834**, *12*, 311–314.

[49] Noble, A. *Ann. Pharm.* **1856**, *98*, 253–256.

[50] Wagner, J. R., Ed. *Jahres-Bericht über die Fortschritte und Leistungen der chemischen Technologie und technischen Chemie*; Verlag von Otto Wigand: Leipzig, 1861; Vol. 7.
[51] Mène, C. *C. r. hebd. séances Acad. sci.* **1861**, 311.
[52] Grieß, P. *Ann. Pharm.* **1858**, *106*, 123–125.
[53] Grieß, P. *Ann. Pharm.* **1860**, *113*, 334–338.
[54] Abelshauser, W., Ed. *Die BASF: Eine Unternehmensgeschichte*, 2nd ed.; Beck: München, 2003.
[55] Blangey, L. *Angew. Chem.* **1927**, *40*, 1127–1130.
[56] Heckl, L. *Fette, Seifen, Anstrichm.* **1958**, *60*, 560–564.
[57] Hartley, G. S. *Nature* **1937**, *140*, 281.
[58] Cammenga, H. K.; Emel'yanenko, V. N.; Verevkin, S. P. *Ind. Eng. Chem. Res.* **2009**, *48*, 10120–10128.
[59] Harada, J.; Ogawa, K.; Tomoda, S. *Acta Crystallogr. B Struct. Sci.* **1997**, *53*, 662–672.
[60] Mostad, A.; Rømming, C.; Hammarström, S.; Lousberg, R. J. J. C.,; Weiss, U. *Acta Chem. Scand.* **1971**, *25*, 3561–3568.
[61] Hugel, T.; Holland, N. B.; Cattani, A.; Moroder, L.; Seitz, M.; Gaub, H. E. *Science* **2002**, *296*, 1103–1106.
[62] Fraleoni-Morgera, A.; Giorgini, L.; Zanirato, P. *Dyes Pigment.* **2008**, *76*, 394–399.
[63] Lameijer, L. N.; Budzak, S.; Simeth, N. A.; Hansen, M. J.; Feringa, B. L.; Jacquemin, D.; Szymanski, W. *Angew. Chem. Int. Ed.* **2020**, *59*, 21663–21670.
[64] Zimmerman, G.; Chow, L.-Y.; Paik, U.-J. *J. Am. Chem. Soc.* **1958**, *80*, 3528–3531.
[65] Haberfield, P.; Block, P. M.; Lux, M. S. *J. Am. Chem. Soc.* **1975**, *97*, 5804–5806.
[66] Wolf, E.; Cammenga, H. K. *Z. Phys. Chem.* **1977**, *107*, 21–38.
[67] Kölle, U.; Schätzle, H.; Rau, H. *Photochem. Photobiol.* **1980**, *32*, 305–311.
[68] Nerbonne, J. M.; Weiss, R. G. *J. Am. Chem. Soc.* **1978**, *100*, 5953–5954.
[69] Crecca, C. R.; Roitberg, A. E. *J. Phys. Chem. A* **2006**, *110*, 8188–8203.
[70] Wei-Guang Diau, E. *J. Phys. Chem. A* **2004**, *108*, 950–956.
[71] Shao, J.; Lei, Y.; Wen, Z.; Dou, Y.; Wang, Z. *J. Chem. Phys.* **2008**, *129*, 164111.
[72] Stuart, C. M.; Frontiera, R. R.; Mathies, R. A. *J. Phys. Chem. A* **2007**, *111*, 12072–12080.
[73] Schultz, T.; Quenneville, J.; Levine, B.; Toniolo, A.; Martínez, T. J.; Lochbrunner, S.; Schmitt, M.; Shaffer, J. P.; Zgierski, M. Z.; Stolow, A. *J. Am. Chem. Soc.* **2003**, *125*, 8098–8099.
[74] Cattaneo, P.; Persico, M. *Phys. Chem. Chem. Phys.* **1999**, *1*, 4739–4743.
[75] Chang, C.-W.; Lu, Y.-C.; Wang, T.-T.; Diau, E. W.-G. *J. Am. Chem. Soc.* **2004**, *126*, 10109–10118.
[76] Cembran, A.; Bernardi, F.; Garavelli, M.; Gagliardi, L.; Orlandi, G. *J. Am. Chem. Soc.* **2004**, *126*, 3234–3243.
[77] Rau, H.; Lüddecke, E. *J. Am. Chem. Soc.* **1982**, *104*, 1616–1620.
[78] Rau, H. *J. Photochem.* **1984**, *26*, 221–225.
[79] Conti, I.; Garavelli, M.; Orlandi, G. *J. Am. Chem. Soc.* **2008**, *130*, 5216–5230.
[80] Bortolus, P.; Monti, S. *J. Phys. Chem.* **1979**, *83*, 648–652.

[81] Schulte-Frohlinde, D. *Ann. Pharm.* **1958**, *612*, 131–138.
[82] Hall, C. D.; Beer, P. D. *J. Chem. Soc., Perkin Trans. 2* **1991**, 1947.
[83] Nakamura, A.; Doi, K.; Tatsumi, K.; Otsuka, S. *J. Mol. Catal.* **1976**, *1*, 417–429.
[84] Yamashita, S. *Bull. Chem. Soc. Jpn.* **1961**, *34*, 842–845.
[85] Arnaud, R.; Lemaire, J. *Can. J. Chem.* **1974**, *52*, 1868–1871.
[86] Laviron, E.; Mugnier, Y. *J. Electroanal. Chem. Interf. Electrochem.* **1978**, *93*, 69–73.
[87] Goulet-Hanssens, A.; Utecht, M.; Mutruc, D.; Titov, E.; Schwarz, J.; Grubert, L.; Bléger, D.; Saalfrank, P.; Hecht, S. *J. Am. Chem. Soc.* **2017**, *139*, 335–341.
[88] Goulet-Hanssens, A.; Rietze, C.; Titov, E.; Abdullahu, L.; Grubert, L.; Saalfrank, P.; Hecht, S. *Chem* **2018**, *4*, 1740–1755.
[89] Whitten, D. G.; Wildes, P. D.; Pacifici, J. G.; Irick, G. *J. Am. Chem. Soc.* **1971**, *93*, 2004–2008.
[90] Ronayette, J.; Arnaud, R.; Lebourgeois, P.; Lemaire, J. *Can. J. Chem.* **1974**, *52*, 1848–1857.
[91] Ronayette, J.; Arnaud, R.; Lemaire, J. *Can. J. Chem.* **1974**, *52*, 1858–1867.
[92] Nishimura, N.; Sueyoshi, T.; Yamanaka, H.; Imai, E.; Yamamoto, S.; Hasegawa, S. *Bull. Chem. Soc. Jpn.* **1976**, *49*, 1381–1387.
[93] Talaty, E. R.; Fargo, J. C. *Chem. Commun.* **1967**, *0*, 65–66.
[94] Nishimura, N.; Kosako, S.; Sueishi, Y. *Bull. Chem. Soc. Jpn.* **1984**, *57*, 1617–1625.
[95] Bunce, N. J.; Ferguson, G.; Forber, C. L.; Stachnyk, G. J. *J. Org. Chem.* **1987**, *52*, 394–398.
[96] Bléger, D.; Schwarz, J.; Brouwer, A. M.; Hecht, S. *J. Am. Chem. Soc.* **2012**, *134*, 20597–20600.
[97] Chinnakali, K.; Fun, H. K.; Shawkataly, O. B.; Teoh, S. G. *Acta Crystallogr. C Cryst. Struct. Commun.* **1993**, *49*, 615–616.
[98] Beharry, A. A.; Sadovski, O.; Woolley, G. A. *J. Am. Chem. Soc.* **2011**, *133*, 19684–19687.
[99] Slavov, C.; Yang, C.; Schweighauser, L.; Boumrifak, C.; Dreuw, A.; Wegner, H. A.; Wachtveitl, J. *Phys. Chem. Chem. Phys.* **2016**, *18*, 14795–14804.
[100] Slavov, C.; Yang, C.; Schweighauser, L.; Wegner, H. A.; Dreuw, A.; Wachtveitl, J. *ChemPhysChem* **2017**, *18*, 2137–2141.
[101] Norikane, Y.; Katoh, R.; Tamaoki, N. *Chem. Commun. (Camb)* **2008**, 1898–1900.
[102] Siewertsen, R.; Neumann, H.; Buchheim-Stehn, B.; Herges, R.; Näther, C.; Renth, F.; Temps, F. *J. Am. Chem. Soc.* **2009**, *131*, 15594–15595.
[103] Heindl, A.; Schweighauser, L.; Logemann, C.; Wegner, H. *Synthesis* **2017**, *49*, 2632–2639.
[104] Slavov, C.; Yang, C.; Heindl, A. H.; Stauch, T.; Wegner, H. A.; Dreuw, A.; Wachtveitl, J. *J. Phys. Chem. Lett.* **2018**, *9*, 4776–4781.
[105] Åstrand, P.-O.; Ramanujam, P. S.; Hvilsted, S.; Bak, K. L.; Sauer, S. P. A. *J. Am. Chem. Soc.* **2000**, *122*, 3482–3487.
[106] Weston, C. E.; Richardson, R. D.; Haycock, P. R.; White, A. J. P.; Fuchter, M. J. *J. Am. Chem. Soc.* **2014**, *136*, 11878–11881.

[107] Wang, Y.-T.; Liu, X.-Y.; Cui, G.; Fang, W.-H.; Thiel, W. *Angew. Chem. Int. Ed.* **2016**, *55*, 14009–14013.

[108] Wendler, T.; Schütt, C.; Näther, C.; Herges, R. *J. Org. Chem.* **2012**, *77*, 3284–3287.

[109] Qi, C.; Li, S.-H.; Li, Y.-C.; Wang, Y.; Chen, X.-K.; Pang, S.-P. *J. Mater. Chem.* **2011**, *21*, 3221.

[110] Yu, Q.; Staples, R. J.; Shreeve, J. M. *Z. Anorg. Allg. Chem.* **2020**, *646*, 1799–1804.

[111] Li, Y.-C.; Qi, C.; Li, S.-H.; Zhang, H.-J.; Sun, C.-H.; Yu, Y.-Z.; Pang, S.-P. *J. Am. Chem. Soc.* **2010**, *132*, 12172–12173.

[112] Hammerl, A.; Hiskey, M. A.; Holl, G.; Klapötke, T. M.; Polborn, K.; Stierstorfer, J.; Weigand, J. J. *Chem. Mater.* **2005**, *17*, 3784–3793.

[113] Thies, S.; Sell, H.; Bornholdt, C.; Schütt, C.; Köhler, F.; Tuczek, F.; Herges, R. *Chem. Eur. .J.* **2012**, *18*, 16358–16368.

[114] Garcia-Amorós, J.; Díaz-Lobo, M.; Nonell, S.; Velasco, D. *Angew. Chem. Int. Ed.* **2012**, *51*, 12820–12823.

[115] Čechová, L.; Filo, J.; Dračínský, M.; Slavov, C.; Sun, D.; Janeba, Z.; Slanina, T.; Wachtveitl, J.; Procházková, E.; Cigáň, M. *Angew. Chem. Int. Ed.* **2020**, *59*, 15590–15594.

[116] Kerth, J.; Löbbecke, S. *Propellants Explos. Pyrotech.* **2002**, *27*, 111.

[117] Crespi, S.; Simeth, N. A.; König, B. *Nat. rev. chem.* **2019**, *3*, 133–146.

[118] Calbo, J.; Weston, C. E.; White, A. J. P.; Rzepa, H. S.; Contreras-García, J.; Fuchter, M. J. *J. Am. Chem. Soc.* **2017**, *139*, 1261–1274.

[119] Vela, S.; Scheidegger, A.; Fabregat, R.; Corminboeuf, C. *Chem. Eur. .J.* **2021**, *27*, 419–426.

[120] Wozniak, D. R.; Salfer, B.; Zeller, M.; Byrd, E. F. C.; Piercey, D. G. *Org. Lett.* **2020**, *22*, 9114–9117.

[121] Garcia-Amorós, J.; Bučinskas, A.; Reig, M.; Nonell, S.; Velasco, D. *J. Mater. Chem. C* **2014**, *2*, 474–480.

[122] Slavov, C.; Yang, C.; Heindl, A. H.; Wegner, H. A.; Dreuw, A.; Wachtveitl, J. *Angew. Chem. Int. Ed.* **2020**, *59*, 380–387.

[123] Heindl, A. H.; Wegner, H. A. *Chem. Eur. .J.* **2020**, *26*, 13730–13737.

[124] Nielsen, C. B.; McCulloch, I. *Prog. Polym. Sci.* **2013**, *38*, 2053–2069.

[125] Garcia-Amorós, J.; R Castro, M. C.; Coelho, P.; M Raposo, M. M.; Velasco, D. *Chem. Commun. (Camb)* **2013**, *49*, 11427–11429.

[126] Andersson, J.-Å.; Petterson, R.; Tegnér, L. *J. Photochem.* **1982**, *20*, 17–32.

[127] Gruber, E.; Strauss, M. A.; Wegner, H. A.; Andersen, L. H. *J. Chem. Phys.* **2019**, *150*, 084303.

[128] Eckardt, N.; Flammersheim, H. J.; Cammenga, H. K. *J. Therm. Anal. Calorim.* **1998**, *52*, 177–185.

[129] Cammenga, H.; Sarge, S.; Eligehausen, S. *Solid State Ion.* **1989**, *32-33*, 625–629.

[130] Bushuyev, O. S.; Tomberg, A.; Friščić, T.; Barrett, C. J. *J. Am. Chem. Soc.* **2013**, *135*, 12556–12559.

[131] Kempfer-Robertson, E. M.; Thompson, L. M. *J. Phys. Chem. A* **2020**, *124*, 3520–3529.

[132] Asano, T.; Okada, T.; Shinkai, S.; Shigematsu, K.; Kusano, Y.; Manabe, O. *J. Am. Chem. Soc.* **1981**, *103*, 5161–5165.

[133] Yu, Y.; Nakano, M.; Ikeda, T. *Nature* **2003**, *425*, 145.

[134] Wang, K.; Yin, L.; Miu, T.; Liu, M.; Zhao, Y.; Chen, Y.; Zhou, N.; Zhang, W.; Zhu, X. *Mater. Chem. Front.* **2018**, *2*, 1112–1118.

[135] Yanai, N.; Uemura, T.; Inoue, M.; Matsuda, R.; Fukushima, T.; Tsujimoto, M.; Isoda, S.; Kitagawa, S. *J. Am. Chem. Soc.* **2012**, *134*, 4501–4504.

[136] Castellanos, S.; Goulet-Hanssens, A.; Zhao, F.; Dikhtiarenko, A.; Pustovarenko, A.; Hecht, S.; Gascon, J.; Kapteijn, F.; Bléger, D. *Chem. Eur. .J.* **2016**, *22*, 746–752.

[137] Hagen, S.; Kate, P.; Peters, M. V.; Hecht, S.; Wolf, M.; Tegeder, P. *Appl. Phys. A* **2008**, *93*, 253–260.

[138] Comstock, M. J.; Levy, N.; Kirakosian, A.; Cho, J.; Lauterwasser, F.; Harvey, J. H.; Strubbe, D. A.; Fréchet, J. M. J.; Trauner, D.; Louie, S. G.; Crommie, M. F. *Phys. Rev. Lett.* **2007**, *99*, 038301.

[139] Simoncelli, S.; Aramendía, P. F. *Catal. Sci. Technol.* **2015**, *5*, 2110–2116.

[140] Hofmann, K.; Brumm, S.; Mende, C.; Nagel, K.; Seifert, A.; Roth, I.; Schaarschmidt, D.; Lang, H.; Spange, S. *New J. Chem.* **2012**, *36*, 1655.

[141] Strauss, M. A.; Wegner, H. A. *ChemPhotoChem* **2019**, *3*, 392–395.

[142] Schanze, K. S.; Mattox, T. F.; Whitten, D. G. *J. Org. Chem.* **1983**, *48*, 2808–2813.

[143] Halicioğlu, T.; Sinanoğlu, O. *Ann. N. Y. Acad. Sci.* **1969**, *158*, 308–317.

4 Contributions to Literature

In the following section, the main research articles published with first authorship are enlisted. The most recent article is presented first.

4.1 London Dispersion in Alkane Solvents

Reference:

M. A. Strauss, H. A. Wegner, *Angew. Chem. Int. Ed.*, **2021**, *60*, 779-786.
German Edition:
M. A. Strauss, H. A. Wegner, *Angew. Chem.*, **2021**, *133*, 792-799.
DOI: 10.1002/anie.202012094 and 10.1002/ange.202012094

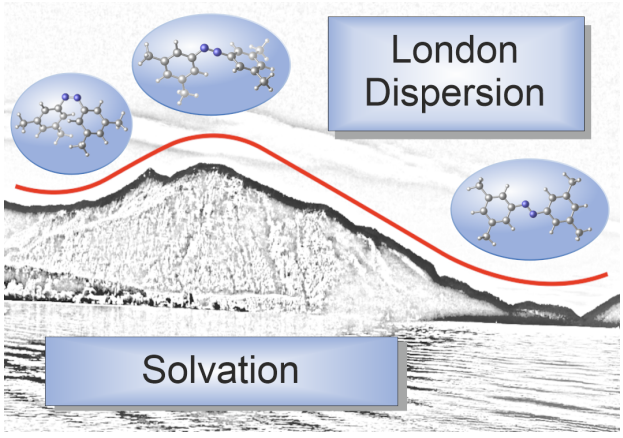

"The importance of London dispersion interactions in solution is an ongoing debate. Although the significance of dispersion for structure and stability is widely accepted, the degree of its attenuation in solution is still not properly understood. Quantitative evaluations are derived mostly from computations. Experimental data provide guidelines to include London dispersion in solution phase design. Herein, dispersive interactions were examined with an azobenzene probe. Alkyl substituents in *meta* positions of the azobenzene core were systematically varied and the effect on the half-lives for the thermally induced *Z* to *E* isomerization in several alkane solvents was determined. The results show that intramolecular dispersion is only marginally influenced. In solvents with low surface tension, reduced destabilizing solvent-solvent interactions increase the half-life up to 20%. Specific individual interactions between alkyl chains on the azobenzene and those of the solvent lead to additional fluctuations of the half-lives. These presumably result from structural changes of the conformer ensemble."

GDCh Research Articles Angewandte International Edition Chemie

Check for updates

Solvent Effects

How to cite: *Angew. Chem. Int. Ed.* **2021**, *60*, 779–786
International Edition: doi.org/10.1002/anie.202012094
German Edition: doi.org/10.1002/ange.202012094

London Dispersion in Alkane Solvents

*Marcel A. Strauss and Hermann A. Wegner**

Abstract: *The importance of London dispersion interactions in solution is an ongoing debate. Although the significance of dispersion for structure and stability is widely accepted, the degree of its attenuation in solution is still not properly understood. Quantitative evaluations are derived mostly from computations. Experimental data provide guidelines to include London dispersion in solution phase design. Herein, dispersive interactions were examined with an azobenzene probe. Alkyl substituents in meta positions of the azobenzene core were systematically varied and the effect on the half-lives for the thermally induced Z to E isomerization in several alkane solvents was determined. The results show that intramolecular dispersion is only marginally influenced. In solvents with low surface tension, reduced destabilizing solvent-solvent interactions increase the half-life up to 20 %. Specific individual interactions between alkyl chains on the azobenzene and those of the solvent lead to additional fluctuations of the half-lives. These presumably result from structural changes of the conformer ensemble.*

Introduction

Solvation dictates all chemical transformations in the liquid phase ranging from processes in the living world to production of bulk chemicals on a multi ton scale. Nevertheless, the specific solvent-solute interactions and their importance on controlling chemical reactions is often underestimated. They can exhibit discrete or bulk effects on molecules and atoms leading to an alteration also of macroscopic properties. In biology, the solvent environment is crucial for the accurate folding and function of proteins.[1] In this way, the catalytic activity and stability can be enhanced tremendously.[2] But the solvent plays a far greater role than just containing the reactants for a chemical transformation. It can influence the selectivity of a chemical reaction by favouring a certain transition state.[3] By the proper selection of the solvent, it is even possible to reverse the enantioselectivity of a reaction.[4]

While in most cases the bulk properties of a solvent can be reliably described, direct interactions of solvent molecules with the solute often require sophisticated and expensive computational approaches. Although hydrogen bonding or formation of Lewis pairs are already well predictable by calculations, the weaker van der Waals interactions are often neglected in more complex systems. Accurate computation of non-covalent interactions and entropies in solution stays a demanding task. Especially, implicit solvent models often show a mediocre correlation with experiments and even explicit methods are in general only slightly better.[5] This emphasizes the need for experimental data to predict also subtle solvent effects and to provide a basis for further improvements of computational models, particularly with regard to a growing interest in evaluating subtle preferences of non-covalent interactions for their consideration in the design of catalysts.[6] The proper selection of an ideal solvent can therefore be decisive in controlling certain molecular processes. Understanding solute-solvent interactions is crucial and promises potential for improvements in industrial solvent purification[7] and recovery.[8]

In this context, London dispersion slowly starts to gain attention as a means to control selectivities in synthesis. Large and polarizable moieties have proven their applicability as dispersion energy donors[9] stabilizing extreme bonding situations.[10] They play an important role in the aggregation of aromatic species,[11] the formation of organometallic complexes[12] and in catalysis.[13] However, there are only a few rare investigations of London dispersion interactions between linear alkyl chains.[14,15] Flexible *n*-alkyl chains can adopt a high number of conformers at elevated temperatures. Due to this fact, an estimation of their dispersion donor abilities is a highly complex task. In recent years numerous computational methods were developed giving access to a comprehensive toolbox for efficiently evaluating the dispersive interactions in molecular systems in the gas phase with high accuracy.[16] The strength of London dispersion in solution, however, is subject of current research interests. Some studies address this by investigating the effect of the solvent on conformer or dimer stability.[17–19]

These approaches were conducted in order to determine the contribution of London dispersion to the stability of their systems. The observed attenuation of the dispersion caused by competitive interactions with the solvent molecules, however, was not complete. For some systems a compensation between 60–80 % was observed.[17,20] We introduced the azobenzene switch as powerful tool to investigate London dispersion

[*] M. A. Strauss, Prof. Dr. H. A. Wegner
Institute of Organic Chemistry, Justus Liebig University Giessen
Heinrich-Buff-Ring 17, 35392 Giessen (Germany)
and
Center for Materials Research (LaMa), Justus Liebig University Giessen
Heinrich-Buff-Ring 16, 35392 Giessen (Germany)
E-mail: hermann.a.wegner@org.chemie.uni-giessen.de
Supporting information and the ORCID identification number(s) for the author(s) of this article can be found under: https://doi.org/10.1002/anie.202012094.

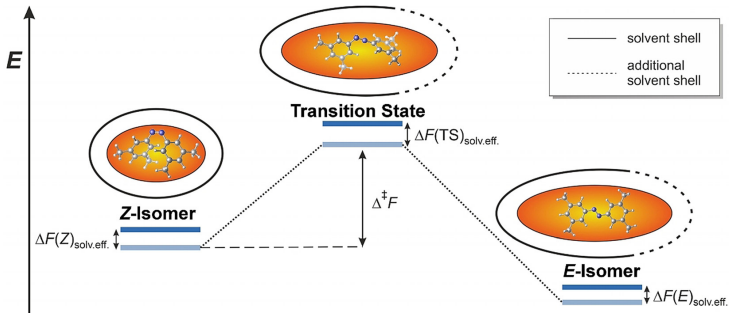

Figure 1. Relative energies for the *Z* to *E* isomerization of an azobenzene. Upon isomerization, the solvent accessible surface of the azobenzene increases, leading to increased solute solvent interactions.

forces. Herein, it was chosen to address these open questions.[19,21–23]

Methods

The present study aims at systematically exploring the interplay of alkane solvents with different alkyl substituents in *meta*-position of the azobenzene by monitoring the thermal $Z \rightarrow E$ isomerization. During this process, the alkyl-alkyl and alkyl-aryl interactions contribute to the stabilization of the *Z*-isomer, which is influenced by the solvent environment. Azobenzene can isomerize between two different states—the *E*-state and the about 11.7 kcal mol^{-1} considerably less stable *Z*-state (Figure 1).[24] Isomerization between the *E*- and *Z*-state can be initiated upon irradiation with light. The transition from the *Z*- to the *E*-isomer can also be achieved by heating. The distance between the carbon atoms in *para*-position of the rings changes from 9.1 Å[25] in the *E*-isomer to about 6.2 Å[26] in the *Z*-isomer. In this way, substituents on the azobenzene can be brought in close proximity. Especially substituents in *meta*-positions come into a distance, where London dispersion donors stabilize the *Z*-isomer of the azobenzene as we could show previously.[21] The general effect of the solvent on the isomerization barrier for azobenzenes can be described as a sum of three parameters [Eq. (1)].[27] First, the contribution from interactions between the solute and the solvent ΔF_{inter}. These forces mainly include dispersive and electrostatic interactions. Second, the ΔF_{cav} term describes the energy necessary to form cavities in the solvent for the solute. Here, the interdependence of solvent surface tension γ and the volume of the solute dominate this parameter. Third, ΔF_{red} stands for the reduction of intramolecular interactions between molecular groups of the solute, which are altered by the solvent environment.

$$\Delta F_{solv.\,eff} = \Delta F_{inter} + \Delta F_{cav} + \Delta F_{red} \quad (1)$$

The contribution of the solvent on the intramolecular interactions in the *Z*-isomer is considered to be constant. This assumption is supported by the fact, that the overall tendency of the half-lives observed in dependence of the substituents stays very similar in all investigated solvents (see Figure 2 and Supporting Information Figure S2–S8). Due to their apolar character, solvophobic contributions to the thermal $Z \rightarrow E$ isomerization barrier should play a minor role here.

The utilized azo compounds **1**–**13** (Scheme 1) for this investigation were prepared by a highly flexible synthesis strategy allowing the introduction of a variety of alkyl substituents (for synthetic details, see Supporting Information).[23] To study the varying interactions in several alkane solvents all azobenzenes investigated were switched from the *E*- to the *Z*-state by irradiation at 302 nm. The thermally induced back isomerization at 40 °C was measured by UV/Vis spectroscopy. In this way, the influence of subtle changes of the solvent environment on the stability of the *Z*-isomer in dependence of the alkyl substituent of the azobenzenes was investigated. In this study, a series of linear alkanes starting from *n*-heptane to *n*-dodecane, as well as 2,2,4-trimethylpentane (*iso*-octane) and cyclooctane were used as solvents. Concentration as well as temperature were kept constant for these measurements.

Results and Discussion

As previously reported[23] substitution of the parent azobenzene **12** with methyl substituents leads first to a decrease of the *Z*-isomer half-life, which results from a change in the electronic properties of the azobenzene motif. Further elongation of the alkyl substituents increases the half-life due to increasing attractive London dispersive interactions with increasing chain length. In the row of all-*meta* *n*-alkylated azobenzenes **1**–**8**, the highest half-life is observed for derivative **4** with *n*-butyl groups. With longer alkyl chains, the unfavourable entropic contributions lead again to slight decrease of the *Z*-isomer stability in **5**–**8**. However, the arrangement of the alkyl groups has a large effect for both the solvent and the substituents on the azobenzene. Replacing the *n*-butyl substituents in **4** with *tert*-butyl groups in azobenzene

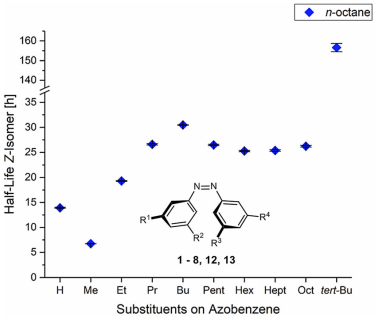

Figure 2. Influence of the substituents on the half-lives for the *Z*-isomers of azobenzenes **1**–**8**, **12** and **13** at 40 °C in *n*-octane. The overall tendency of the half-lives in dependence of the substituents is in most cases minorly affected by the solvent (see also Supporting Information Figure S2–S8).

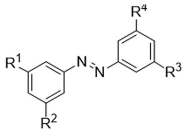

1: $R^{1\text{-}4}$ = methyl
2: $R^{1\text{-}4}$ = ethyl
3: $R^{1\text{-}4}$ = *n*-propyl
4: $R^{1\text{-}4}$ = *n*-butyl
5: $R^{1\text{-}4}$ = *n*-pentyl
6: $R^{1\text{-}4}$ = *n*-hexyl
7: $R^{1\text{-}4}$ = *n*-heptyl
8: $R^{1\text{-}4}$ = *n*-octyl
9: $R^{1,2}$ = methyl; $R^{3,4}$ = H
10: $R^{1,2}$ = *n*-heptyl; $R^{3,4}$ = H
11: $R^{1,3}$ = n-heptyl; $R^{2,4}$ = H
12: $R^{1\text{-}4}$ = H
13: $R^{1\text{-}4}$ = *tert*-butyl

Scheme 1. Overview of the investigated azobenzene derivatives with different substitution patterns and sizes.

13 leads to a tremendous increase in the half-life of the *Z*-isomer by a factor >4. The reason for this is that all alkyl groups in **13** are now in an optimal distance for establishing attractive alkyl-alkyl and alkyl-aryl interactions caused by London dispersion. In **4**, the linear alkyl chains bear more conformational flexibility and due to the higher distance from the azobenzene core exhibit weaker attractive interactions in the *Z*-isomer.

A surprisingly large increase of the half-lives for all compounds was determined, when the solvent was changed from *n*-octane to *iso*-octane. The increase varies between $\approx 5\,\%$ for small azobenzenes to around 20 % for those with larger alkyl substituents (Figure 3. By applying the Arrhenius law, the difference in the activation barrier for the isomerization of **4** for example can be calculated as 0.1 kcal mol^{-1}. This change just derives from replacing the linear alkane *n*-octane with the more spherical formed *iso*-octane. The opposite effect is observed, when cyclooctane instead of *n*-octane is used. Here, the half-life of the *Z*-isomer is reduced

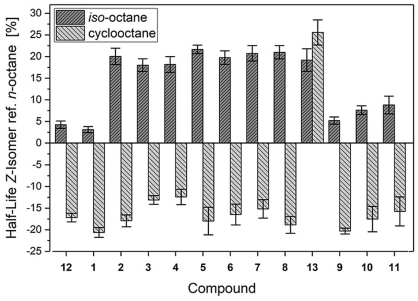

Figure 3. Relative changes of the *Z*-isomer half-lives for the azobenzenes **1**–**13** with different substituents at 40 °C relative to *n*-octane. The highest deviations were observed for *iso*-octane and cyclooctane showing increases of the half-lives up to 20 %.

between 12 and 21 % compared to *n*-octane for all compounds in this study except for azobenzene **13** with the *tert*-butyl groups. To evaluate the origin of these solvent effects, the details of the alteration of half-lives were looked at for the whole series of solvents. The main reason for these observations can be correlated to a change in the solute-solvent interaction term ΔF_{inter} or by changes in ΔF_{cav}.

At first, the influence on the solute-solvent interactions were examined regarding a change of electrostatic or van der Waals contributions. Especially the *Z*-isomer is affected by changes in the electrostatic environment due to the larger dipole. For unsubstituted azobenzene, an increase of the relative permittivity ε_r of the solvent environment normally leads to an increase in the half-life of the *Z*-isomer. This was demonstrated by the work of Winkler and co-workers, who determined the half-lives of azobenzene (**12**) for solvents with a relative permittivity ε_r between 1.92 and 80.10.[28] Most measurements were performed in solvents with a relative permittivity higher than 7. Their results can be explained by a thermodynamic stabilization of the *Z*-isomer in a solvent with a substantially higher polarity. This is supported by the findings of Haberfield and co-workers,[29] who calorimetrically investigated the enthalpies for the $Z \rightarrow E$ isomerization of *Z*-azobenzene in cyclohexane and cyclohexanone. Furthermore, an energetic increase of the transition state due to less favoured solute-solvent interactions was detected.

When the half-lives in different alkanes as solvents are determined, however, a negative linear dependence on the solvent permittivity is observed for azobenzenes with small alkyl groups (Figure 4 a). In contrast to the investigation of Winkler, a decrease of the half-lives with increasing permittivity ε_r was detected. It can be assumed, that for the investigated permittivity range, destabilization of the *Z*-isomer occurs rather than stabilization. The dipole moment of *Z*-azobenzene can be calculated with 3.2 D.[30] This value is close to the one of acetone with 2.9 D.[31] Studies show, that the mixing enthalpy of acetone with *n*-alkanes increases with increasing chain length of the *n*-alkanes, indicating less favourable interactions between solute and solvent.[32] This would also be the case for the *Z*-azobenzene, leading to

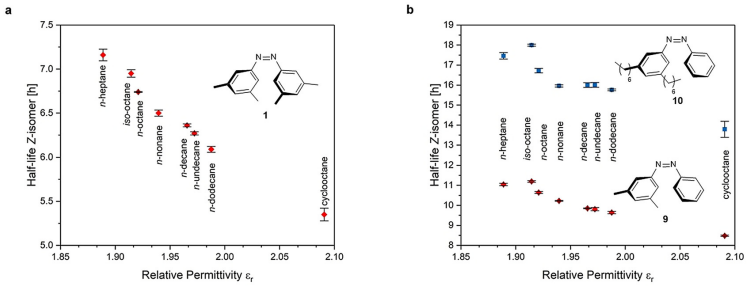

Figure 4. The half-lives of *Z*-isomer of azobenzene **1** (**a**) and **9** and **10** (**b**) in different alkanes as solvent in dependency of the relative solvent permittivity[31] at 40 °C. **a** Azobenzene **1** still shows a linear dependency on the relative permittivity. **b** Half-lives for **9** and **10** show already a higher deviation from linearity for *iso*-octane as solvent.

a lowering of the $Z \rightarrow E$ isomerization barrier by increasing the energy of the *Z*-isomer and therefore a shorter half-life.

Modification of the degree of substitution of the azobenzene provides further insights: For compounds **9** and **10** the overall relative permittivity dependency of the half-lives seems to stay the dominant factor, although the course of the half-lives is less steep (Figure 4b). This is most likely caused by the changed electron distribution of the azobenzene core, since two alkyl substituents were replaced with hydrogen. However, a deviation from linearity for the measurements in *iso*-octane is emerging here, which seems to be even higher for the derivative with the longer alkyl chains **10**. For longer alkyl groups, also the linear correlation shows significantly less coherence, indicating a growing influence of other types of interactions.

Since the actual volume or solvent accessible surface of the azobenzenes changes upon isomerization, it is very likely that for larger substituents a greater effect is observed. This will then contribute mainly to the ΔF_{cav} term, describing the compensation of solvent-solvent interactions, which have to be overcome to accommodate the solute. The dominant parameter here to describe the changes in the solvent shell is the surface tension. When the half-lives of the azobenzenes **9** and **10** are plotted against the surface tension γ (Figure 5a) a linear correlation is again obtained for these solvents with similar γ values. It can be argued, that in solvents with less surface tension, that is, *iso*-octane, the dipolar *Z*-isomer of the azobenzenes is less destabilized in these apolar solvents, leading to the higher half-lives. Cyclooctane, however, exhibits very strong internal solvent-solvent interactions, which can be derived from the rather high melting point of 14.6 °C.[31] These forces have to be overcome upon solvation of the azobenzene, resulting in less favouring solute-solvent interactions. In contrast, *iso*-octane might provide a less favourable interaction surface to interact with the linear alkyl substituents due to its more spherical shape. This would lead to a less solvated transition state compared to linear alkanes as solvents resulting in longer half-lives.

For all-*meta* alkylated azobenzenes with longer alkyl chains, a higher fluctuation of the half-lives is observed, though the overall trend of decreasing half-lives with increasing surface tension remains. The additional methylene units in longer chains bear more degrees of rotational freedom. At such elevated temperatures, already an ensemble of conformers is adopted for these flexible alkyl chains of the substituents but also of the solvents. For *n*-octane, already ten conformers are less than 0.6 kcal mol^{-1} higher in energy than the all-*trans* conformer.[33] It is not unlikely that discrete solvent-solute interdependency of the alkyl chains with the solvent lead to a kind of match-mismatch interaction. This special type of interaction contributes to the ΔF_{inter} term. The importance of the right geometrical match for such weak London dispersion interactions was just recently demonstrated by Chen and co-worker, who showed that disadvantageous interaction geometries can exceed the contribution of higher polarizability upon formation of perfluoroalkane-alkane dimers.[15]

The results of azobenzene **4** with *n*-butyl chains are not only special for exhibiting the longest half-lives of all *n*-alkyl substituted azobenzenes (Figure 5b). They further show significant breaks in the tendency of decreasing half-lives for the row of linear alkane solvents. However, their conformational freedom still seems to be limited enough, so that attractive London dispersive interactions in the *Z*-isomer are not overcompensated by entropic contributions in any solvent. The trend of fluctuating half-lives for the row of linear alkane solvents is continued for other all-*meta* *n*-alkylated azobenzenes like **7** with *n*-heptyl chains in Figure 5c. The energetic differences in the isomerization barrier for the $Z \rightarrow E$ isomerization of these derivatives in *n*-alkanes are so small that even subtle changes of entropic contributions have a detectable impact. This includes changes in the conformer distribution.

Rigidity can have an advantageous effect for the interactions of two molecular entities. For linear alkyl chains the entropic contributions to the free energy of interaction upon approaching is much higher compared to rigid alkyl structures. They exhibit weaker enthalpic attraction but a much less entropic penalty for association due to their conformational rigidity.[34] Therefore, rigid *tert*-butyl groups as sub-

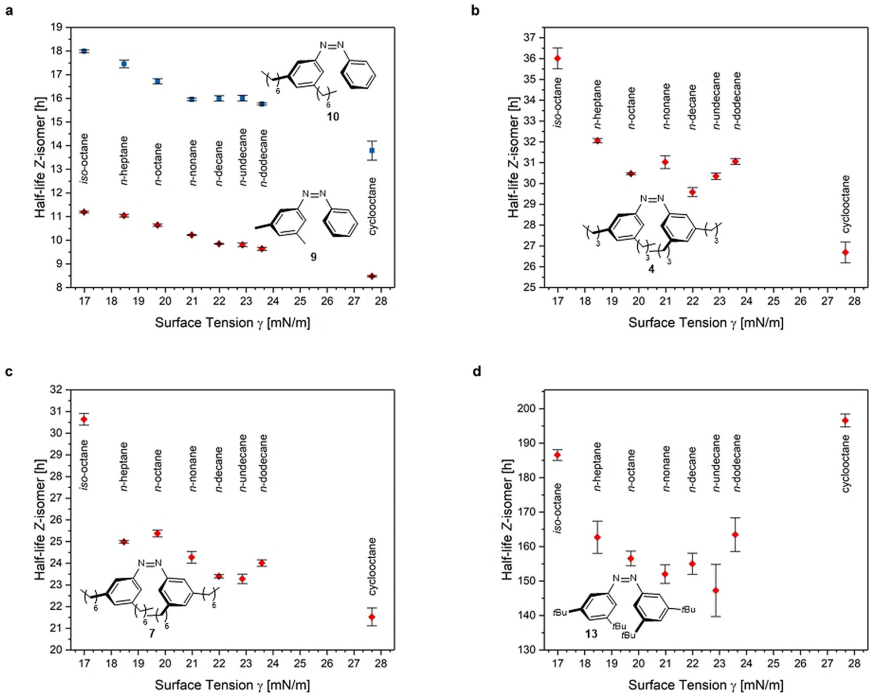

Figure 5. The half-lives of *Z*-isomer of azobenzene **9** and **10** (**a**), **4** (**b**), **7** (**c**) and **13** (**d**) in different alkanes as solvent in dependency of the surface tension[41] at 40 °C. **a** In contrast to Figure 3 b the half-lives for **9** and **10** show a better linear correlation with the surface tension of the solvents. This observation goes along with an increasing importance of the ΔF_{cav} term for these derivatives. **b** Elongation of the alkyl chains leads to higher fluctuations from linearity for *n*-alkanes as solvent. **c** These data differ also with the chain length of the substituents on the azobenzene. These fluctuations can be contributed to the ΔF_{inter} term. **d** This solute-solvent interaction is also the reasonable cause for the large increase of *Z*-isomer stability of **13** in cyclooctane.

stituents were introduced with the incentive to evaluate the influence of spatial extent on the solvent effect (Figure 5 d). Azobenzene **13** is the only derivative in this study, for which the half-life of the *Z*-isomer in cyclooctane is higher than in *n*-octane and even in *iso*-octane. Since the *tert*-butyl substituents are isoelectronic compared to *n*-butyl, this stability change is most likely based on a structural effect. The predominant conformer of cyclooctane is the boat-chair,[35] which exhibits a very flat interaction surface. The better capability of cyclooctane for interaction with more globular structures is reflected that is, by the lower mixing enthalpy of the more spherical 2,3-dimethylbutane compared to *n*-hexane[36] and for other spherical solutes.[37] This should in our case then result in an increased interaction of the *tert*-butyl groups with the cyclooctane solvent compared to the linear alkanes, leading to a better solvation of the *Z*-isomer and, therefore, an increased half-life.

Computational Conformer Analysis

With the introduction of new sophisticated computational tools, it was possible to evaluate the influence of the conformational and rotational flexibility of the alkyl chains on the stabilisation within the *Z*-isomer. The *Conformer-Rotamer Ensemble Sampling Tool* (CREST) by Grimme was used to perform such a conformational analysis.[38] The structures of the *E*-state, the transition state and the *Z*-state of azobenzene **1** were first optimized on a PBE0[39] level of theory and used as template for other derivatives. Afterwards, the core structure of the azobenzene was constrained allowing only rotation of the alkyl substituents. In this way, hundreds of conformers for azobenzenes **2**, **4** and **7** were computed. Single point energies on the B97-3c[40] level of this conformer ensemble were calculated for allowing a better selection of the relevant structures. Conformers up to 3 kcal mol^{-1} higher

in energy than the lowest energy structure were considered for further analysis.

In the next step, distances between the carbon atoms on opposing alkyl chains were determined to find close contacts for non-covalent interactions. Results were limited to distances below 5 Å, therefore including H-H distances of 4.2 Å or lower where dispersive interactions start to contribute significantly to the stability of molecular entities.[42] To obtain a more meaningful picture of the contact distribution, the considered conformers were weighed by their single point energies with a Boltzmann distribution. The in this way determined average number of C–C contacts over the conformer ensemble within this 3 kcal mol^{-1} energy window are listed in Table 1. For compound **2**, the distances between the ethyl side chains are too short for relevant attractive interactions between the alkyl chains in the *E*- as well as the transition state. Only in the *Z*-state, the ethyl groups mesh well. For longer chains, like *n*-butyl in **4**, this kind of interactions are also to a minor extent present in the transition state but ≈5.7 times more dominant in the *Z*-state. In the *n*-heptyl derivative **7**, these interactions occur in all three states. While the differences between the *E*-state and the transition state are quite small, the number of contacts in the *Z*-state are here only ≈3.4 times higher than in the transition state. Noteworthy, that the same number of average interactions are present in the *E*-state, supporting the correlation between transition and *E*-state projected in the introduction. This analysis emphasizes that the observed kinetic trend for linear alkyl substituted azobenzenes is mainly driven by increased stabilisation of the *Z*-isomer up to mid-length chains. With further increasing chain length, these interactions start to occur also more and more in the transition state and seem to compensate further elongation of the alkyl substituents.

These interactions can also be visualized by an NCI analysis, which is depicted in Figure 6.[43] This non-covalent interaction analysis indicates the regions in the molecules as isosurfaces, where these contacts occur. The colour code further allows to differentiate between attractive (blue), repulsive (red) and weak interactions (green). In the transition state of derivative **4** weak alkyl-alkyl interactions start to form as can be seen in the right part of the molecule. In the *Z*-state additional alkyl-aryl interactions emerge, providing a much larger interaction surface leading to a large stabilization of the *Z*-state. For the *n*-heptyl derivative **7**, a similar analysis can be done (see Supporting Information Figure S9 and S10). It has to be pointed out, that the alkyl chains in the *Z*-state intercalate with the ones on the opposing aryl ring, leading to larger stabilizing effects on the structure. In the transition state, the alkyl chains tend to preferentially interact with the ones on the same aryl ring due to an unfavourable core geometry of the transition state. These interactions are most likely competing with interactions with solvent molecules due to the less restricted geometry. It can be assumed that specific solute-solvent interactions mainly affect the transition state.

Table 1: Average Number of opposing C–C contacts below 5 Å over all conformers within 3 kcal mol^{-1}.

Cpd	*E*-state	Transition state	*Z*-state
2	0.00	0.00	0.73
4	0.00	2.04	11.68
7	12.81	12.74	42.70

Conclusion

Three main effects governing the London dispersion between alkyl groups and alkyl solvents could be established:

1. The intramolecular dispersion interactions are only marginally influenced by the solvent since the overall tendency of the half-lives in dependency of the substituents stays very similar.
2. It was shown that in solvents with low surface tension, destabilizing contributions due to solvent-solvent interac-

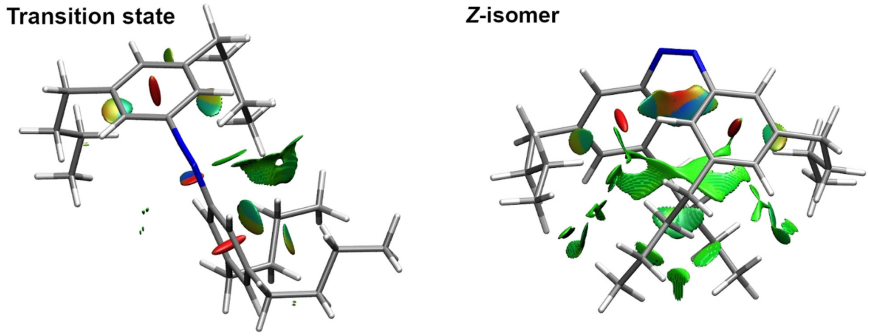

Figure 6. NCI[43] analysis of the optimized structures for the lowest energy conformers of the transition state and the *Z*-state of azobenzene **4** [PBE0-D3BJ/def2-TZVP].[39,44] Visualization was created with VMD.[45]

tions can contribute up to 0.1 kcal mol^{-1} or an increase of the *Z*-isomer half-life up to 20%.

3. Specific individual interactions between the alkyl chains on the azobenzene and those of the solvent lead to additional fluctuations of the half-lives. These are presumably caused by structural changes of the conformer ensemble both of the *n*-alkyl substituents and of the *n*-alkanes as solvents.

This investigation using azobenzene as a molecular probe reveals that even small structural changes of an alkane solvent can have substantial effects on the stability of an organic compound. A detailed computational evaluation of the conformer ensemble supports the taken approach. These new insights provide general guidelines to design solvent-solute interactions for all kinds of processes in the liquid state.

Acknowledgements

Financial support was provided by the Justus Liebig University Giessen and by the Deutsche Forschungsgemeinschaft (SPP1807). We thank Dr. Heike Hausmann and Anja Platt for NMR support and Jan M. Schümann for the fruitful discussions. Open access funding enabled and organized by Projekt DEAL.

Conflict of interest

The authors declare no conflict of interest.

Keywords: azobenzene · London dispersion · molecular probe · solvent effects · spectroscopy

[1] Y. Levy, J. N. Onuchic, *Annu. Rev. Biophys. Biomol. Struct.* **2006**, *35*, 389 – 415.
[2] a) A. M. Klibanov, *Nature* **2001**, *409*, 241 – 246; b) M.-H. Wu, M.-C. Lin, C.-C. Lee, S.-M. Yu, A. H.-J. Wang, T.-H. D. Ho, *Sci. Rep.* **2019**, *9*, 9754.
[3] H. Yorimitsu, T. Nakamura, H. Shinokubo, K. Oshima, K. Omoto, H. Fujimoto, *J. Am. Chem. Soc.* **2000**, *122*, 11041 – 11047.
[4] J. Flores-Ferrándiz, B. Fiser, E. Gómez-Bengoa, R. Chinchilla, *Eur. J. Org. Chem.* **2015**, 1218 – 1225.
[5] J. Zhang, H. Zhang, T. Wu, Q. Wang, D. van der Spoel, *J. Chem. Theory Comput.* **2017**, *13*, 1034 – 1043.
[6] F. D. Toste, M. S. Sigman, S. J. Miller, *Acc. Chem. Res.* **2017**, *50*, 609 – 615.
[7] B. Liang, H. Wang, X. Shi, B. Shen, X. He, Z. A. Ghazi, N. A. Khan, H. Sin, A. M. Khattak, L. Li, et al., *Nat. Chem.* **2018**, *10*, 961 – 967.
[8] Y. Cui, T.-S. Chung, *Nat. Commun.* **2018**, *9*, 1426.
[9] a) J. P. Wagner, P. R. Schreiner, *Angew. Chem. Int. Ed.* **2015**, *54*, 12274 – 12296; *Angew. Chem.* **2015**, *127*, 12446 – 12471; b) J. Hwang, P. Li, M. D. Smith, K. D. Shimizu, *Angew. Chem. Int. Ed.* **2016**, *55*, 8086 – 8089; *Angew. Chem.* **2016**, *128*, 8218 – 8221.
[10] a) S. Rösel, H. Quanz, C. Logemann, J. Becker, E. Mossou, L. Cañadillas-Delgado, E. Caldeweyher, S. Grimme, P. R. Schreiner, *J. Am. Chem. Soc.* **2017**, *139*, 7428 – 7431; b) A. A. Fokin, T. S. Zhuk, S. Blomeyer, C. Pérez, L. V. Chernish, A. E. Pashenko, J. Antony, Y. V. Vishnevskiy, R. J. F. Berger, S. Grimme, et al., *J. Am. Chem. Soc.* **2017**, *139*, 16696 – 16707; c) P. R. Schreiner, L. V. Chernish, P. A. Gunchenko, E. Y. Tikhonchuk, H. Hausmann, M. Serafin, S. Schlecht, J. E. P. Dahl, R. M. K. Carlson, A. A. Fokin, *Nature* **2011**, *477*, 308 – 311.
[11] M. Fatima, A. L. Steber, A. Poblotzki, C. Pérez, S. Zinn, M. Schnell, *Angew. Chem. Int. Ed.* **2019**, *58*, 3108 – 3113; *Angew. Chem.* **2019**, *131*, 3140 – 3145.
[12] a) D. J. Liptrot, J.-D. Guo, S. Nagase, P. P. Power, *Angew. Chem. Int. Ed.* **2016**, *55*, 14766 – 14769; *Angew. Chem.* **2016**, *128*, 14986 – 14989; b) M. S. G. Ahlquist, P.-O. Norrby, *Angew. Chem. Int. Ed.* **2011**, *50*, 11794 – 11797; *Angew. Chem.* **2011**, *123*, 11998 – 12001.
[13] a) V. R. Yatham, W. Harnying, D. Kootz, J.-M. Neudörfl, N. E. Schlörer, A. Berkessel, *J. Am. Chem. Soc.* **2016**, *138*, 2670 – 2677; b) E. Lyngvi, I. A. Sanhueza, F. Schoenebeck, *Organometallics* **2015**, *34*, 805 – 812.
[14] a) D. van Craen, W. H. Rath, M. Huth, L. Kemp, C. Räuber, J. M. Wollschläger, C. A. Schalley, A. Valkonen, K. Rissanen, M. Albrecht, *J. Am. Chem. Soc.* **2017**, *139*, 16959 – 16966; b) C. Ray, J. R. Brown, A. Kirkpatrick, B. B. Akhremitchev, *J. Am. Chem. Soc.* **2008**, *130*, 10008 – 10018; c) R. G. Snyder, H. L. Strauss, C. A. Elliger, *J. Phys. Chem.* **1982**, *86*, 5145 – 5150; d) S. Tsuzuki, K. Honda, T. Uchimaru, M. Mikami, *J. Phys. Chem. A* **2004**, *108*, 10311 – 10316.
[15] R. Pollice, P. Chen, *J. Am. Chem. Soc.* **2019**, *141*, 3489 – 3506.
[16] a) C. Riplinger, P. Pinski, U. Becker, E. F. Valeev, F. Neese, *J. Chem. Phys.* **2016**, *144*, 024109; b) S. Grimme, A. Hansen, J. G. Brandenburg, C. Bannwarth, *Chem. Rev.* **2016**, *116*, 5105 – 5154; c) E. Caldeweyher, C. Bannwarth, S. Grimme, *J. Chem. Phys.* **2017**, *147*, 034112.
[17] R. Pollice, M. Bot, I. J. Kobylianskii, I. Shenderovich, P. Chen, *J. Am. Chem. Soc.* **2017**, *139*, 13126 – 13140.
[18] a) L. Yang, C. Adam, G. S. Nichol, S. L. Cockroft, *Nat. Chem.* **2013**, *5*, 1006 – 1010; b) C. Adam, L. Yang, S. L. Cockroft, *Angew. Chem. Int. Ed.* **2015**, *54*, 1164 – 1167; *Angew. Chem.* **2015**, *127*, 1180 – 1183; c) J. Hwang, B. E. Dial, P. Li, M. E. Kozik, M. D. Smith, K. D. Shimizu, *Chem. Sci.* **2015**, *6*, 4358 – 4364.
[19] M. A. Strauss, H. A. Wegner, *Eur. J. Org. Chem.* **2019**, 295 – 302.
[20] R. Pollice, F. Fleckenstein, I. Shenderovich, P. Chen, *Angew. Chem. Int. Ed.* **2019**, *58*, 14281 – 14288; *Angew. Chem.* **2019**, *131*, 14419 – 14426.
[21] L. Schweighauser, M. A. Strauss, S. Bellotto, H. A. Wegner, *Angew. Chem. Int. Ed.* **2015**, *54*, 13436 – 13439; *Angew. Chem.* **2015**, *127*, 13636 – 13639.
[22] A. H. Heindl, R. C. Wende, H. A. Wegner, *Beilstein J. Org. Chem.* **2018**, *14*, 1238 – 1243.
[23] M. A. Strauss, H. A. Wegner, *Angew. Chem. Int. Ed.* **2019**, *58*, 18552 – 18556; *Angew. Chem.* **2019**, *131*, 18724 – 18729.
[24] A. R. Dias, M. E. Minas Da Piedade, J. A. Martinho Simões, J. A. Simoni, C. Teixeira, H. P. Diogo, Y. Meng-Yan, G. Pilcher, *J. Chem. Thermodyn.* **1992**, *24*, 439 – 447.
[25] J. Harada, K. Ogawa, S. Tomoda, *Acta Crystallogr. Sect. B* **1997**, *53*, 662 – 672.
[26] A. Mostad, C. Rømming, S. Hammarström, R. J. J. C. Lousberg, U. Weiss, *Acta Chem. Scand.* **1971**, *25*, 3561 – 3568.
[27] T. Halicioglu, O. Sinanoglu, *Ann. N. Y. Acad. Sci.* **1969**, *158*, 308 – 317.
[28] C. A. Winkler, J. Halpern, G. W. Brady, *Can. J. Res.* **1950**, *28*, 140 – 155.
[29] P. Haberfield, P. M. Block, M. S. Lux, *J. Am. Chem. Soc.* **1975**, *97*, 5804 – 5806.
[30] J. Dokić, M. Gothe, J. Wirth, M. V. Peters, J. Schwarz, S. Hecht, P. Saalfrank, *J. Phys. Chem. A* **2009**, *113*, 6763 – 6773.
[31] D. R. Lide, *CRC handbook of chemistry and physics. A ready-reference book of chemical and physical data*, **2004**,CRC Press, Boca Raton, Florida.
[32] S. Shen, Y. Wang, J. Shi, G. C. Benson, B. C.-Y. Lu, *J. Chem. Thermodyn.* **1990**, *22*, 387 – 392.

[33] D. Gruzman, A. Karton, J. M. L. Martin, *J. Phys. Chem. A* **2009**, *113*, 11974 – 11983.
[34] E. M. King, M. A. Gebbie, N. A. Melosh, *Langmuir* **2019**, *35*, 16062 – 16069.
[35] a) O. V. Dorofeeva, V. S. Mastryukov, N. L. Allinger, A. Almenningen, *J. Phys. Chem.* **1985**, *89*, 252 – 257; b) K. B. Wiberg, *J. Org. Chem.* **2003**, *68*, 9322 – 9329.
[36] a) W. L. Spiteri, T. M. Letcher, *Thermochim. Acta* **1982**, *59*, 73 – 80; b) M. B. Ewing, K. N. Marsh, *J. Chem. Thermodyn.* **1973**, *5*, 651 – 657.
[37] B. Marongiu, S. Porcedda, L. Lepori, E. Matteoli, *Fluid Phase Equilib.* **1995**, *108*, 167 – 183.
[38] a) S. Grimme, *J. Chem. Theory Comput.* **2019**, *15*, 2847 – 2862; b) P. Pracht, F. Bohle, S. Grimme, *Phys. Chem. Chem. Phys.* **2020**, *22*, 7169 – 7192.
[39] C. Adamo, V. Barone, *J. Chem. Phys.* **1999**, *110*, 6158 – 6170.
[40] J. G. Brandenburg, C. Bannwarth, A. Hansen, S. Grimme, *J. Chem. Phys.* **2018**, *148*, 064104.
[41] M. D. Lechner, *Surface Tension of Pure Liquids and Binary Liquid Mixtures*, Springer, Berlin, Heidelberg, **1997**.
[42] S. Grimme, R. Huenerbein, S. Ehrlich, *ChemPhysChem* **2011**, *12*, 1258 – 1261.
[43] E. R. Johnson, S. Keinan, P. Mori-Sánchez, J. Contreras-García, A. J. Cohen, W. Yang, *J. Am. Chem. Soc.* **2010**, *132*, 6498 – 6506.
[44] a) S. Grimme, S. Ehrlich, L. Goerigk, *J. Comput. Chem.* **2011**, *32*, 1456 – 1465; b) S. Grimme, J. Antony, S. Ehrlich, H. Krieg, *J. Chem. Phys.* **2010**, *132*, 154104; c) F. Weigend, R. Ahlrichs, *Phys. Chem. Chem. Phys.* **2005**, *7*, 3297 – 3305.
[45] W. Humphrey, A. Dalke, K. Schulten, *J. Mol. Graphics* **1996**, *14*, 33 – 38.

Manuscript received: September 4, 2020
Accepted manuscript online: October 1, 2020
Version of record online: November 5, 2020

4.2 Exploring London Dispersion and Solvent Interactions at Alkyl–Alkyl Interfaces Using Azobenzene Switches

Reference:

M. A. Strauss, H. A. Wegner, *Angew. Chem. Int. Ed.*, **2019**, *58*, 18552–18556.
German Edition:
M. A. Strauss, H. A. Wegner, *Angew. Chem.*, **2019**, *131*, 18724–18729.
DOI: 10.1002/anie.201910734 and 10.1002/ange.201910734

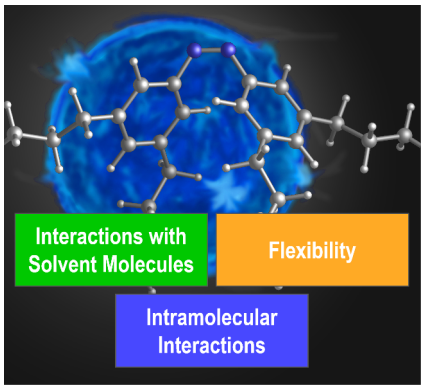

"Interactions on the molecular level control structure as well as function. Especially interfaces between innocent alkyl groups are hardly studied although they are of great importance in larger systems. Herein, London dispersion in conjunction with solvent interactions between linear alkyl chains was examined with an azobenzene-based experimental setup. Alkyl chains in all *meta* positions of the azobenzene core were systematically elongated, and the change in rate for the thermally induced $Z \rightarrow E$ isomerization in *n*-decane was determined. The stability of the *Z*-isomer increased with longer chains and reached a maximum for *n*-butyl groups. Further elongation led to faster isomerization. The origin of the intramolecular interactions was elaborated by various techniques, including ^{1}H NOESY NMR spectroscopy. The results indicate that there are additional long-range interactions between *n*-alkyl chains with the opposite phenyl core in the *Z*-state. These interactions are most likely dominated by attractive London dispersion. This work provides rare insight into the stabilizing contributions of highly flexible groups in an intra- as well as an intermolecular setting."

GDCh Communications Angewandte International Edition Chemie

Check for updates

Dispersion Interactions

International Edition: DOI: 10.1002/anie.201910734
German Edition: DOI: 10.1002/ange.201910734

Exploring London Dispersion and Solvent Interactions at Alkyl–Alkyl Interfaces Using Azobenzene Switches

*Marcel A. Strauss and Hermann A. Wegner**

Abstract: *Interactions on the molecular level control structure as well as function. Especially interfaces between innocent alkyl groups are hardly studied although they are of great importance in larger systems. Herein, London dispersion in conjunction with solvent interactions between linear alkyl chains was examined with an azobenzene-based experimental setup. Alkyl chains in all meta positions of the azobenzene core were systematically elongated, and the change in rate for the thermally induced Z→E isomerization in n-decane was determined. The stability of the Z-isomer increased with longer chains and reached a maximum for n-butyl groups. Further elongation led to faster isomerization. The origin of the intramolecular interactions was elaborated by various techniques, including ^{1}H NOESY NMR spectroscopy. The results indicate that there are additional long-range interactions between n-alkyl chains with the opposite phenyl core in the Z-state. These interactions are most likely dominated by attractive London dispersion. This work provides rare insight into the stabilizing contributions of highly flexible groups in an intra- as well as an intermolecular setting.*

The interaction of chemical entities on the molecular level is crucial for their structure and, therefore, for their properties as well as function. While stronger interactions, such as hydrogen bonds or Lewis pairs, are well-established, weak ones such as van der Waals interactions still have not been studied in depth and are usually neglected in more complex systems. London dispersion represents the attractive part of the van der Waals potential and was first introduced by Fritz London in 1930.[1] While London dispersion plays a dominant role in the interaction of hydrocarbons, these non-covalent interactions are omnipresent and not limited to a certain type of functional group.[2] In synthesis, large and polarizable moieties—in most cases rigid alkyl groups—can be utilized as dispersion energy donors if placed at the correct distance.[3] They allow the stabilization of extreme bonding situations,[4] therefore overcompensating repulsive forces to generate, for example, the longest carbon–carbon bond in alkanes reported to date.[5] Biological systems[6] are also stabilized by the significant contributions of dispersion forces. In addition, they dominate the interaction energy in frustrated Lewis pairs (FLPs)[7] or in the aggregation of aromatic species.[8] Other studies have demonstrated their substantial influence on the stability of organometallic complexes[9] and in catalysis.[10] In recent years, numerous computational methods were developed that give access to a comprehensive toolbox for efficiently evaluating the dispersion interactions in molecular systems with high accuracy.[11]

Nevertheless, London dispersion is often regarded as negligible in solution. However, studies have been conducted towards addressing this statement and investigating the influence of the solvent on conformer or dimer stability.[12,13] In these studies, it was tried to dissect the different contributions to the total energy of the molecular system. The authors observed a very large attenuation of dispersion forces due to competitive dispersion interactions with the solvent, which were not completely cancelled out.

In contrast to rigid alkyl dispersion donors, such as adamantyl or *tert*-butyl moieties, highly flexible *n*-alkyl chains bear more complex challenges for estimating their dispersion donor abilities. Therefore, London dispersion interactions between linear alkyl chains have still only marginally been explored.[14,15] At elevated temperatures, a large number of different conformers have to be considered for these alkanes for a conclusive evaluation of the experimental findings. For *n*-pentane, the *gauche* conformer is already the most abundant one at room temperature.[16] Furthermore, the potential formation of hairpin structures for longer alkyl chains complicates meaningful interpretation.[17] Computational analysis of the large number of possible conformers often turns out to be very challenging with standard resources. Therefore, experimental data is essential to understand these fundamental interactions. The azobenzene switch has been established as a powerful tool to investigate London dispersion forces and was chosen to address these open questions (Scheme 1).[13,18,19]

Azobenzenes are photoswitchable molecules, which can isomerize from the thermodynamically most stable *E*-state to the metastable *Z*-state, which is about 11.7 kcal mol^{-1} higher in energy (Scheme 2).[20] An important change upon isomerization is the reduction of the distance between the carbon atoms in the *para* position of the rings from 9.1 Å[21] to about

[*] M. A. Strauss, Prof. Dr. H. A. Wegner
Institute of Organic Chemistry
Justus-Liebig University Giessen
Heinrich-Buff-Ring 17, 35392 Giessen (Germany)
and
Center for Materials Research (LaMa)
Justus-Liebig University Giessen
Heinrich-Buff-Ring 16, 35392 Giessen (Germany)
E-mail: hermann.a.wegner@org.chemie.uni-giessen.de
Supporting information and the ORCID identification number(s) for the author(s) of this article can be found under: https://doi.org/10.1002/anie.201910734.

GDCh Communications Angewandte International Edition Chemie

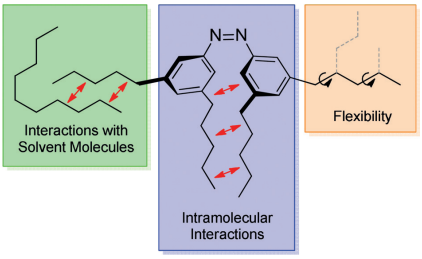

Scheme 1. Intra- and intermolecular interactions, as well as flexibility in all-*meta* *n*-alkylated azobenzenes.

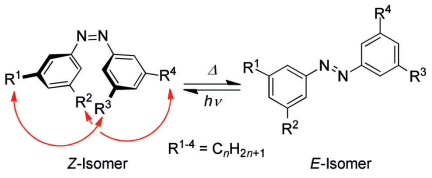

Scheme 2. Isomerization of all-*meta* *n*-alkylated azobenzene systems.

6.2 Å,[22] bringing substituents on the azobenzene rings in close proximity. In a previous study, we had demonstrated that for azobenzene derivatives substituted in the *meta* positions, the substituents come into a distance where London dispersion donors stabilize the *Z*-isomer of the azobenzene.[18]

For the current study, *n*-alkyl substituents were systematically attached in the *meta* positions of the azobenzene scaffold with increasing lengths, ranging from methyl up to *n*-octyl chains. The system was deliberately designed such that each of the two alkyl chains on a phenyl ring faces another one on the opposite ring in the *Z*-isomer. Therefore, the overall interaction contacts are increased, leading to high sensitivity towards small changes in the system.

For the synthesis of the azobenzene probes, a highly flexible strategy was designed. The side chains of choice were introduced by a Wittig reaction using 5-nitroisophthalaldehyde. Subsequent hydrogenation and oxidative azo coupling yielded the symmetric all-*meta* *n*-alkylated azobenzenes **1**–**8** (Scheme 3). The modular synthesis of this azobenzene probe can be conveniently altered to modify the substituents as desired.

To study the alkyl–alkyl interactions, all azobenzenes were switched from the *E*- to the *Z*-state by irradiation at 302 nm. The thermally induced back-isomerization at a given temperature was then followed by UV/Vis spectroscopy to directly correlate the chain length of the alkyl substituents with the stability of the *Z*-isomer of the azobenzene.

The measurements were conducted in *n*-decane to minimize solvophobic contributions to the thermally induced *Z*→*E* isomerization barrier. As can be seen in Figure 1, the half-lives of the *Z*-isomers of the all-*meta*-substituted azobenzenes

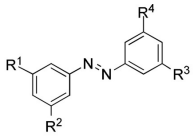

1: R^{1-4} = methyl
2: R^{1-4} = ethyl
3: R^{1-4} = *n*-propyl
4: R^{1-4} = *n*-butyl
5: R^{1-4} = *n*-pentyl
6: R^{1-4} = *n*-hexyl
7: R^{1-4} = *n*-heptyl
8: R^{1-4} = *n*-octyl
9: R^{1-4} = H
10: $R^{1,2}$ = methyl; $R^{3,4}$ = H
11: $R^{1,2}$ = *n*-heptyl; $R^{3,4}$ = H
12: $R^{1,3}$ = *n*-heptyl; $R^{2,4}$ = H
13: $R^{1,2}$ = *n*-propyl; $R^{3,4}$ = H

Scheme 3. Overview of azobenzene derivatives investigated in this study.

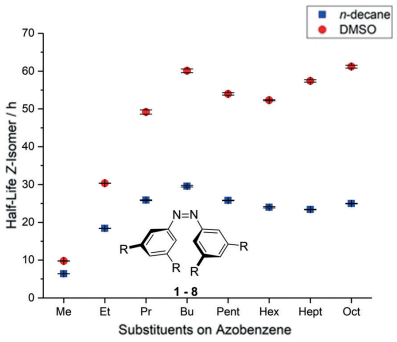

Figure 1. Half-lives of all-*meta*-substituted azobenzenes **1**–**8** with different chain lengths at 40 °C in *n*-decane and DMSO.

at 40 °C increased dramatically at the beginning upon elongation of the alkyl substituents. This observation is in accordance with the expectation of increasing attractive London dispersion interactions with increasing chain length. For the *n*-butyl chains, a maximum is reached with a half-life that is about five times higher than that for the tetramethyl-substituted derivative **1**. Further elongation leads to a decrease in the half-lives down to approximately 23 h. This decrease might be caused by competitive alkyl–alkyl interactions between alkyl chains on the same phenyl ring, which would reduce the overall interaction strength with alkyl groups on the opposite phenyl ring.

In an analogous study, van Craen and co-workers had investigated the effect of *n*-alkyl-substituted ligands on the stabilization of dimers of titanium(IV) helicate complexes. They had also observed a higher degree of dimerization with increased chain length up to *n*-heptyl.[14] However, for solubility reasons, the dimerization of the titanium complexes had to be studied in THF, which should add solvophobic contributions to the attractive interactions in favor of the dimer formation.

It therefore seemed quite likely that in solvents such as THF or dimethyl sulfoxide (DMSO), our system would also show an increased half-life for the *Z*-isomer for the elongated chains, and this was indeed observed. When the measurements were conducted in DMSO, an overall increase in the *Z*-isomer half-lives was observed (Figure 1). This can be rationalized by a thermodynamic stabilization of the *Z*-isomer in a more polar solvent. This was also demonstrated by Haberfield and co-workers, who calorimetrically examined the enthalpies for the $Z \rightarrow E$ isomerization of *Z*-azobenzene in cyclohexane versus cyclohexanone.[23] In addition, they found a slight energetic increase in the transition state due to less favored solute–solvent interactions. This observation further helps explaining the changed course of the half-lives for the azobenzenes **6**–**8** with *n*-hexyl or longer chains. Here, strong solvophobic interactions contribute extensively to a higher-energy transition state with increasing chain length and therefore a longer half-life for these compounds. The preference for solvent–solvent over solute–solvent interactions corresponds also to the observed, drastically decreased solubility of these azobenzenes in DMSO.

At different temperatures, the overall trend of the isomerization rates stays essentially the same (Figure 2). The lowest isomerization rate at each temperature, and therefore the most stable *Z*-isomer, was observed for

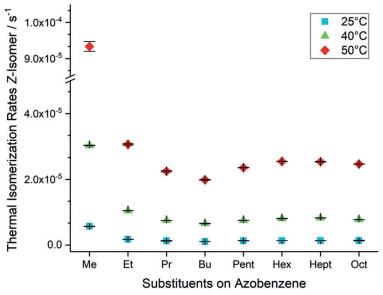

Figure 2. Thermal isomerization rates of all-*meta*-substituted azobenzenes **1**–**8** with different chain lengths in *n*-decane at three different temperatures.

azobenzene **4** with the *n*-butyl substituents. Furthermore, the isomerization rate decreased again from **7** to **8**. Although this did not seem to be the case at 25 °C, a higher error for this measurement might influence the result here. Overall, a threefold increase in the isomerization rates was observed upon increasing the temperature by 10 °C. This acceleration is independent of the chain length of the alkyl substituents and was observed for each azobenzene investigated.

In total, isomerization rates were measured at five different temperatures. An Exner plot was constructed to exclude a change in the isomerization mechanism (see Figure S2 in the Supporting Information). The plot shows a high linear correlation indicating a constant mechanism for the investigated temperature range. The collected kinetic data allowed us to further evaluate the enthalpies and entropies of activation for the $Z \rightarrow E$ isomerization for all compounds (Table 1).

Table 1: Experimental kinetic data of the thermal $Z \rightarrow E$ isomerization of **1**–**8** in *n*-decane as the solvent. Energies are given in kcal mol^{-1}, entropies in cal K^{-1} mol^{-1}. Errors were calculated from the highest slope and *y*-intercept error out of three Eyring–Polanyi fits.

Compound	$\Delta H^{+}_{Z\text{-}E}$	$\Delta S^{+}_{Z\text{-}E}$	$\Delta G^{+}_{Z\text{-}E}$[a]
1	20.1 ± 0.3	−12.5 ± 1.0	24.6 ± 0.6
2	21.5 ± 0.2	−12.9 ± 0.5	25.3 ± 0.3
3	21.6 ± 0.5	−13.3 ± 1.7	25.5 ± 1.1
4	21.9 ± 0.3	−12.4 ± 0.9	25.6 ± 0.6
5	21.9 ± 0.5	−12.0 ± 1.6	25.5 ± 1.0
6	21.9 ± 0.2	−12.1 ± 0.6	25.5 ± 0.4
7	22.0 ± 0.1	−11.8 ± 0.4	25.5 ± 0.2
8	21.7 ± 0.4	−12.8 ± 1.3	25.5 ± 0.8

[a] At 25 °C, 1 atm.

The enthalpy of activation shows a large increase with longer chains from **1** to **3**. For compounds **4**–**7**, the values stay constant with a small decrease for **8**. This is not surprising as elongation of the alkyl substituents increases the possible number of attractive contacts between the chains. The contributions to the increasing enthalpy of activation are dominated by London dispersion interactions. However, insertion of additional methylene units also enhances the degrees of rotational and vibrational freedom, leading to a compensation of the attraction for longer alkyl substituents. This also explains why for these linear alkyl chains, a plateau is reached. Interpretation of the experimentally determined entropic contributions to the isomerization barrier is complex. Extending the chains should increase the conformational freedom, and hence increase the destabilizing entropic contributions. However, it can be expected that London dispersion interactions will restrict the flexibility of the chains, counteracting the effect of larger substituents to the entropic contributions to a certain degree. Additionally, interactions with the solvent have to be considered. Solvophobic effects based on cohesive properties of the solvent should be less important for our experiments in *n*-decane, but have to be taken into account for solvents with higher polarity such as DMSO. Although a qualitative estimation is reasonable, the calculated error of the entropies is too large to quantify and dissect individual contributions.

It is expected that the strength of London dispersion interactions should correlate with the number as well as the position of the substituents. Therefore, different substitution patterns were examined. By exchanging two *n*-heptyl substituents in **7** for hydrogen atoms, either azobenzene **12** with alkyl chains on opposite phenyl rings or compound **11** with both substituents on the same phenyl ring were obtained. Additionally, the dimethyl analogue **10** was prepared. Hydrogen substituents are not isoelectronic to alkyl substituents. Hence, the overall electron distribution in the phenyl rings is different, which also influences the isomerization rates. Therefore, unsubstituted azobenzene (**9**) was also investigated for comparison. In Figure 3, the half-lives of the *Z*-isomers of these compounds are depicted.

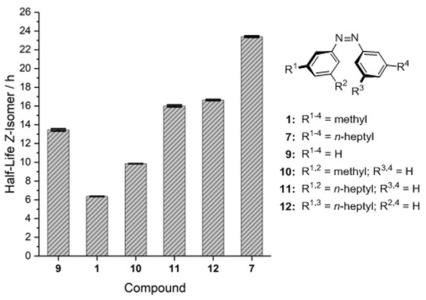

Figure 3. Half-lives of azobenzenes with different substitution patterns and/or different chain lengths at 40 °C in *n*-decane.

As expected, the substitution of two Me groups with H atoms in compound **10** led to an increase in the half-life by approximately 3 h, illustrating the electronic difference of H versus alkyl substitution. When all alkyl substituents are replaced by hydrogen atoms, the half-life further increases. This observation correlates well with the change in electron density. An increase in the electron density leads to faster isomerization, and therefore, to a shorter half-life. The diheptyl derivatives **11** and **12** show substantially longer half-lives than the Me derivatives **1** and **10** because of the increased attractive London dispersion interactions resulting from alkyl–alkyl as well as alkyl–aryl interactions. The similar half-lives of azobenzenes **11** and **12** result from the same number of alkyl–aryl contacts, indicating that alkyl–alkyl contacts are of minor importance here. However, compound **11**, with both heptyl chains on the same phenyl ring, only shows a marginally shorter half-life, which can be rationalized by considering the altered electronic structure compared to compound **12**.

To further elucidate the large difference between **10** and **11**, 3,5-di-*n*-propyl-substituted azobenzene **13** was synthesized, and switched to the photostationary state under continuous irradiation at 302 nm. Afterwards, a ^{1}H NOESY NMR spectrum was recorded (Figure 4). This technique can be used to identify hydrogen atoms that are up to 5 Å apart from each other. Between 3 and 5 Å, London dispersion interactions can contribute significantly to the stability of molecular entities. The marked cross-peaks show that the methyl groups of the *n*-propyl substituents are close enough to interact with the opposite phenyl ring. This long-range interaction of the alkyl chains with the Ph moiety is attractive in character and significantly contributes to the longer half-life of **11** compared to **10**. This finding further indicates that attractive alkyl–aryl interactions have a considerable impact on the stability of the *Z*-isomer.

An additional ^{1}H NOESY NMR experiment with compound **11** also revealed the close proximity of the alkyl substituents and the opposite phenyl ring. Interestingly, here the interaction with the fourth methylene unit counted from the phenyl ring was clearly observed, which is in a similar distance range as for **13**. The small deviation can be rationalized by a different conformation for **11**.

In conclusion, we have observed subtle changes in London dispersion interactions by measuring the isomerization rates of *n*-alkyl-substituted azobenzenes. The presented experimental setup allowed us to determine the changes occurring upon stepwise elongation of the *n*-alkyl chains with high precision and reproducibility. The $Z \rightarrow E$ isomerization decelerated from methyl to *n*-butyl substituents, maximizing London dispersion from alkyl–alkyl and alkyl–aryl interactions. With longer alkyl substituents, the isomerization is again accelerated up to a certain threshold because of the higher entropic contributions that overcompensate the stabilization of the *Z*-state by London dispersion. Furthermore, solvophobic contributions dominate in solvents with higher polarity such as DMSO for alkyl chains longer than *n*-hexyl.

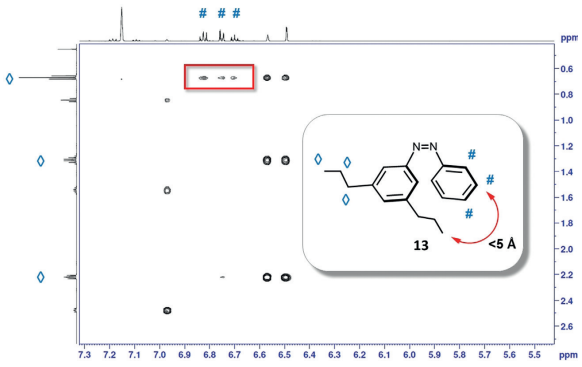

Figure 4. ^{1}H NOESY NMR spectrum of the *Z*-isomer of compound **13** in benzene-d_6 in the photostationary state. The marked cross-peaks indicate the close proximity of the methyl groups with the adjacent phenyl ring, leading to attractive London dispersion.

This work provides further evidence that London dispersion interactions in solution are still contributing in a relevant way even to chemical systems with a high degree of flexibility. These results provide deeper insight into how the subtle balance between steric repulsion, attractive London dispersion, and entropy can be adjusted with flexible dispersion energy donors. The excellent solubility of these azobenzenes in a broad range of solvents as well as their modular synthesis provides the possibility to extend the investigation also to other types of interactions, such as

fluoroalkyl–fluoroalkyl or fluoroalkyl–alkyl interactions, as well as other solvent systems in the future.

Acknowledgements

Financial support was provided by the Justus Liebig University Giessen and by the Deutsche Forschungsgemeinschaft (SPP1807). We thank Dr. Heike Hausmann and Anja Platt for NMR support and Jan M. Schümann for fruitful discussions.

Conflict of interest

The authors declare no conflict of interest.

Keywords: azobenzenes · London dispersion · molecular probes · solvent effects · spectroscopy

How to cite: *Angew. Chem. Int. Ed.* **2019**, *58*, 18552 – 18556
Angew. Chem. **2019**, *131*, 18724 – 18729

[1] F. London, *Z. Phys.* **1930**, *63*, 245 – 279.
[2] F. London, *Trans. Faraday Soc.* **1937**, *33*, 8b.
[3] a) J. P. Wagner, P. R. Schreiner, *Angew. Chem. Int. Ed.* **2015**, *54*, 12274 – 12296; *Angew. Chem.* **2015**, *127*, 12446 – 12471; b) J. Hwang, P. Li, M. D. Smith, K. D. Shimizu, *Angew. Chem. Int. Ed.* **2016**, *55*, 8086 – 8089; *Angew. Chem.* **2016**, *128*, 8218 – 8221.
[4] a) S. Rösel, C. Balestrieri, P. R. Schreiner, *Chem. Sci.* **2017**, *8*, 405 – 410; b) S. Rösel, H. Quanz, C. Logemann, J. Becker, E. Mossou, L. Cañadillas-Delgado, E. Caldeweyher, S. Grimme, P. R. Schreiner, *J. Am. Chem. Soc.* **2017**, *139*, 7428 – 7431; c) S. Rösel, J. Becker, W. D. Allen, P. R. Schreiner, *J. Am. Chem. Soc.* **2018**, *140*, 14421 – 14432; d) A. A. Fokin, T. S. Zhuk, S. Blomeyer, C. Pérez, L. V. Chernish, A. E. Pashenko, J. Antony, Y. V. Vishnevskiy, R. J. F. Berger, S. Grimme, et al., *J. Am. Chem. Soc.* **2017**, *139*, 16696 – 16707.
[5] P. R. Schreiner, L. V. Chernish, P. A. Gunchenko, E. Y. Tikhonchuk, H. Hausmann, M. Serafin, S. Schlecht, J. E. P. Dahl, R. M. K. Carlson, A. A. Fokin, *Nature* **2011**, *477*, 308 – 311.
[6] a) J. P. Wagner, P. R. Schreiner, *J. Chem. Theory Comput.* **2014**, *10*, 1353 – 1358; b) J. Vondrásek, T. Kubar, F. E. Jenney, M. W. W. Adams, M. Kozísek, J. Cerný, V. Sklenár, P. Hobza, *Chem. Eur. J.* **2007**, *13*, 9022 – 9027; c) S. Hanlon, *Biochem. Biophys. Res. Commun.* **1966**, *23*, 861 – 867; d) M. Kolář, T. Kubař, P. Hobza, *J. Phys. Chem. B* **2011**, *115*, 8038 – 8046; e) C. Nick Pace, J. M. Scholtz, G. R. Grimsley, *FEBS Lett.* **2014**, *588*, 2177 – 2184.
[7] G. Bistoni, A. A. Auer, F. Neese, *Chem. Eur. J.* **2017**, *23*, 865 – 873.
[8] M. Fatima, A. L. Steber, A. Poblotzki, C. Pérez, S. Zinn, M. Schnell, *Angew. Chem. Int. Ed.* **2019**, *58*, 3108 – 3113; *Angew. Chem.* **2019**, *131*, 3140 – 3145.
[9] a) S. Löffler, J. Lübben, A. Wuttke, R. A. Mata, M. John, B. Dittrich, G. H. Clever, *Chem. Sci.* **2016**, *7*, 4676 – 4684; b) D. J. Liptrot, J.-D. Guo, S. Nagase, P. P. Power, *Angew. Chem. Int. Ed.* **2016**, *55*, 14766 – 14769; *Angew. Chem.* **2016**, *128*, 14986 – 14989; c) M. S. G. Ahlquist, P.-O. Norrby, *Angew. Chem. Int. Ed.* **2011**, *50*, 11794 – 11797; *Angew. Chem.* **2011**, *123*, 11998 – 12001; d) C.-Y. Lin, J.-D. Guo, J. C. Fettinger, S. Nagase, F. Grandjean, G. J. Long, N. F. Chilton, P. P. Power, *Inorg. Chem.* **2013**, *52*, 13584 – 13593; e) L. Song, J. Schoening, C. Wölper, S. Schulz, P. R. Schreiner, *Organometallics* **2019**, *38*, 1640 – 1647.
[10] a) T. H. Meyer, W. Liu, M. Feldt, A. Wuttke, R. A. Mata, L. Ackermann, *Chem. Eur. J.* **2017**, *23*, 5443 – 5447; b) E. Procházková, A. Kolmer, J. Ilgen, M. Schwab, L. Kaltschnee, M. Fredersdorf, V. Schmidts, R. C. Wende, P. R. Schreiner, C. M. Thiele, *Angew. Chem. Int. Ed.* **2016**, *55*, 15754 – 15759; *Angew. Chem.* **2016**, *128*, 15986 – 15991; c) V. R. Yatham, W. Harnying, D. Kootz, J.-M. Neudörfl, N. E. Schlörer, A. Berkessel, *J. Am. Chem. Soc.* **2016**, *138*, 2670 – 2677; d) E. Lyngvi, I. A. Sanhueza, F. Schoenebeck, *Organometallics* **2015**, *34*, 805 – 812; e) E. Detmar, V. Müller, D. Zell, L. Ackermann, M. Breugst, *Beilstein J. Org. Chem.* **2018**, *14*, 1537 – 1545.
[11] a) C. Riplinger, P. Pinski, U. Becker, E. F. Valeev, F. Neese, *J. Chem. Phys.* **2016**, *144*, 024109; b) S. Grimme, A. Hansen, J. G. Brandenburg, C. Bannwarth, *Chem. Rev.* **2016**, *116*, 5105 – 5154; c) S. Grimme, J. Antony, S. Ehrlich, H. Krieg, *J. Chem. Phys.* **2010**, *132*, 154104; d) S. Grimme, S. Ehrlich, L. Goerigk, *J. Comput. Chem.* **2011**, *32*, 1456 – 1465; e) E. Caldeweyher, C. Bannwarth, S. Grimme, *J. Chem. Phys.* **2017**, *147*, 034112; f) S. Grimme, C. Bannwarth, E. Caldeweyher, J. Pisarek, A. Hansen, *J. Chem. Phys.* **2017**, *147*, 161708.
[12] a) R. Pollice, M. Bot, I. J. Kobylianskii, I. Shenderovich, P. Chen, *J. Am. Chem. Soc.* **2017**, *139*, 13126 – 13140; b) L. Yang, C. Adam, G. S. Nichol, S. L. Cockroft, *Nat. Chem.* **2013**, *5*, 1006 – 1010; c) C. Adam, L. Yang, S. L. Cockroft, *Angew. Chem. Int. Ed.* **2015**, *54*, 1164 – 1167; *Angew. Chem.* **2015**, *127*, 1180 – 1183; d) J. Hwang, B. E. Dial, P. Li, M. E. Kozik, M. D. Smith, K. D. Shimizu, *Chem. Sci.* **2015**, *6*, 4358 – 4364.
[13] M. A. Strauss, H. A. Wegner, *Eur. J. Org. Chem.* **2019**, 295 – 302.
[14] D. van Craen, W. H. Rath, M. Huth, L. Kemp, C. Räuber, J. M. Wollschläger, C. A. Schalley, A. Valkonen, K. Rissanen, M. Albrecht, *J. Am. Chem. Soc.* **2017**, *139*, 16959 – 16966.
[15] a) C. Ray, J. R. Brown, A. Kirkpatrick, B. B. Akhremitchev, *J. Am. Chem. Soc.* **2008**, *130*, 10008 – 10018; b) R. G. Snyder, H. L. Strauss, C. A. Elliger, *J. Phys. Chem.* **1982**, *86*, 5145 – 5150; c) S. Tsuzuki, K. Honda, T. Uchimaru, M. Mikami, *J. Phys. Chem. A* **2004**, *108*, 10311 – 10316.
[16] A. Salam, M. S. Deleuze, *J. Chem. Phys.* **2002**, *116*, 1296 – 1302.
[17] a) N. O. B. Lüttschwager, T. N. Wassermann, R. A. Mata, M. A. Suhm, *Angew. Chem. Int. Ed.* **2013**, *52*, 463 – 466; *Angew. Chem.* **2013**, *125*, 482 – 485; b) D. G. Liakos, F. Neese, *J. Chem. Theory Comput.* **2015**, *11*, 2137 – 2143.
[18] L. Schweighauser, M. A. Strauss, S. Bellotto, H. A. Wegner, *Angew. Chem. Int. Ed.* **2015**, *54*, 13436 – 13439; *Angew. Chem.* **2015**, *127*, 13636 – 13639.
[19] A. H. Heindl, R. C. Wende, H. A. Wegner, *Beilstein J. Org. Chem.* **2018**, *14*, 1238 – 1243.
[20] a) A. R. Dias, M. E. Minas Da Piedade, J. A. Martinho Simões, J. A. Simoni, C. Teixeira, H. P. Diogo, Y. Meng-Yan, G. Pilcher, *J. Chem. Thermodyn.* **1992**, *24*, 439 – 447; b) A. W. Adamson, A. Vogler, H. Kunkely, R. Wachter, *J. Am. Chem. Soc.* **1978**, *100*, 1298 – 1300.
[21] J. Harada, K. Ogawa, S. Tomoda, *Acta Crystallogr. Sect. B* **1997**, *53*, 662 – 672.
[22] A. Mostad, C. Rømming, *Acta Chem. Scand.* **1971**, *25*, 3561 – 3568.
[23] P. Haberfield, P. M. Block, M. S. Lux, *J. Am. Chem. Soc.* **1975**, *97*, 5804 – 5806.

Manuscript received: August 22, 2019
Accepted manuscript online: September 26, 2019
Version of record online: November 7, 2019

4.3 Influence of an Ammonium Tag on the Switching Dynamics of Azobenzenes in Polar Solvents

Reference:

M. A. Strauss, H. A. Wegner, *ChemPhotoChem*, **2019**, *3*, 392-395.
DOI: 10.1002/cptc.201800264

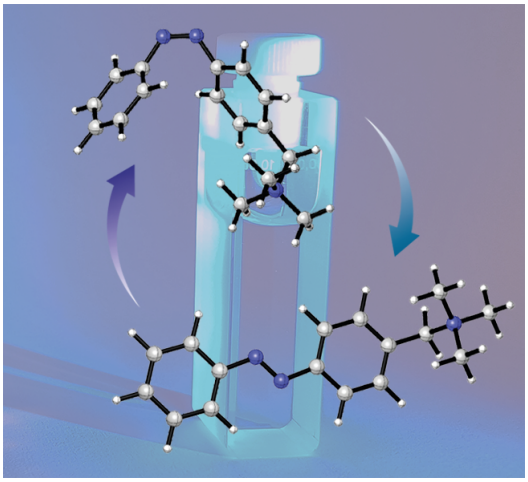

"Herein, we present a comprehensive study of the photophysical properties of an ammonium-tagged azobenzene in comparison to the unsubstituted compound in different solvents. It was shown that the thermal $Z \rightarrow E$ isomerization rate is decreased for the ammonium-tagged azobenzene. Additionally, the rate is higher with increased permittivity of the solvent. The results have been supported by DFT computations."

ChemPubSoc Europe
DOI: 10.1002/cptc.201800264
CHEMPHOTOCHEM Communications
Check for updates

Special Issue

Influence of an Ammonium Tag on the Switching Dynamics of Azobenzenes in Polar Solvents

Marcel A. Strauss[a] and Hermann A. Wegner*[a]

Herein, we present a comprehensive study of the photophysical properties of an ammonium-tagged azobenzene in comparison to the unsubstituted compound in different solvents. It was shown that the thermal *Z*→*E* isomerization rate is decreased for the ammonium-tagged azobenzene. Additionally, the rate is higher with increased permittivity of the solvent. The results have been supported by DFT computations.

Nature has successfully employed chromophores in a wide variety of photoreceptive systems of which the rhodopsin, based on the isomerization of 11-*cis*-retinal, is responsible for the human vision.[1] Equipped with synthetic photoactivated tools, scientists have been able to control the shape and activity of various biological systems. In this way, the usage of light enabled them to study and interfere with complex biological processes, also often in a reversible manner.[2] An additional advantage lies in the possibility to regulate these processes with high spatial and temporal resolution as well as the light intensity.[3] Optical control of endogenous and exogenous gene activation by introduction of photosensitive groups, for example, allowed the development of new methods for genome engineering and gene therapy, extending the concept of optogenetics.[4]

In recent years, chemists and pharmacologists have successfully implemented parts of optogenetic strategies into their research aiming at altering medically relevant targets like ion channels,[5] G-protein coupled receptors,[6] enzymes,[7] microtubules[8] and lipids[9] in a reversible fashion. As a result, the term *photopharmacology* was introduced to emphasize the focus on the development of synthetic photoswitches to control biological function.[10] Experiments *in vitro* demonstrated the capability to photocontrol the contraction of muscle fibers,[11] enzymatic cleavage of RNA[12] or a DNA polymerase reaction[13] and even antibacterial activity.[14] Also a flexible method to generate light-activated peptide ligands to targets of choice has been reported.[15] The advantages of photopharmacology for addressing a certain target offer a promising approach for applications *in vivo*.[16] This was further demonstrated by the development of synthetic photoswitches to restore the visual responses in blind mice.[17]

Azobenzenes have proven to provide a reliable scaffold for their application *in vitro* as well as *in vivo*, especially, since substituents can be conveniently altered by numerous synthetic methods, resulting in a high number of possibilities to tune their photochemical behavior. One requirement to initiate the *E* to *Z* switching *in vivo* is to tune the wavelength for photoisomerization, which is often initiated by UV-light, to the visible red or even infrared region, allowing deeper penetration of tissue. In recent years a number of publications were presented providing several strategies how this can be achieved.[18] Different approaches focus on the use of two-photon absorption of near-infrared light to photoswitch azobenzenes.[19]

Another issue, which has to be addressed, is the solubility. Unsubstituted azobenzene has only a low solubility in water, which makes it difficult for applications under physiological conditions. The incorporation of an ammonium tag can be an opportunity to provide high solubility in physiological relevant media. Such modified azobenzene moieties have gained growing interest for biomedical research. They are further discussed as potential drug delivery systems in the context of photoswitchable host-guest complexes.[20,21] However, a detailed investigation of the influence of the ammonium tag on the switching behavior of the azobenzene system has to our knowledge not been reported yet. Our study aims at filling this gap by providing extensive data for evaluating the impact of an ammonium tag on the isomerization and other photophysical properties of such a modified azobenzene derivative (Scheme 1).

Since the solvent environment has an important impact on the position of the maxima of absorption as well as stabilizing or destabilizing effects on the *Z*-isomer of the respective azobenzene, solvent influence should be considered for the design of photoresponsive systems. Initially, the influence of

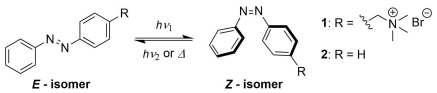

Scheme 1. Isomeric forms of two different azobenzenes investigated in this study.

[a] *M. A. Strauss, Prof. Dr. H. A. Wegner*
Institute of Organic Chemistry
Justus Liebig University Giessen
Heinrich-Buff-Ring 17, 35392 Giessen (Germany)
and
Center for Materials Research (LaMa)
Justus Liebig University Giessen
Heinrich-Buff-Ring 16, 35392 Giessen (Germany)
E-mail: hermann.a.wegner@org.chemie.uni-giessen.de

Supporting information for this article is available on the WWW under https://doi.org/10.1002/cptc.201800264

An invited contribution to a Special Issue on Photoresponsive Molecular Switches and Machines.

ChemPubSoc Europe

CHEMPHOTOCHEM Communications

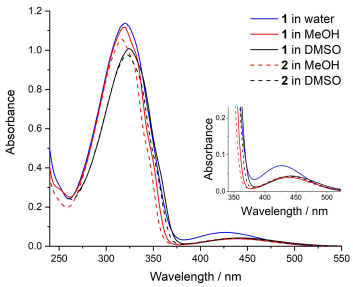

Figure 1. UV/Vis absorption spectra of azobenzenes **1** and **2** in different solvents at 25 °C (6×10^{-5} M).

the solvent on the absorption spectra of the selected azobenzenes was investigated. Water, methanol (MeOH) and dimethyl sulfoxide (DMSO) were chosen as solvents in this study. Figure 1 exemplifies the results of the solvent environment on the absorption of **1** and **2.**

As can be seen the impact on the π-π^* and the n-π^* absorption varies. In water or MeOH, the position of the π-π^* band is almost identical for **1** and only slightly blue-shifted for **2**. However, the n-π^* absorption for **1** in water shows an intensive blue shift, whereas for all other investigated samples, the position of the n-π^* band stays the same for both **1** and **2**. A distinct effect can also be observed in DMSO. Here, the π-π^* band is red shifted to a similar degree for both azobenzene derivatives compared to the protic solvents investigated.

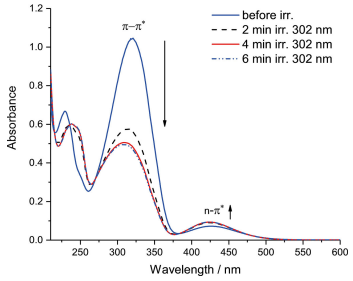

Figure 2. Changes in the UV/Vis absorption spectra of azobenzene **1** upon irradiation at 302 nm in water at 25 °C (6×10^{-5} M).

By irradiation at 302 nm, the ammonium-tagged compound **1** and the unsubstituted azobenzene **2** can be switched from the *E* to the *Z* state in all solvents examined. An example of the spectral changes upon isomerization in water for **1** is depicted in Figure 2. The decrease of the π-π^* band and the slight increase of the n-π^* is clearly visible upon irradiation. After 6 min, no further spectral changes were observed in this solvent. Both azobenzene derivatives can be switched by irradiation at this wavelength in the course of several minutes. Complete back-isomerization can be achieved by irradiating at 448 nm.

The rates for the *Z* to *E* isomerization in different solvents and at different temperatures were determined in order to gain insight into the stabilizing or destabilizing influence of the ammonium tag on the *Z*-isomer. Due to the different boiling points of the solvents, rates in methanol had to be measured at lower temperatures compared to water and DMSO. Table 1 shows the results of the determined isomerization rates at 30 °C as well as the activation parameters, which were determined by an Eyring-Polani analysis.

An accelerated isomerization for **1** in MeOH and DMSO compared to **2** was detected. This goes along with a higher activation enthalpy for the unsubstituted azobenzene **2**. The free energies of activation differ only to a small degree. Furthermore, it should be noted, that both compounds showed a slower isomerization in MeOH compared to DMSO. The highest difference was observed for the measurement in water. The isomerization of **1** proceeded about 75% slower than in the other solvents. This could be caused by a higher stabilization of the *Z*-isomer as our computations indicated (see below).

The solvents play not only an important role on the stability of the isomers, but also on the maximum accumulation of *Z*-isomer in solution. This is based on the often not well separated π-π^* absorption bands of the *E*- and the *Z*-isomer. The degree of overlap at a certain wavelength is responsible for the incomplete switching. This aspect was investigated by ^{1}H NMR, which allowed a very accurate quantification of the isomer composition in the respective solvents after irradiation to the photostationary states. As can be seen in Figure 3, the solvent has a significant effect on the isomer distribution at the photostationary state. Especially high polar solvents with a high permittivity (water: $\varepsilon = 78.36$, $\mu = 1.85$ D; DMSO: $\varepsilon = 46.84$, $\mu =$

Table 1. Experimental kinetic data of the thermal *Z* to *E* isomerization of **1** and **2** in different solvents. Energies are given in [kcal mol^{-1}], entropies in [cal K^{-1} mol^{-1}] and k values in [s^{-1}].

Cmpd.	Solvent	$k_{Z\text{-}E}$ [a]	$\Delta H^{\ddagger}_{Z\text{-}E}$	$\Delta S^{\ddagger}_{Z\text{-}E}$	$\Delta G^{\ddagger}_{Z\text{-}E}$ [b]
1	Water	$5.63\times10^{-7}\pm3\times10^{-9}$	24.6 ± 0.4	-6 ± 1	26.4 ± 0.7
	MeOH	$2.10\times10^{-6}\pm5\times10^{-8}$	22.9 ± 0.6	-9 ± 2	26 ± 1
	DMSO	$2.38\times10^{-6}\pm2\times10^{-8}$	22.1 ± 0.2	-11.6 ± 0.5	25.5 ± 0.3
2	MeOH	$1.48\times10^{-6}\pm2\times10^{-8}$	23.5 ± 0.3 [c]	-7.7 ± 0.7 [c]	25.8 ± 0.5 [c]
	DMSO	$2.07\times10^{-6}\pm3\times10^{-8}$	22.0 ± 0.6	-12 ± 2	26 ± 1

[a] At 30 °C; [b] at 25 °C; [c] calculated with results from Winkler et al.[22] Half-lives and isomerization rates for all measured temperatures are listed in the Supporting Information.

ChemPubSoc Europe
CHEMPHOTOCHEM Communications

3.96 D)[23] allow the enrichment of *Z*-isomer for **1** up to 20% more compared to methanol ($\varepsilon = 32.64$, $\mu = 1.70$ D).[23] The dipole moment seems to play only a minor role here. As Huang and co-workers reported, isomerization at 365 nm in D_2O can be performed to switch up to 70% of azobenzene **1** to the *Z*-isomer.[20] For azobenzene **2**, the differences between MeOH and DMSO are less significant, though more of the *Z*-isomer can be generated in DMSO.

Additionally, a computational study was performed to support the obtained experimental data. Special focus was laid on the activation parameters for the thermal *Z* to *E* isomerization. These results are depicted in Table 2 and allow the reproduction of the observed tendencies. The computations predict for both compounds a higher activation barrier in MeOH compared to DMSO, which was also observed in the experiments by the slower isomerization in MeOH. Furthermore, the free energy of activation for **1** in water was calculated to be the highest of all investigated samples, which was confirmed by the experiments.

Also the higher activation barrier for **2** in comparison to **1** is reproduced correctly. A minor discrepancy is that the computed total values of the free energies of activation is systematically too high, whereas the enthalpy of activation is underestimated in comparison to the experimental data. Application of a coupled-cluster method for determination of the single point energies might account for this problem. However, the data provide a valuable starting point for the evaluation of the isomerization pathway of **1**.

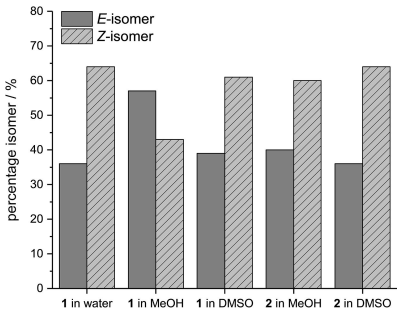

Figure 3. Isomer distribution in solutions of **1** and **2** at the photostationary state upon irradiation at 302 nm at 25 °C (3.7×10^{-2} M).

Table 2. Computed thermodynamic parameters [B2PLYP-D3/def2-TZVP//B3LYP-D3/def2-TZVP, SMD[26] solvent model for single point energies] at 25 °C ($\Delta H_{Z\text{-}E}$, $\Delta G_{Z\text{-}E}$) and the computed activation energy of the thermal conversion from *Z* to *E* in [kcal mol^{-1}] ($\Delta H^{\ddagger}_{Z\text{-}E}$, $\Delta G^{\ddagger}_{Z\text{-}E}$).

Cmpd.	Solvent	$\Delta H_{Z\text{-}E}$	$\Delta G_{Z\text{-}E}$	$\Delta H^{\ddagger}_{Z\text{-}E}$	$\Delta G^{\ddagger}_{Z\text{-}E}$
1	Water	10.5	11.1	28.2	28.1
	MeOH	11.8	12.3	26.9	26.9
	DMSO	12.2	12.7	26.7	26.6
2	MeOH	12.2	12.7	28.1	27.6
	DMSO	12.6	13.1	27.8	27.2

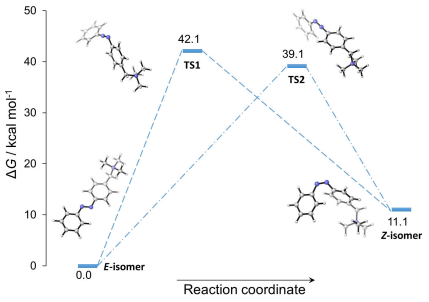

Figure 4. Computed relative energies for the *E*→*Z* transition of **1** at 25 °C in methanol. Structures were visualized by CYLview.[24] [B2PLYP-D3/def2-TZVP//B3LYP-D3/def2-TZVP, SMD solvent model].

As can be seen by the computed energies in Figure 4, the isomerization of **1** is most likely proceeding via the transition state **TS2** with the linear N–N–C moiety including the phenyl ring with the ammonium tag. The activation barrier here is about 3 kcal/mol lower than for the transition via **TS1**. The geometries of the transition states are consistent with previously reported geometries for non-push-pull azobenzenes for which an isomerization pathway dominated by inversion is assumed.[25] Our studies indicate, that rotating the ammonium tag by 180° has only a minor effect (~0.5 kcal/mol) on the total energy of the structures. This energy difference lies in the range of the uncertainty of the computational method. Further detailed information concerning the structures at several states is displayed in the SI.

In conclusion, we presented a comprehensive study on the influence of an ammonium tag substituent on the photophysical properties of an azobenzene derivative. Furthermore, the effect of different solvents has been evaluated. The results provide essential background information on the influence of the charge attached on the switching properties, which will be of special interest for applications in photopharmacology or water-based host-guest chemistry.

Experimental Section

Detailed information on the applied synthesis procedures can be derived from the Supporting Information.

The computations were performed with the Gaussian 16 software package.[27] Geometry optimizations were performed at a B3LYP-D3 level using the def2-TZVP basis set.[28] Molecular structures were visualized using the CYLview software.[24] Single point energy (SPE) computations on a B2PLYP-D3/def2-TZVP level were conducted using the previously optimized B3LYP structures.[29]

ChemPubSoc Europe

CHEMPHOTOCHEM Communications

Acknowledgements

Financial support was provided by the Justus Liebig University Giessen and by the Deutsche Forschungsgemeinschaft (SPP1807). We thank Dr. Heike Hausmann and Anja Platt for NMR support, Simon Becher for FT-ICR-MS measurements and Julia Ruhl for the fruitful discussions.

Conflict of Interest

The authors declare no conflict of interest.

Keywords: azobenzene · kinetics · molecular switches · photopharmacology · solvent effects

[1] a) R. R. Birge, *Biochim. Biophys. Acta Bioenerg.* **1990**, *1016*, 293–327; b) T. Yamashita, H. Ohuchi, S. Tomonari, K. Ikeda, K. Sakai, Y. Shichida, *Proc. Natl. Acad. Sci. USA* **2010**, *107*, 22084–22089; c) A. Möglich, X. Yang, R. A. Ayers, K. Moffat, *Annu. Rev. Plant Biol.* **2010**, *61*, 21–47; d) G. Nagel, D. Ollig, M. Fuhrmann, S. Kateriya, A. M. Musti, E. Bamberg, P. Hegemann, *Science* **2002**, *296*, 2395–2398; e) M. Chen, M. Schliep, R. D. Willows, Z.-L. Cai, B. A. Neilan, H. Scheer, *Science* **2010**, *329*, 1318–1319; f) A. Losi, W. Gärtner, *Photochem. Photobiol. Sci.* **2008**, *7*, 1168–1178.

[2] a) Y. Liu, X. Gao, D. Wei, Y. Ren, *ChemPhotoChem* **2017**, *1*, 393–396; b) W. Szymański, J. M. Beierle, H. A. V. Kistemaker, W. A. Velema, B. L. Feringa, *Chem. Rev.* **2013**, *113*, 6114–6178; c) B. Schierling, A.-J. Noël, W. Wende, T. Le Hien, E. Volkov, E. Kubareva, T. Oretskaya, M. Kokkinidis, A. Römpp, B. Spengler, *Proc. Natl. Acad. Sci. USA* **2010**, *107*, 1361–1366; d) R. Mogaki, K. Okuro, T. Aida, *J. Am. Chem. Soc.* **2017**, *139*, 10072–10078; e) W. Heu, J. M. Choi, H.-H. Kyeong, Y. Choi, H. Y. Kim, H.-S. Kim, *Angew. Chem. Int. Ed.* **2018**, *57*, 10859–10863.

[3] a) X. M. M. Weyel, M. A. H. Fichte, A. Heckel, *ACS Chem. Biol.* **2017**, *12*, 2183–2190; b) W. A. Velema, J. P. van der Berg, W. Szymanski, A. J. M. Driessen, B. L. Feringa, *ACS Chem. Biol.* **2014**, *9*, 1969–1974; c) N. J. Hauwert, T. A. M. Mocking, D. Da Costa Pereira, A. J. Kooistra, L. M. Wijnen, G. C. M. Vreeker, E. W. E. Verweij, A. H. de Boer, M. J. Smit, C. de Graaf, *J. Am. Chem. Soc.* **2018**, *140*, 4232–4243; d) S. Passlick, M. T. Richers, G. C. R. Ellis-Davies, *Angew. Chem. Int. Ed.* **2018**, *57*, 12554–12557.

[4] a) J. Hemphill, E. K. Borchardt, K. Brown, A. Asokan, A. Deiters, *J. Am. Chem. Soc.* **2015**, *137*, 5642–5645; b) Y. Nihongaki, S. Yamamoto, F. Kawano, H. Suzuki, M. Sato, *Chem. Biol.* **2015**, *22*, 169–174.

[5] a) N. H. Wassermann, E. Bartels, B. F. Erlanger, *Proc. Natl. Acad. Sci. USA* **1979**, *76*, 256–259; b) N. H. Wassermann, A. S. Penn, P. I. Freimuth, N. Treptow, S. Wentzel, W. L. Cleveland, B. F. Erlanger, *Proc. Natl. Acad. Sci. USA* **1982**, *79*, 4810–4814.

[6] a) J. Broichhagen, T. Podewin, H. Meyer-Berg, Y. von Ohlen, N. R. Johnston, B. J. Jones, S. R. Bloom, G. A. Rutter, A. Hoffmann-Röder, D. J. Hodson, *Angew. Chem. Int. Ed.* **2015**, *54*, 15565–15569; b) J. Broichhagen, T. Podewin, H. Meyer-Berg, Y. von Ohlen, N. R. Johnston, B. J. Jones, S. R. Bloom, G. A. Rutter, A. Hoffmann-Röder, D. J. Hodson, *Angew. Chem.* **2015**, *127*, 15786–15790.

[7] Y.-H. Tsai, S. Essig, J. R. James, K. Lang, J. W. Chin, *Nat. Chem.* **2015**, *7*, 554–561.

[8] M. Borowiak, W. Nahaboo, M. Reynders, K. Nekolla, P. Jalinot, J. Hasserodt, M. Rehberg, M. Delattre, S. Zahler, A. Vollmar, *Cell* **2015**, *162*, 403–411.

[9] J. A. Frank, H. G. Franquelim, P. Schwille, D. Trauner, *J. Am. Chem. Soc.* **2016**, *138*, 12981–12986.

[10] J. Broichhagen, J. A. Frank, D. Trauner, *Acc. Chem. Res.* **2015**, *48*, 1947–1960.

[11] C. Hoppmann, P. Schmieder, P. Domaing, G. Vogelreiter, J. Eichhorst, B. Wiesner, I. Morano, K. Rück-Braun, M. Beyermann, *Angew. Chem. Int. Ed.* **2011**, *50*, 7699–7702.

[12] S. Keiper, J. S. Vyle, *Angew. Chem. Int. Ed.* **2006**, *45*, 3306–3309.

[13] A. Yamazawa, X. Liang, H. Asanuma, M. Komiyama, *Angew. Chem. Int. Ed.* **2000**, *39*, 2356–2357.

[14] W. A. Velema, J. P. van der Berg, M. J. Hansen, W. Szymanski, A. J. M. Driessen, B. L. Feringa, *Nat. Chem.* **2013**, *5*, 924–928.

[15] S. Bellotto, S. Chen, I. Rentero Rebollo, H. A. Wegner, C. Heinis, *J. Am. Chem. Soc.* **2014**, *136*, 5880–5883.

[16] C. Matera, A. M. J. Gomila, N. Camarero, M. Libergoli, C. Soler, P. Gorostiza, *J. Am. Chem. Soc.* **2018**, *140*, 15764–15773.

[17] a) A. Polosukhina, J. Litt, I. Tochitsky, J. Nemargut, Y. Sychev, I. de Kouchkovsky, T. Huang, K. Borges, D. Trauner, R. N. van Gelder, *Neuron* **2012**, *75*, 271–282; b) L. Laprell, K. Hüll, P. Stawski, C. Schön, S. Michalakis, M. Biel, M. P. Sumser, D. Trauner, *ACS Chem. Neurosci.* **2016**, *7*, 15–20.

[18] a) M. J. Hansen, M. M. Lerch, W. Szymanski, B. L. Feringa, *Angew. Chem. Int. Ed.* **2016**, *55*, 13514–13518; b) M. J. Hansen, M. M. Lerch, W. Szymanski, B. L. Feringa, *Angew. Chem.* **2016**, *128*, 13712–13716; c) M. Dong, A. Babalhavaeji, S. Samanta, A. A. Beharry, G. A. Woolley, *Acc. Chem. Res.* **2015**, *48*, 2662–2670.

[19] E. C. Carroll, S. Berlin, J. Levitz, M. A. Kienzler, Z. Yuan, D. Madsen, D. S. Larsen, E. Y. Isacoff, *Proc. Natl. Acad. Sci. USA* **2015**, *112*, E776-85.

[20] D. Xia, G. Yu, J. Li, F. Huang, *Chem. Commun.* **2014**, *50*, 3606–3608.

[21] a) L. Shao, B. Hua, J. Sun, Q. Li, J. Yang, G. Yu, *Tetrahedron Lett.* **2017**, *58*, 1863–1867; b) G. Yu, C. Han, Z. Zhang, J. Chen, X. Yan, B. Zheng, S. Liu, F. Huang, *J. Am. Chem. Soc.* **2012**, *134*, 8711–8717.

[22] C. A. Winkler, J. Halpern, G. W. Brady, *Can. J. Res.* **1950**, *28b*, 140–155.

[23] D. R. Lide (Ed.) *CRC handbook of chemistry and physics. A ready-reference book of chemical and physical data*, CRC Press, Boca Raton, **2004**.

[24] C. Y. Legault, *CYLview*, **2009**, Université de Sherbrooke, Quebec, Canada, can be found under http://www.cylview.org.

[25] J. Dokić, M. Gothe, J. Wirth, M. V. Peters, J. Schwarz, S. Hecht, P. Saalfrank, *J. Phys. Chem. A* **2009**, *113*, 6763–6773.

[26] A. V. Marenich, C. J. Cramer, D. G. Truhlar, *J. Phys. Chem. B* **2009**, *113*, 6378–6396.

[27] M. J. Frisch, G. W. Trucks, H. B. Schlegel, G. E. Scuseria, M. A. Robb, J. R. Cheeseman, G. Scalmani, V. Barone, G. A. Petersson, H. Nakatsuji, *Gaussian 16 Rev. B.01*, **2016**, Wallingford, CT.

[28] a) A. D. Becke, *J. Chem. Phys.* **1993**, *98*, 5648–5652; b) C. Lee, W. Yang, R. G. Parr, *Phys. Rev. B* **1988**, *37*, 785–789; c) S. Grimme, *J. Comput. Chem.* **2004**, *25*, 1463–1473; d) F. Weigend, R. Ahlrichs, *Phys. Chem. Chem. Phys.* **2005**, *7*, 3297–3305.

[29] S. Grimme, *J. Chem. Phys.* **2006**, *124*, 34108.

Manuscript received: December 22, 2018
Revised manuscript received: January 22, 2019
Accepted manuscript online: January 24, 2019
Version of record online: February 13, 2019

4.4 Molecular Systems for the Quantification of London Dispersion Interactions

Reference:

M. A. Strauss, H. A. Wegner, *Eur. J. Org. Chem.*, **2019**, *2-3*, 295-302.
DOI: 10.1002/ejoc.201800970

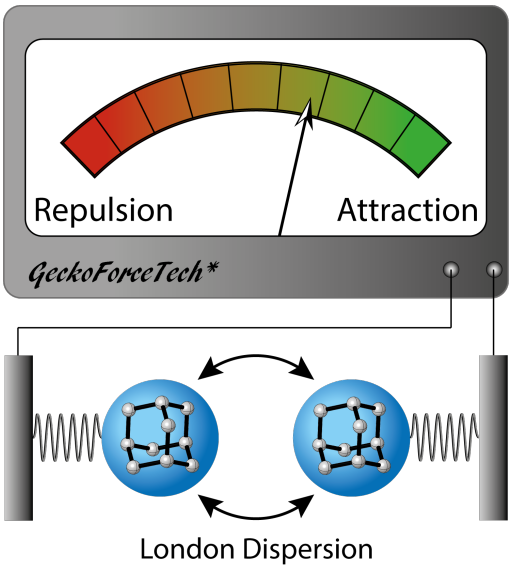

"In recent years the importance of London dispersion forces as the attractive part of the van der Waals potential has been recognized for structural stability, catalysis and chemical reactivity. Though known for decades, the determination of the strength of dispersive interactions between certain groups remains a challenging task. Geometrically well-defined molecular model systems offer the possibility to systematically examine and quantify the London dispersion contribution to interaction energies. The incorporation of control systems in the analysis allows dissecting the interaction of interest from other effects. The knowledge gained from these endeavours will provide the necessary basis to include London dispersion in the design of chemical processes and functional materials."

ChemPubSoc Europe
DOI: 10.1002/ejoc.201800970
EurJOC European Journal of Organic Chemistry
Microreview
Check for updates

Measuring London Dispersion* | *Very Important Paper* | SPECIAL ISSUE

VIP

Molecular Systems for the Quantification of London Dispersion Interactions

Marcel A. Strauss[a] and Hermann A. Wegner*[a]

Abstract: In recent years the importance of London dispersion forces as the attractive part of the van der Waals potential has been recognized for structural stability, catalysis and chemical reactivity. Though known for decades, the determination of the strength of dispersive interactions between certain groups remains a challenging task. Geometrically well-defined molecular model systems offer the possibility to systematically examine and quantify the London dispersion contribution to interaction energies. The incorporation of control systems in the analysis allows dissecting the interaction of interest from other effects. The knowledge gained from these endeavours will provide the necessary basis to include London dispersion in the design of chemical processes and functional materials.

1. Introduction

Van der Waals interactions are a unique type of non-covalent interactions, which play a significant, but often underestimated, role for structural stability[1] as well as catalysis[2] and chemical reactivity. The attractive part of the van der Waals interaction has been termed "London dispersion", after F. London,[3] who formulated its existence already more than eight decades ago. Only in recent years the implementation of the concept of London dispersion in molecular synthesis has been proven very effective, allowing to compose compounds with extreme long C–C bonds,[4] stabilize organometallic compounds,[5] such as iron and cobalt complexes in an unusually high +4 oxidation state[6] or to overcome repulsion by accomplishing the shortest intermolecular H–H contact,[7] just to name a few examples. Also in nature the importance of London-dispersion forces has been shown by a multitude of scientific investigations.[8] They play a significant role, in particular for large molecules such as proteins, and can greatly contribute to their thermal stability.[9] In addition, they also take part in the formation of bacterial biofilms[10] or allow densely packed membranes in certain bacteria.[11] Moreover, analytical applications can benefit from integrating London dispersion in auxiliary tools. For example, a crystalline porous material was accessed via self-assembling induced by London dispersion and aromatic interactions, which permits X-ray characterization of built-in molecular guests.[12]

Due to the ubiquitous appearance of such a fundamental interaction, several attempts for investigating attractive dispersive effects in molecules were initiated, which were further driven by increased performance in the field of computational chemistry.[13] In recent years, the term "dispersion energy donors" was proposed for substituents in close proximity with

[a] *Institute of Organic Chemistry, Justus-Liebig University Giessen, Heinrich-Buff-Ring 17, 35392 Giessen, Germany*
E-mail: hermann.a.wegner@org.chemie.uni-giessen.de
http://www.uni-giessen.de/fbz/fb08/Inst/organische-chemie/Wegner
ORCID(s) from the author(s) for this article is/are available on the WWW under https://doi.org/10.1002/ejoc.201800970.

Hermann A. Wegner studied chemistry in Göttingen, Boston and Stanford. After a postdoc at the University of Oxford he started his independent career at the University of Basel before taking up his current position as Professor of Organic Chemistry at the Justus Liebig University, Giessen. His research is driven by investigating and applying fundamental concepts of physical organic chemistry in the area of catalysis (bidentate Lewis acid catalysis), and molecular materials (molecular switches and non-planar aromatics).

Marcel A. Strauss started his studies in chemistry at the Justus Liebig University Giessen in 2009. He received a bachelor degree in 2012 and his master degree in 2015. He is currently working towards his PhD in organic chemistry in the group of Prof. Hermann A. Wegner. His research is focused on azobenzenes and London dispersion interactions.

ChemPubSoc Europe
EurJOC European Journal of Organic Chemistry
Microreview

high polarizability due to their stabilizing contribution for exceptional bonding situations.[14]

London dispersion forces have their origin in an electron correlation effect, which can be described as an induced-dipol-induced-dipole interaction. This effect can be divided further into a short range and a long rage effect.[15] The maximum of attraction is reached when two molecular fragments A and B are situated in a distance, which equals the sum of their van der Waals radii. Further approach then leads to repulsion caused by the Pauli exclusion.

$$E_{\mathrm{Disp}} = -\frac{1}{2}\sum_{\mathrm{A,B}} C_6^{AB}/r_{AB}^6$$

The mathematical description for the attraction is shown by the equation above, where C_6 stands for empirical polarization coefficients of the involved atoms. The distance contributes with r^{-6} to the dispersion energy, demonstrating that the dispersion interaction through space attenuates much faster than Coulomb interactions. Although known for a long time, the specific effect of a particular group on London dispersion is difficult to quantify. However, such knowledge would greatly enhance the possibility to utilize London dispersion as design element in synthesis and molecular structure.

2. Quantifying London Dispersion

The evaluation of London dispersion by experimental methods is challenging due to the low energy contributions within medium-sized organic molecules. Apart from simple alkanes, for which London dispersion contributes the most to the attractive interactions, more complex molecules often provide anchor points for other non-covalent interactions exceeding the London dispersion in strength. This includes interactions such as hydrogen-bonding,[16] π–π-,[17] CH–π-[18] or ionic interactions[19] and even chalcogen–chalcogen bonds.[20] Hence, in most of the cases, London dispersion is the least dominant interaction, which provides difficulties to separate the dispersion effects from others. Furthermore, the origin of weak interactions in solution might also be solvophobic interactions, especially in high polar solvents such as DMSO.[21] In order to rule out solvophobic effects as the main source for weak interactions, screening of solvents with different polarity can be helpful.[22] In this context different experimental approaches have been tested. One most promising one is the use of molecular scaffolds which can adopt two different conformations of which one is stabilized by the interactions to be measured (Figure 1).[23] Such molecular balances, however, require consideration of the relative stabilities of all accessible conformations, which for very flexible molecules are not possible to address by experimental means. Therefore, it is necessary to confine the number of conformations in such a model system to obtain reliable thermodynamic information. This is often done by introducing sterically demanding groups for increasing the strain limiting the conformational freedom. One of the most important aspects in designing a probe for London dispersion remains the unambiguous assignment of the conformers since chemical intuition is sometimes misleading like in the case of trineopentylbenzene (Scheme 1).[24]

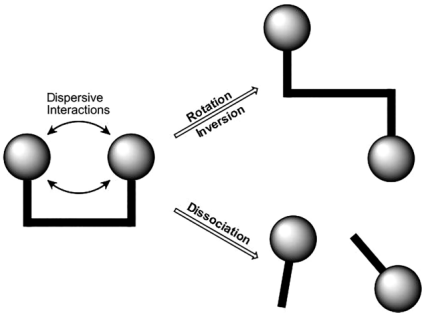

Figure 1. Conceptual model system for determination of equilibria positions influenced by London dispersion forces.

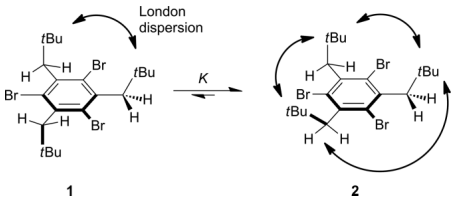

Scheme 1. Dynamic NMR measurements of 1,3,5-tribromo-2,4,6-trineopentylbenzene in fluorobenzene showed that the *all-cis* conformation **2** is favoured over its conformer **1**.

In addition, application of a thermodynamic double-mutant cycle has turned out to be beneficial in several investigations for experimental determination of non-covalent interactions in synthetic systems.[25] The concept stems from biology, where it is applied to determine the strength of intramolecular and intermolecular non-covalent interactions in proteins or protein–ligand complexes.[26] Referencing to suitable control compounds permits to dissect the desired interaction energy from other background influences like solvent or secondary intramolecular interactions. Sigman and co-workers could recently show the potential of having a precise model with defined interaction parameters helping to develop structure–function relationships for catalytic systems.[27] Their concept is currently under investigation for dispersion forces.

Despite the conceptual difficulties, benefits from an extensive data set allowing evaluating stabilizing effects of specific dispersion energy donors will be of enormous value in many fields of chemistry like catalysis, total synthesis or material science.

3. Molecular Balances for Determination of London Dispersion

An effective approach for the investigation of dispersion contribution lies in the use of molecular balances. These systems normally can adopt two different states, which are associated with

ChemPubSoc Europe
EurJOC European Journal of Organic Chemistry
Microreview

either a dispersion stabilized conformer or with the conformer destabilized by steric repulsion. A high degree of symmetry in these model systems simplifies the analysis, allowing determination of the equilibrium positions with reliable spectroscopic methods such as NMR spectroscopy.

3.1. Torsion Balances for Determination of London Dispersion Interactions

In 1994 Wilcox and co-workers used derivatives of Tröger's base of which two conformers can interconvert by slow rotation to determine edge-to-face aromatic interactions. They measured the ratio of the two conformers in equilibrium by NMR at 298 K (Scheme 2).[28] Surprisingly, they observed that the influence of cyclohexyl–aryl interactions or *tert*-butyl–aryl interactions on the dynamic equilibrium leading to folding of the molecule is equally important than the edge-to-face interaction of the aryl esters. Furthermore, they found that changing the solvent had only a negligible effect on the observed folded:unfolded ratio.

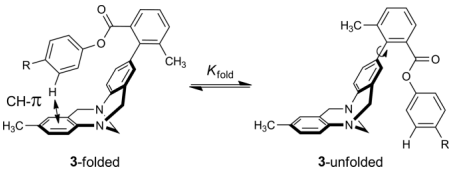

Scheme 2. Rotamer equilibrium of Wilcox' balance **3**.

A successive project by the Wilcox group with such type of balances aimed at determining the importance of changes in molecular electrostatic potential or dispersion forces on aryl–aryl or alkyl–aryl interactions.[29] The data was consistent with the dominance of dispersion forces for such edge-to-face binding events.

Due to good synthetic accessibility of derivatives of this Tröger's base torsion balance, many research groups applied this concept for their investigations of intramolecular interactions. The group of Cockroft further developed such molecular balances with the intent to measure interactions between apolar alkyl chains in 31 organic, fluorous and aqueous solvent environments.[30] For this endeavor, they modified the framework with alkyl chains providing an extended alkyl–alkyl contact in order to maximize the contribution of dispersion forces on the conformational equilibrium. The contact of the alkyl chains in the folded conformer was also confirmed by X-ray crystallography. This study further included a thermodynamic double-mutant cycle, which allowed them to estimate the alkyl–alkyl interaction energy of interest from the experimental interaction energies. Their findings revealed a very large cancellation of dispersion forces due to competitive dispersion interactions with the solvent. In apolar organic solvents, the alkyl–alkyl interactions were marginally disfavored, whereas they were slightly favored in organic solvents with increased polarity. In high polar solvents, they found evidence, that solvophobic effects are driving the alkyl–alkyl association to the folded state (Scheme 3).

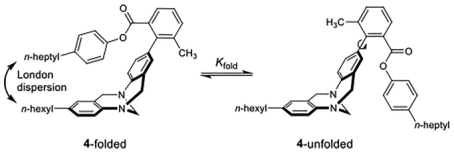

Scheme 3. Rotamer equilibrium of modified balance **4** by Cockroft.

According to Cockroft, the cancellation of dispersion forces is likely to be highly dependent on the solvent accessibility of the interacting molecular surfaces. Furthermore, competitive dispersion interactions of the solute with the solvent can be an explanation for the reduced alkyl–alkyl interaction energies. Since these observations could not accurately be described by computational models that take dispersion forces into account, they suggest to use them with caution in situations where competitive dispersion interactions with the solvent are possible.

In another study, the group of Cockroft further extended their investigations to perfluoroalkyl-perfluoroalkyl cohesion applying the same methodology using synthetic molecular torsion balances.[31] The dissected alkyl–alkyl and perfluoroalkyl-perfluoroalkyl interaction energies were in a range of $<\pm$ 2 kJ mol^{-1}. These results were consistent with a large attenuation of intramolecular dispersion forces due to competitive interactions with the solvent. Experimental differences for the self-assembling of alkyl vs. perfluoroalkyl chains corroborate dependency of the degree of attenuation on the bulk polarizability of the solvent. The contributions of van der Waals dispersion and solvophobic effects to the position of the equilibrium geometries of the molecular balances could be dissected by linear regression. Their results indicate a dominant influence in fluorous and apolar organic solvents due to differences in dispersion interactions. They further demonstrated the utility of solvent cohesive energy density as parameter for quantifying the solvophobic effects in a range of organic solvents.[32]

A rigid bicyclic *N*-arylimide framework was used as a template for Shimizu's balance system (Scheme 4). They aimed at determining the contributions of London dispersion forces to the strength of aromatic stacking interactions in solution.[33] Intramolecular stacking interactions were measured via a conformational equilibrium. Size and polarizability of one of the aromatic surfaces were systematically increased and the stacking interaction energies were corrected for solvophobic, linker, and electrostatic substituent effects by using control systems, geometrical constraints and various solvents. The variations due to polarizability were found to be an order of magnitude smaller in solution than in comparison to analogous computational studies in vacuo. Their results indicated relatively minor dispersion contributions to the aromatic stacking interaction in solution. They further concluded that dispersion interactions of aromatic surfaces formed with solvent molecules dominate in solution, which attenuates the overall magnitude of the dispersion term within the molecules. This deduction, however, contrasts with computational studies and gas-phase studies. A closer look at the stabilizing and destabilizing effects of alkyl groups on an intramolecular aromatic interaction revealed the

ChemPubSoc Europe
EurJOC European Journal of Organic Chemistry
Microreview

sensitive interplay of distance and van der Waals contact areas.[34] The surface contact areas derived from the van der Waals contact areas of X-ray structures turned out to be a powerful parameter for predicting stabilizing and repulsive effects of alkyl groups. The optimal H–H contact distances for stabilization could thereby be determined in the range of 2.5 to 3.0 Å.

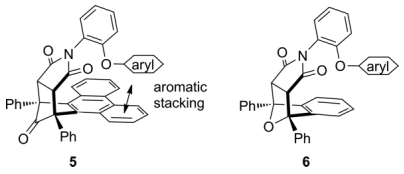

Scheme 4. Balance scaffold **5** used by Shimizu to investigate aromatic stacking reactions and control balance **6** showing no interactions.

The application of torsion balances for investigation of weak dispersive interactions provided substantial insights into the sensitivity of the strength of interactions towards solvent effects and interacting surface areas. However, the need to use control systems for effectively dissecting secondary effects like solvophobic, linker or electrostatic interactions complicate the studies of the targeted weak dispersion forces.

3.2. Cyclooctatetraene Balances

With the intent to design a new ligand, Streitwieser et al. prepared 1,4-di-*tert*-butylcyclooctatetraene and observed an unanticipated effect in regard to double bond isomerism.[35] The compound exists as an equilibrium mixture of the two double bond isomers, 1,4-di-*tert*-butylcyclooctatetraene **7d** and the 1,6-isomer **8d** (Scheme 5). In contradiction to the general expectation, the 1,6-isomer, in which both *tert*-butyl groups are located on the same side of the molecule, is actually more stable. It was reasoned, that the *tert*-butyl groups in the 1,6-isomer

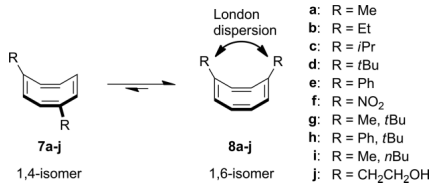

Scheme 5. Inversion of 1,4-substituted cyclooctatetraene **7** to the more stable 1,6-substituted cyclooctatetraene **8** by double bond isomerism.

are positioned at the edge of steric repulsion and intramolecular van der Waals attraction dominates.

The group of Paquette et al. were able to confirm this unusual stability for 1,6-di-*tert*-butylcyclooctatetraene **8d** by their studies. They also observed a solvent dependency of this phenomenon.[36] The exceptional system with its distinct property also raised the interest of theoreticians, who performed computational studies and supported the assumption of Streitwieser, that van der Waals attraction is responsible for the counterintuitive observed stability of the 1,6-di-*tert*-butylcyclooctatetraene **8d**.[37]

Kirsch and co-workers intensified the NMR experiments on the bond-shift equilibrium between the 1,6- **8** and 1,4-dialkylcyclooctatetraenes **7**.[38] They increased stepwise the size of the alkyl substituents from methyl to *tert*-butyl and prepared also derivatives with two nitro- or two phenyl residues. They confirmed the temperature-dependency of the equilibria position of the 1,6-isomer **8** for each derivative and determined a lower enthalpy and entropy than for the 1,4-isomer **7**. Although they detected only minor changes of the equilibrium position, the overall tendency that with increasing size of the alkyl substituents, the 1,6-isomer **8** is more preferred, is clearly observed (Table 1). To obtain a greater insight into this phenomenon, they further conducted molecular mechanics calculations for some derivatives. These studies revealed that the difference in energy of the 1,4- and 1,6-isomers is based on attractive interactions in the latter compound.

The cyclooctatetraene model has the potential as a convenient probe to determine the influence of the solvent system on dispersion interactions since minor changes can be easily followed by NMR spectroscopy. Applying up-to-date computational methods might further help to describe the strength of London dispersion contribution to the increased stability of the 1,6-isomer **8**, which might provide useful guidelines for the design of other systems. The absence of heteroatoms further excludes electrostatic interactions.

3.3. Thiobarbiturate Balance System

In 1987 Berg et al. developed a model system based on thiobarbiturates **9** (Scheme 6), for which the conformational distribution is mainly caused by attractive van der Waals interactions. The structural composition allows the unequivocal assignments of NMR signals to the corresponding conformers.[39] Utilization of the six-membered barbiturate system increased the barrier for rotation, allowing to detect even changes with substituents smaller than neopentyl. At −70 °C subspectra were observed, which could be assigned to the *syn* and *anti* conformers. The

Table 1. Experimental enthalpy and entropy differences for the **8** ⇄ **7** equilibrium for dialkylcyclooctatetraenes.[a]

Compound and alkyl group	$-\Delta H$ [kcal mol^{-1}]	$-\Delta S$ [cal mol^{-1} K^{-1}]	Correlation coefficient	$-\Delta G$ 20 °C [kcal mol^{-1}]
8a-7a Methyl	0.05	+0.3	0.064	0.08
8b-7b Ethyl	0.52	−1.0	0.851	0.24
8c-7c Isopropyl	0.61	−1.0	0.837	0.36
8d-7d *tert*-Butyl	1.14	−2.5	0.952	0.39[b]

[a] Calculated from $\log_{10}K_{eq} = -\Delta H\,(2.3RT)^{-1} + -\Delta S\,(2.3R)^{-1}$. The 1,6-isomer **8** is the more stable in each case and has the lower entropy, except for the methyl compound **8a**. [b] 25 °C in deuteriochloroform, whereas other results are in benzene.

ChemPubSoc Europe
EurJOC European Journal of Organic Chemistry
Microreview

correct identification of the signals was further confirmed by an NOE difference experiment.

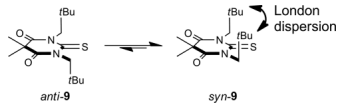

Scheme 6. Two conformers of thiobarbiturate balance **9** for determination of solvent influence on *syn*/*anti* equilibrium position.

For these experiments, signals of the *gem*-dimethyl groups of **9** functioned as the conformational probe. Solvent effects on the equilibrium position between the *syn*/*anti* conformers seemed to result from an interaction with the thiobarbiturate system **9** and the solvent. This assumption is indicated by comparison with a similar 1,3-dineopentyl-4,5-dimethyl-imidazoline-2-thione probe **10** (Scheme 7). For the second system, the relation of *syn* and *anti* conformers is not changed by the solvent. Their conclusion, that the more crowded *syn* conformation of **10** is preferred mainly due to intramolecular attractive dispersion forces was also supported by molecular mechanics calculations.

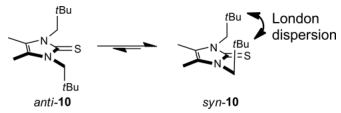

Scheme 7. Two conformers of imidazoline-2-thione based system **10** for determination of solvent influence on *syn*/*anti* equilibrium position.

The reliable assignment of the NMR signals to the corresponding conformers and the easy monitoring of the equilibrium positions are definitely an advantage of this system. However, allocating solvent effects on dispersive interactions to the interacting alkyl residues is difficult due to the high sensitivity of the thiobarbiturate scaffold for solvent interactions.

4. Dissociation Systems

Another way to quantify the contribution of dispersion donors can be done by investigating the stability of a parent molecular system, which is modified systematically by different dispersion donor groups. Direct comparison of kinetic or thermodynamic data will provide insight into the attractive or repulsive contributions of the investigated groups when other parameters are kept constant. Such experimentally well accessible data could be equilibrium constants or bond dissociation energies. Furthermore, rate constants for isomerization allow in accordance with the Bell-Evans-Polany principle to deduce changes of the reaction enthalpies.[40,41]

4.1. The Azobenzene Molecular Switch as Tool for Quantification of London Dispersion

General textbook knowledge states that the *Z*-isomer of double bonds, including azobenzenes, is less stable due to steric strain, which is supported in the case of aliphatic azo compounds by the group of Ruechardt.[41] However, this explanation seems to be not universally applicable to azobenzenes. By direct comparison of thermal *Z*→*E* isomerization rates of unsubstituted azobenzene (**11a**)[42] with 3,3′,5,5′-tetra-*tert*-butylazobenzene (**11e**),[43] it is observed that the *Z*-isomer of the more crowded *tert*-butyl-substituted compound is kinetically more stable by nearly one order of magnitude (Scheme 8).

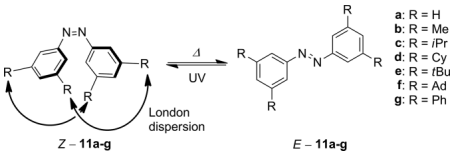

Scheme 8. Investigation of the thermal *Z*→*E* isomerization of seven differently substituted azobenzenes **11**. (Ad = adamantyl, Cy = cyclohexyl).

In a recent study, we were able to show that substitution with bulky alkyl residues, which function as large dispersion energy donors, stabilize the *Z*-isomer of azobenzenes **11** (Scheme 8).[44] For this systematic study, seven differently substituted azobenzenes were prepared and by measuring the rates for thermally induced *Z*- to *E*-isomerization, a distinct tendency was observed, which contradicts the intuitive expectation, that bulky substituents destabilize *Z*-azobenzenes.

The experimental results clearly show that the larger the alkyl residues, the higher the half-lives of the *Z*-isomer. The effect was also present independent of the solvent, in *n*-octane as well as in a very polar solvent such as DMSO (Figure 2).

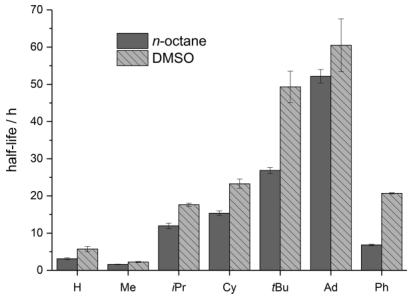

Figure 2. Half-lives of all-*meta*-substituted azobenzenes **11a**–**g** in *n*-octane and DMSO at 53 °C.[44]

Computations revealed, that the contributions of London dispersion for stabilization are mainly present in the *Z*-isomer and not in the transition state. Since the activation barrier for *E*- to *Z*-isomerization was only marginally changed by different substituents, we concluded, that a thermodynamic stabilization of the *Z*-isomer is responsible for these findings, which is mainly caused by attractive London dispersion interactions (Figure 3).

The ease of modifying the azobenzene scaffold as well as measuring the isomerization rates, render the azobenzene

ChemPubSoc Europe
EurJOC European Journal of Organic Chemistry
Microreview

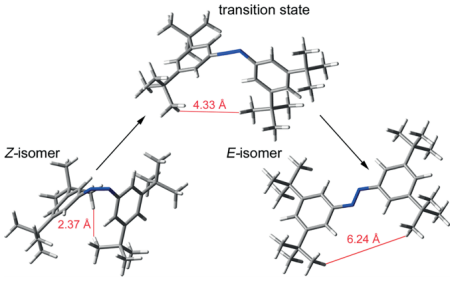

Figure 3. Optimized geometries of the *Z*-, the *E*-isomer and the transition state of the thermal isomerization of all-*meta*-*tert*-butylazobenzene **11e** [B3LYP-D3/6-311G(d,p)].[44]

molecular switch highly suitable to investigate the stabilizing effect of various dispersion donors, even in case of two different interacting groups. In contrast to the molecular balances described in section 3 the azobenzene isomerization from *Z* to *E* is not an equilibrium as there is no *Z*-isomer present at the end of the isomerization and can be treated like dissociation of two (dispersion donor) groups.

4.2. Proton-Bound-*N*-Heterocyclic Dimer Dissociation for Investigating London Dispersion

Peter Chen and co-workers examined the degree of contribution of London dispersion to the bond dissociation energy of a wide variety of proton-bound *N*-heterocyclic dimers in the gas phase as well as in solution (Scheme 9).[45] Gas-phase dissociation energies were determined experimentally by threshold collision-induced-dissociation measurements (T-CID) and compared with values obtained by computational methods. NMR studies were conducted over a wide temperature range to obtain free dissociation energies in solution by measurement of the equilibrium constants.

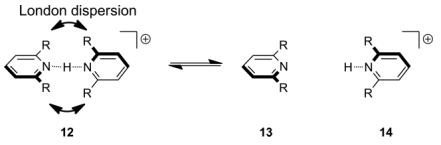

Scheme 9. Proton-bound *N*-heterocyclic dimer scaffold for determination of the influence of different substituents on the bond dissociation energy in solution.

Their test-systems are based *i.a.* on pyridines, quinolines, acridines, and tertiary amines. These core structures were modified remote from the central N–H–N bond with substituents with limited flexibility to reduce entropic effects and which exhibit interaction mainly by dispersion. With this approach, variations in the bond dissociation energy can be correlated to the change in the substitution pattern. Based on this data, the substituents can be classified by their strength of London dispersion interactions. Additionally, comparison of the results in the gas phase and in solution allowed estimating the dispersive interactions with the solvent (Figure 4).

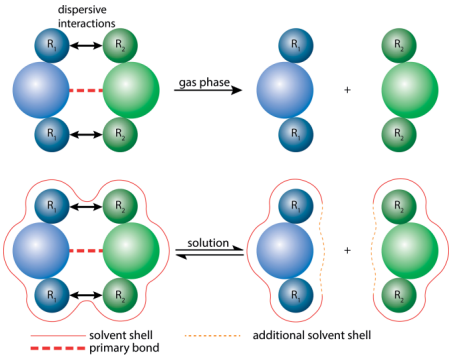

Figure 4. Concept for investigation of differently substituted proton-bound *N*-heterocyclic dimers in the gas phase and in solution with expected interactions.[45]

Evaluation of the applied methods for computations was performed by comparing the computed bond dissociation energies with the experimentally obtained data for a designed probe with an alternative weak bond, offering a second dissociation pathway in a CID experiment as reference. The validated data revealed, that in the gas phase, attractive dispersion is more important than repulsive exchange. Computed free energies of dissociation in solution were estimated by applying the dispersion-corrected implicit solvent models SMD[46] and COSMO-RS.[47] However, with both implicit solvent models, the trends or the magnitude for Gibbs free energies of bond dissociation for the larger test systems could not be reproduced. They further concluded that London dispersion plays a major role for the bond dissociation energies in the gas phase with increasing size of the substituents. Stabilization by London dispersion attenuates in dichloromethane solution by about 70% due to compensatory interactions of solvent molecules with newly exposed surfaces upon cleavage of the central N-H–N bond. These effects are still measurable at temperatures relevant for chemical reactions.

Their investigation clearly showed, that results from computations with dispersion corrected implicit solvent models should be interpreted carefully since especially for larger systems with dispersive interactions significant deviations from the experiment are to be expected. The high number of compounds measured provide a comprehensive overview on the stabilization capabilities of different substituents by dispersive interactions in the gas phase and in dichloromethane solution.

4.3. Dimerization Equilibrium of a Titanium Complex Controlled by London Dispersion

Albrecht, Rissanen and Schalley investigated the effect of altering the outer sphere of ligands with different dispersion donor

ChemPubSoc Europe
EurJOC European Journal of Organic Chemistry
Microreview

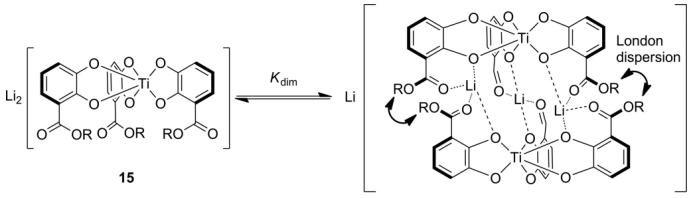

Scheme 10. Dimerisation of titanium triscatecholate helicate **16** with several alkyl substituents.[21]

groups on the stabilization of dinuclear titanium(IV) helicate complexes **16** (Scheme 10).[21] Based on a previously reported monomer–dimer equilibrium of titanium triscatecholate units **15** in the presence of lithium ions in solution,[48] they determined the influence of linear, branched and cyclic alkyl residues on the ester moieties as well as *n*-fluoroalkyl side chains on the equilibrium position. The threefold symmetry of the system led to a high sensitivity towards subtle changes due to a threefold amplification of the weak interaction energies.

The equilibrium constant as well as other thermodynamic parameters were determined by NMR spectroscopy. As can be seen from the crystal structures of the dimers, short alkyl–alkyl contacts which indicate London dispersion stabilization are only possible in the dimer. Van't Hoff analyses revealed that dimerization of the *n*-alkyl-substituted complexes is enthalpically more favored by stepwise elongation of the chain. Entropy, on the other hand, is less favored due to the restricted conformational freedom of the side chains caused by attractive interactions. For the *n*-fluoroalkyl derivatives, enthalpic contributions are less significant. Here, the entropy term is always favorable, which the authors explain by the liberation of solvent molecules upon dimerization. In the case of open-chain branched alkyl compounds, the increasing steric demand of the substituents seems to disfavor the dimerization. For the cycloalkyl derivatives, however, dimer formation is enthalpically favored for larger rings, which stems from the higher interacting contact areas. Kinetic studies on the exchange of two separately generated homodimeric helicates were performed in THF by ESI mass spectrometry. This approach allowed determining the exchange trends caused by weak interactions giving an estimation of the dissociation barrier for the dimeric helicate **16** into the monomers **15**. The increase of the dissociation barrier indicates stabilizing interactions in the transition state for dimer-to-monomer dissociation. Evaluation of selected examples provided support for the assumption that London dispersion interactions and not solvophobic effects are mainly responsible for the observed increased stability with larger alkyl substituents. Therefore, complexes from the four different series with similar dimerization constants or similar sizes were considered. Upon dimerization, the alkyl residues were less exposed to the solvent, which could also be shown by the crystal structures. Though the space requirements of *isopropyl* and cyclobutyl substituents are very similar, the dimerization constants differ significantly, which would not be the case if solvophobic effects were the major driving forces for dimerization.

Examinations of London dispersion between linear alkyl chains are still only marginal explored. This work offers a rare insight into the difficulties faced when working with highly flexible groups. Especially entropic contributions due to this high flexibility and possible formation of "loops" complicate meaningful interpretation. Due to this, also computational analysis of the large number of possible conformers often turns out impossible with standard resources. A minor drawback is the limited solubility of this system, prohibiting extensive studies of solvent effects.

5. Conclusion

Different approaches were utilized to quantify the degree of London dispersion interactions. Systems based on molecular torsion balances provided an extensive insight into the stabilizing effects of dispersion energy donors and could illuminate the influence of solvophobic effects leading to a preference of a certain rotamer. However, a higher degree of flexibility often raises the complexity for interpretation of measurements and leads to a higher impact of entropic effects. Also, the inclusion of heteroatoms in such model systems can make it necessary to consider further secondary interactions like hydrogen-bonding and, therefore, complicate the determination of the dispersion energy. Certainly, the powerful tool of the double mutant cycles provides a possibility to dissect the interaction of interest in a concise manner. The cyclooctatetraene balances offer the advantage, that secondary interactions are mostly obviated due to the absence of heteroatoms. The challenging part, however, is the elaborate synthesis of substituted derivatives and its sensitivity, e.g. towards light. In thiobarbiturate balances solvent interactions with the barbiturate scaffold overcompensate dispersive interactions and prevent a systematic study of solvent effects on London dispersion. Furthermore, measurements at lower temperatures are required due to the low rotational barrier between *syn*- and *anti*-conformers.

Azobenzenes offer the advantage that its isomerization can precisely be followed by UV/Vis or NMR spectroscopy and changes in activation energies can therefore easily be determined. Also, the synthesis of derivatives can be accomplished in a convenient manner. Easy handling and long-term stability are also beneficial.

The studied proton-bound *N*-heterocyclic dimers show the advantage that measurements in the gas phase are possible,

ChemPubSoc Europe

EurJOC European Journal of Organic Chemistry
Microreview

allowing, by comparison, a direct observation of the attenuation of dispersive interactions in solution. Since charged molecules function as dispersive probes, the number of accessible solvents for screening is limited. The same applies to the dinuclear titanium(IV) helicate complexes, of which the solubility is a limiting factor in its application. However, the threefold symmetry resulting in multiplication of dispersive interactions leads to a beneficial increase of sensitivity.

A number of approaches with a large scope of molecular model systems were so far studied providing a valuable insight into the energetic contributions of London dispersion in the gas phase and in solution. Indeed, the perfect system still has to be established. Some of the presented systems already contributed to our understanding of the strength of dispersive interactions in solution. Further optimization of these dispersion probes will be the subject of future investigations. The ultimate goal to create a universal scale of the strength for various dispersion donors is still a dream. The high dependence of London dispersion interactions on the environment makes it challenging to draw general conclusions. However, collaborative efforts to unify the data obtained by the various methods described above will bring the field a big step closer to this dream. Such detailed knowledge of the contribution of London dispersion will provide valuable data to guide the design of molecular structures as well as processes.

Acknowledgments

The authors thank Jan M. Schümann for the fruitful discussions. Financial support was provided by the Justus-Liebig University Giessen and by the Deutsche Forschungsgemeinschaft (SPP1807).

Keywords: London dispersion · Sensors · Molecular balance · Solvent effects · Interactions

[1] C.-Y. Lin, J.-D. Guo, J. C. Fettinger, S. Nagase, F. Grandjean, G. J. Long, N. F. Chilton, P. P. Power, *Inorg. Chem.* **2013**, *52*, 13584.
[2] a) E. Lyngvi, I. A. Sanhueza, F. Schoenebeck, *Organometallics* **2015**, *34*, 805; b) M. S. G. Ahlquist, P.-O. Norrby, *Angew. Chem. Int. Ed.* **2011**, *50*, 11794; *Angew. Chem.* **2011**, *123*, 11998.
[3] F. London, *Z. Phys.* **1930**, *63*, 245.
[4] P. R. Schreiner, L. V. Chernish, P. A. Gunchenko, E. Y. Tikhonchuk, H. Hausmann, M. Serafin, S. Schlecht, J. E. P. Dahl, R. M. K. Carlson, A. A. Fokin, *Nature* **2011**, *477*, 308.
[5] D. J. Liptrot, P. P. Power, *Nat. Rev. Chem.* **2017**, *1*, 0004.
[6] D. J. Liptrot, J.-D. Guo, S. Nagase, P. P. Power, *Angew. Chem. Int. Ed.* **2016**, *55*, 14766; *Angew. Chem.* **2016**, *128*, 14986.
[7] S. Rösel, H. Quanz, C. Logemann, J. Becker, E. Mossou, L. Cañadillas-Delgado, E. Caldeweyher, S. Grimme, P. R. Schreiner, *J. Am. Chem. Soc.* **2017**, *139*, 7428.
[8] M. Kolář, T. Kubař, P. Hobza, *J. Phys. Chem. B* **2011**, *115*, 8038.
[9] J. Vondrásek, T. Kubar, F. E. Jenney, M. W. W. Adams, M. Kozísek, J. Cerný, V. Sklenár, P. Hobza, *Chem. Eur. J.* **2007**, *13*, 9022.
[10] C. Mayer, R. Moritz, C. Kirschner, W. Borchard, R. Maibaum, J. Wingender, H.-C. Flemming, *Int. J. Biol. Macromol.* **1999**, *26*, 3.
[11] a) J. A. M. Mercer, C. M. Cohen, S. R. Shuken, A. M. Wagner, M. W. Smith, F. R. Moss, M. D. Smith, R. Vahala, A. Gonzalez-Martinez, S. G. Boxer et al., *J. Am. Chem. Soc.* **2016**, *138*, 15845; b) J. P. Wagner, P. R. Schreiner, *J. Chem. Theory Comput.* **2014**, *10*, 1353.
[12] E. Sanna, E. C. Escudero-Adán, A. Bauzá, P. Ballester, A. Frontera, C. Rotger, A. Costa, *Chem. Sci.* **2015**, *6*, 5466.
[13] S. Grimme, *WIREs Comput. Mol. Sci.* **2011**, *1*, 211.
[14] a) J. P. Wagner, P. R. Schreiner, *Angew. Chem. Int. Ed.* **2015**, *54*, 12274; *Angew. Chem.* **2015**, *127*, 12446; b) S. Grimme, R. Huenerbein, S. Ehrlich, *ChemPhysChem* **2011**, *12*, 1258.
[15] Stefan Grimme in *The chemical bond. Fundamental aspects of chemical bonding* (Eds.: G. Frenking, S. S. Shaik), Wiley-VCH Verlag, Weinheim, **2014**, pp. 477–499.
[16] a) A. H. Heindl, R. C. Wende, H. A. Wegner, *Beilstein J. Org. Chem.* **2018**, *14*, 1238; b) U. Lüning, C. Kühl, A. Uphoff, *Eur. J. Org. Chem.* **2002**, 4063.
[17] C. A. Hunter, J. K. M. Sanders, *J. Am. Chem. Soc.* **1990**, *112*, 5525.
[18] A. Nijamudheen, D. Jose, A. Shine, A. Datta, *J. Phys. Chem. Lett.* **2012**, *3*, 1493.
[19] a) T. Grawe, T. Schrader, R. Zadmard, A. Kraft, *J. Org. Chem.* **2002**, *67*, 3755; b) A. Bencini, A. Bianchi, M. I. Burguete, P. Dapporto, A. Doménech, E. García-España, S. V. Luis, P. Paoli, J. A. Ramírez, *J. Chem. Soc., Perkin Trans. 2* **1994**, *67*, 569.
[20] D. J. Pascoe, K. B. Ling, S. L. Cockroft, *J. Am. Chem. Soc.* **2017**, *139*, 15160.
[21] D. van Craen, W. H. Rath, M. Huth, L. Kemp, C. Räuber, J. M. Wollschläger, C. A. Schalley, A. Valkonen, K. Rissanen, M. Albrecht, *J. Am. Chem. Soc.* **2017**, *139*, 16959.
[22] J. Catalán, H. Hopf, *Eur. J. Org. Chem.* **2004**, 4694.
[23] I. K. Mati, S. L. Cockroft, *Chem. Soc. Rev.* **2010**, *39*, 4195.
[24] B. Nilsson, T. Drakenberg, *Org. Magn. Reson.* **1974**, *6*, 155.
[25] S. L. Cockroft, C. A. Hunter, *Chem. Soc. Rev.* **2007**, *36*, 172.
[26] A. Horovitz, *Folding and Design* **1996**, *1*, R121–R126.
[27] M. Orlandi, J. A. S. Coelho, M. J. Hilton, F. D. Toste, M. S. Sigman, *J. Am. Chem. Soc.* **2017**, *139*, 6803.
[28] S. Paliwal, S. Geib, C. S. Wilcox, *J. Am. Chem. Soc.* **1994**, *116*, 4497.
[29] E.-i. Kim, S. Paliwal, C. S. Wilcox, *J. Am. Chem. Soc.* **1998**, *120*, 11192.
[30] L. Yang, C. Adam, G. S. Nichol, S. L. Cockroft, *Nat. Chem.* **2013**, *5*, 1006.
[31] C. Adam, L. Yang, S. L. Cockroft, *Angew. Chem. Int. Ed.* **2015**, *54*, 1164; *Angew. Chem.* **2015**, *127*, 1180.
[32] L. Yang, C. Adam, S. L. Cockroft, *J. Am. Chem. Soc.* **2015**, *137*, 10084.
[33] J. Hwang, B. E. Dial, P. Li, M. E. Kozik, M. D. Smith, K. D. Shimizu, *Chem. Sci.* **2015**, *6*, 4358.
[34] J. Hwang, P. Li, M. D. Smith, K. D. Shimizu, *Angew. Chem. Int. Ed.* **2016**, *55*, 8086; *Angew. Chem.* **2016**, *128*, 8218.
[35] M. H. Lyttle, A. Streitwieser, R. Q. Kluttz, *J. Am. Chem. Soc.* **1981**, *103*, 3232.
[36] L. A. Paquette, G. J. Hefferon, R. Samodral, Y. Hanzawa, *J. Org. Chem.* **1983**, *48*, 1262.
[37] a) N. L. Allinger, M. Frierson, F. A. Van-Catledge, *J. Am. Chem. Soc.* **1982**, *104*, 4592; b) C. Tosi, *J. Comput. Chem.* **1984**, *5*, 248.
[38] J. E. Anderson, P. A. Kirsch, *J. Chem. Soc., Perkin Trans. 2* **1992**, 1951.
[39] U. Berg, I. Pettersson, *J. Org. Chem.* **1987**, *52*, 5177.
[40] in *IUPAC Compendium of Chemical Terminology* (Eds.: M. Nič, J. Jirát, B. Košata, A. Jenkins, A. McNaught), IUPAC, Research Triagle Park, NC, **2009**.
[41] M. Schmittel, C. Ruechardt, *J. Am. Chem. Soc.* **1987**, *109*, 2750.
[42] T. Asano, T. Okada, S. Shinkai, K. Shigematsu, Y. Kusano, O. Manabe, *J. Am. Chem. Soc.* **1981**, *103*, 5161.
[43] J. Dokić, M. Gothe, J. Wirth, M. V. Peters, J. Schwarz, S. Hecht, P. Saalfrank, *J. Phys. Chem. A* **2009**, *113*, 6763.
[44] L. Schweighauser, M. A. Strauss, S. Bellotto, H. A. Wegner, *Angew. Chem. Int. Ed.* **2015**, *54*, 13436; *Angew. Chem.* **2015**, *127*, 13636.
[45] R. Pollice, M. Bot, I. J. Kobylianskii, I. Shenderovich, P. Chen, *J. Am. Chem. Soc.* **2017**, *139*, 13126.
[46] A. V. Marenich, C. J. Cramer, D. G. Truhlar, *J. Phys. Chem. B* **2009**, *113*, 6378.
[47] F. Eckert, A. Klamt, *AIChE J.* **2002**, *48*, 369.
[48] M. Albrecht, S. Mirtschin, M. de Groot, I. Janser, J. Runsink, G. Raabe, M. Kogej, C. A. Schalley, R. Fröhlich, *J. Am. Chem. Soc.* **2005**, *127*, 10371.

Received: June 12, 2018

5 Additional Contributions to Literature

This section lists contributions to articles covering mostly other research areas of the Wegner group. The most recent article is presented first.

5.1 Mechanistic Study of Domino Processes Involving the Bidentate Lewis Acid Catalyzed Inverse Electron-Demand Diels-Alder Reaction

Reference:

M. A. Strauss, D. Kohrs, J. Ruhl, H. A. Wegner, *Eur. J. Org. Chem.*, **2021**, *Accepted Article*
DOI: 10.1002/ejoc.202100486

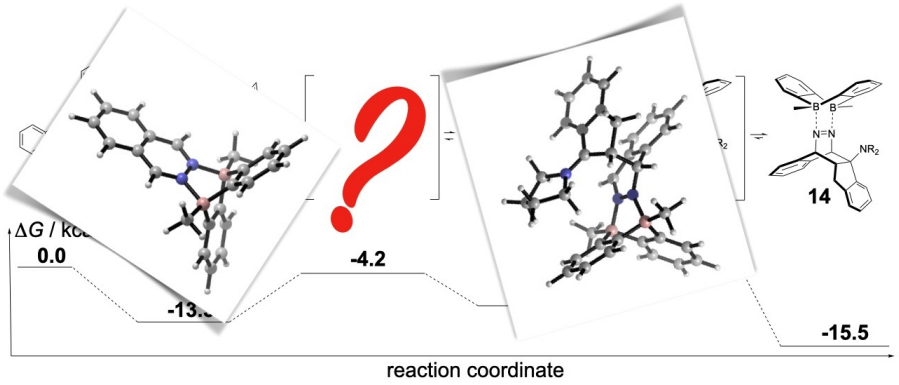

"The detailed understanding of mechanisms is the basis to design new reactions. Herein, we studied the domino bidentate Lewis acid catalyzed inverse electron-demand Diels-Alder (IEDDA) reaction developed in our laboratory computationally as well as with support by synthetic experiments. That way, we could characterize different pathways. A quinodimethane intermediate was identified as key structure, which is the basis for all subsequent transformations: Elimination to an aromatic naphthalene, rearrangement to a dihydroaminonaphthalene and a photo-induced ring opening. These insights allow to optimize reaction conditions, such as catalytic utilization of amine, as well as to advance new reactions in the future."

5.2 Synthesis of Medium-Sized Carbocycles via Bidentate Lewis Acid Catalyzed Inverse Electron-Demand Diels-Alder Reaction Followed by Photoinduced Ring-Opening

Reference:

J. Ruhl, S. Ahles, M. A. Strauss, C. M. Leonhardt, H. A. Wegner, *Org. Lett.*, **2021**, *23*, 2089–2093.
DOI: 10.1021/acs.orglett.1c00249

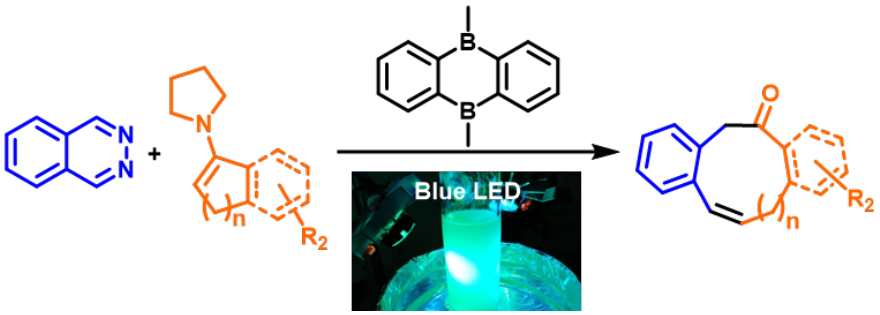

"The combination of a Lewis acid-catalyzed inverse electron-demand Diels–Alder (IEDDA) reaction with a photoinduced ring-opening (PIRO) reaction in a domino process has been established as an efficient synthetic method to access medium-sized carbocycles. From readily available electron-rich and electron-poor phthalazines and enamines, respectively, as starting materials, various 9- and 11-membered carbocycles were prepared. This versatile transition-metal-free tool will be valuable for broadening the structural space in biologically active compounds and functional materials."

5.3 Combining Bidentate Lewis Acid Catalysis and Photochemistry: Formal Insertion of *o*-Xylene into an Enamine Double Bond

Reference:

S. Ahles, J. Ruhl, M. A. Strauss, H. A. Wegner, *Org. Lett.*, **2019**, *21*, 3927-3930.
DOI: 10.1021/acs.orglett.9b01020

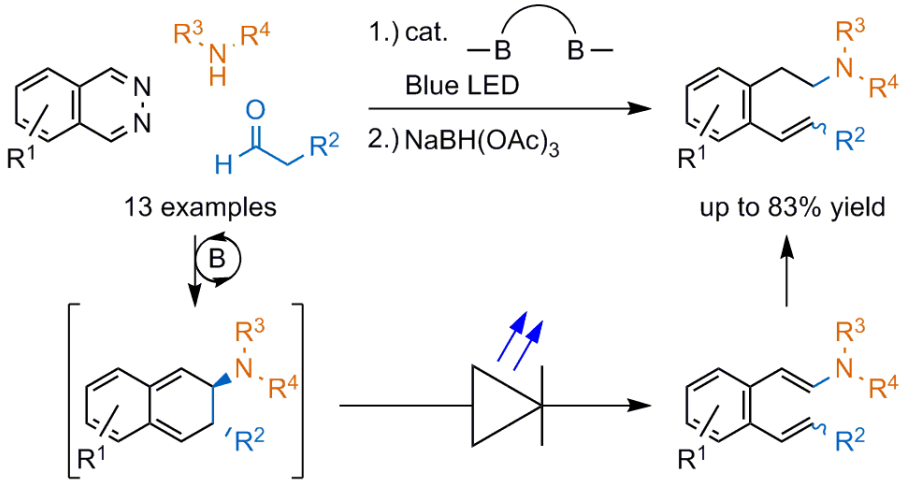

"A bidentate Lewis acid catalyzed domino inverse-electron-demand Diels–Alder reaction combined with a photoinduced ring opening formally inserts *o*-xylene moieties into enamine double bonds. After reduction, phenethylamines were obtained in good yields. The scope of the reaction was determined by variation of all three starting compounds: phthalazines, aldehydes, and amines."

5.4 Action-Spectroscopy Studies of Positively Charge-tagged Azobenzene in Solution and in the Gas-phase

Reference:

E. Gruber, M. A. Strauss, H. A. Wegner, L. H. Andersen, *J. Chem. Phys.*, **2019**, *150*, 084303.
DOI: 10.1063/1.5085743

"The absorption of a positively charge-tagged azobenzene molecule is studied in the gas-phase by measuring photoinduced fragmentation of ions as a function of time. This technique provides information on prompt as well as delayed fragmentation, and a single dissociation channel after one-photon absorption is identified. The spectra in solution, as well as in the gas-phase, show a weak $S_0 \rightarrow S_1$, a strong $S_0 \rightarrow S_2$, and a broad absorption band in the UV regime. The bands are assigned through time dependent density functional theory calculations. The ratio of the various absorption bands depends on the *trans* to *cis* isomerization fraction and may be tuned by light irradiation. Gas-phase absorption spectra are presented and discussed in terms of *trans* and *cis* isomers."

5.5 Synthesis of 2,3-Diaza-Anthraquinones via the Bidentate Lewis Acid Catalysed Inverse Electron-demand Diels–Alder (IEDDA) Reaction

Reference:

L. Hong, S. Ahles, M. A. Strauss, C. Logemann, H. A. Wegner, *Org. Chem. Front.*, **2017**, *4*, 871-875.
DOI: 10.1039/C7QO00172J

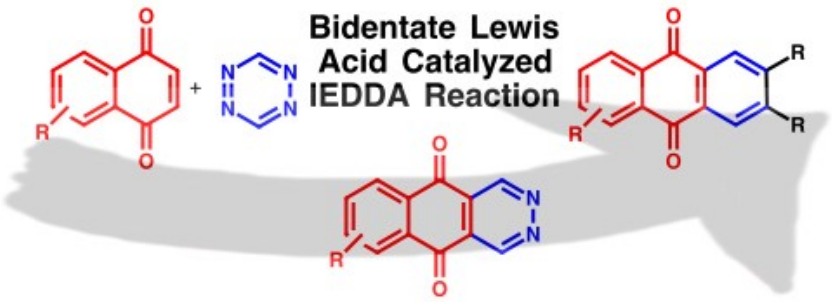

"The bidentate bisborane Lewis acid catalysed inverse electron-demand Diels–Alder (IEDDA) reaction of 1,4-naphthoquinones (1,4-NQs) with 1,2,4,5-tetrazine (**TZ**) has been developed for the synthesis of 2,3-diaza-anthraquinones (2,3-DAAQs). Only due to the coordination of **TZ** with the bisborane catalyst, the IEDDA reaction of electron-deficient 1,4-NQs is possible. The use of **TZ** as the nitrogen source provides an efficient strategy to the 2,3-diaza-anthraquinones. The 2,3-DAAQs themselves are suitable dienes for a second bidentate Lewis acid catalysed IEDDA reaction with various dienophiles to afford substituted AQs. AQs have been discussed as privileged structures for applications in medicinal as well as materials science."

5.6 Attraction or Repulsion? London Dispersion Forces Control Azobenzene Switches

Reference:

L. Schweighauser, M. A. Strauss, S. Bellotto, H. A. Wegner, *Angew. Chem. Int. Ed.*, **2015**, *54*, 13436-13439.
German Edition:
L. Schweighauser, M. A. Strauss, S. Bellotto, H. A. Wegner, *Angew. Chem.*, **2015**, *127*, 13636-13639.
DOI: 10.1002/anie.201506126 and 10.1002/ange.201506126

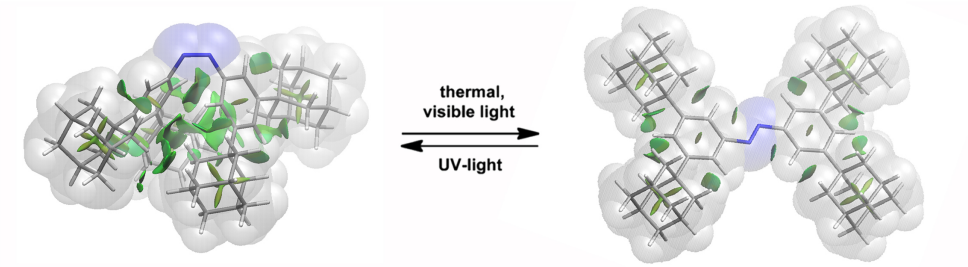

"Large substituents are commonly seen as entirely repulsive through steric hindrance. Such groups have additional attractive effects arising from weak London dispersion forces between the neutral atoms. Steric interactions are recognized to have a strong influence on isomerization processes, such as in azobenzene-based molecular switches. Textbooks indicate that steric hindrance destabilizes the *Z* isomers. Herein, we demonstrate that increasing the bulkiness of electronically equal substituents in the *meta*-position decreases the thermal reaction rates from the *Z* to the *E* isomers. DFT computations revealed that attractive dispersion forces essentially lower the energy of the *Z* isomers."

6 Danksagung

Als Erstes möchte ich mich bei Prof. Dr. Hermann A. Wegner bedanken für die Möglichkeit meine Doktorarbeit in seiner Arbeitsgruppe anzufertigen, seine vertrauensvolle Unterstützung und den Freiraum, den er mir beim Überwinden einiger Herausforderungen eingeräumt hat.

Bei Prof. Dr. Peter R. Schreiner bedanke ich mich dafür, dass er sich als Zweitgutachter für meine Dissertation zur Verfügung stellt.

Meiner lieben Carolin danke ich ganz herzlich für ihre Geduld und Verständnis, wenn das ein oder andere Wochenende mal wieder im Labor verbracht wurde und für ihren motivierenden Zuspruch.

Meiner Familie danke ich für ihre große Unterstützung in all der Zeit ohne die mein Studium so nicht möglich gewesen wäre.

Weiterhin danke ich Dr. Sebastian Ahles und Dr. Luca Schweighauser für ihre vielen hilfreichen Ratschläge, die bei der Überwindung der ein oder anderen kinetischen und thermodynamischen Hürde sehr geholfen haben.

Ganz großer Dank gebührt der gesamten Arbeitsgruppe Wegner für die herrlichen Jahre. Im Besonderen danke ich Julia Ruhl, Daniel Kohrs, Anne Kunz, Jan Griwatz, Dr. Longcheng Hong, Mari Janse van Rensburg, Dr. Andreas Heindl, Sebastian Beeck und Jannis Volkmann für die gemeinsame Zeit im Labor und die vielen anregenden und lustigen Gespräche in der Mensa und beim ein oder anderen Apéro. Außerdem danke für die schönen Stunden bei den Gruppenausflügen, welche ich sehr genossen habe.

Bei meinen Freunden und Kommilitonen Dr. Dominik Niedek, Alexander Seitz, Dr. Miriam Wern, Dr. Andreas Miska, Jean-Marie Pohl, Christof Barth, Dr. Christian Sack und bei Jan Schümann – der mit mir die Dispersion durchdrungen hat – bedanke ich mich für die schönen außeruniversitären Aktivitäten und die willkommenen Ablenkungen vom Alltag und den ein oder anderen fachlichen Rat.

Dr. Dennis Gerbig, Henrik Quanz, Dr. Urs Gellrich, Tizian Müller und Jama Ariai bin ich zutiefst dankbar für das geduldige Beantworten meiner vielen Fragen zur Computerchemie.

Außerdem möchte ich mich bei den Arbeitsgruppen Göttlich und Schreiner bedanken für die super Zusammenarbeit, spontane Hilfsbereitschaft und die schöne Zeit auf vielen gemeinsamen Konferenzen bedanken.

Keine Doktorarbeit kommt ohne die Hilfe der technischen und administrativen Mitarbeiter aus, die mit ihrer Unterstützung unsere Forschung sehr stark weiter bringen. Daher gebührt auch ganz großer Dank Dr. Heike Hausmann, Anika Bernhardt, Anja Platt, Dr. Raffael Wende, Stefan Bernhardt, Steffen Wagner, Edgar Reitz, Anja Beneckenstein, Inna Klein, Brigitte Weinl-Boulakhrouf, Dr. Erwin Röcker, Dr. Jörg Neudert, Eike Santowski, Mario Daubner, sowie Doris Verch und Michaela Richter, die unablässig halfen viele bürokratische Hürden zu umschiffen.